Antigen-specific T cell turnover and expansion *in vivo* during chronic immune stimulation

Kristin I. Ladell

Cardiff University School of Medicine
Institute of Infection & Immunity

PhD thesis
2013

Supervised by: Professor David A. Price, Institute of Infection & Immunity, Cardiff University School of Medicine, Cardiff, UK (supervisor)

Dr. Linda Wooldridge, Institute of Infection & Immunity, Cardiff University School of Medicine, Cardiff, UK (co-supervisor)

Abstract

Effective immunity is fundamental to life on a dirty planet. Appropriate immune responses control infections and protect against cancer. Inappropriate immune responses lead to autoimmunity and allergy. A fine balance between aggression and tolerance is therefore central to effective immune function at the system level. This is a particular problem for T cells, which recognize peptide antigens bound to host major histocompatibility complex (MHC) molecules. Faced with a composite antigenic structure, the distinction between "foreign and dangerous" and "self and harmless" becomes both difficult and imperative, especially when the antigen persists. In this thesis, antigen-specific T cell responses were investigated under conditions of chronic antigenic stimulation to inform our understanding of this process.

In T cell receptor transgenic mice, continuous antigenic stimulation without adjuvant lead to increased *in vivo* turnover of antigen-specific $CD4^+$ T cells but "aborted" immune activation, characterized by depletion of these cells from the circulation and spleen. Full immune activation and expansion of antigen-specific memory/effector $CD4^+$ T cells required the presence of adjuvant, in this case IL-1β, which induces an inflammatory environment.

Further isotope labelling studies in human immunodeficiency virus-infected subjects suggested that the surface marker CD57 demarcates a "steady state" within the $CD8^+$ T cell memory compartment, whereby $CD57^+$ cells have lower *in vivo* turnover rates compared to their $CD57^-$ counterparts. These observations provide a potential mechanistic explanation for the preferential accumulation of $CD57^+CD8^+$ cells under conditions of chronic antigenic stimulation.

Another persistent pathogen, cytomegalovirus (CMV), expresses a viral interleukin (IL)-10 homologue. Memory T cell inflation and antiviral cytokine production in murine CMV(MCMV)-infected mice were suppressed by IL-10. Conversely, IL-10 blockade or deficiency lead to the inflation of certain antigen-specific T cell populations and reduced viral load, most likely as a consequence of the enhanced immune response.

Reactivation of human CMV was also apparent in subjects with dasatinib-associated large granular lymphocyte expansions. Consistent with a causative association, the expanded T cell and NK cell populations in these subjects were oligoclonal and exhibited a late differentiated ($CD27^-CD57^+$) phenotype, indicative of chronic antigenic stimulation. In addition, $CD8^{high}$ and $CD8^{low}$ T cells were observed within both the total and CMV-specific $CD8^+$ T cell compartments, consistent with CMV-driven activation.

In summary, these data show that antigen alone is not sufficient to induce full immune activation, even under conditions of chronic stimulation. Additional signals, such as those provided by an inflammatory environment, are required to trigger full T cell activation and expansion. Persistent viruses attempt to undermine this process, for example by the expression of homologues that mimic host immune regulators. Even in the presence of viral reactivation and immune system perturbations, however, the T cell compartment can demonstrate remarkable resilience in its ability to generate fully differentiated and functional expansions. The persistence of certain memory T cell subsets under such conditions appears to play an important role in the immune response to chronic "dangerous" antigens.

Acknowledgements

I am very grateful for the funding that was available to conduct the projects described in this thesis. Primary funding sources were the National Institutes of Health (NIH grant RO1 AI43866 to Prof. Marc Hellerstein at the University of California Berkeley and NIH award U01 AI43641 to Prof. “Mike” McCune, who is the recipient of the Burroughs Wellcome Fund Clinical Scientist Award in Translational Research and the NIH Director’s Pioneer Award Program, part of the NIH Roadmap for Medical Research, through grant number DPI OD00329), the Medical Research Council UK (Prof. David Price, Prof. Derek Macallan and myself) and the Wellcome Trust (Prof. David Price, Prof. Derek Macallan, Dr. Ian Humphreys and myself). Funding for the optimization of the low-count techniques by mass spectrometry was provided by KineMed Inc. (Emeryville, CA, USA). Funding for other collaborators is not listed, but can be found in the original articles that were published with data from this thesis.

In days past, it was possible for a single author to publish biomedical research articles, but this is not possible nowadays unless one has a very unique and novel idea that one can realize on one’s own. Therefore, I have numerous people to thank, without whom the described projects would not have been possible. First of all, I thank Prof. David Price very much for all his support, for getting me involved in numerous research projects and for taking the time to read and give advice on my thesis. I also thank Prof. “Mike” McCune, Chief of the Division of Experimental Medicine, University of California San Francisco (UCSF) in San Francisco, CA, USA, who together with Prof. Marc Hellerstein (UC Berkeley, Berkley, CA, USA) made it possible for me to come back to San Francisco to carry out a key set of experiments. I am honoured that Dr. Linda Wooldrige agreed to be my co-supervisor and I thank her very much for her input and for the time that she took to give advice on my thesis. I thank all of my collaborators, especially the following: Prof. Marc Hellerstein, Prof. Derek Macallan (London, UK), Dr. Ian Humphreys (Cardiff, UK), Dr. Ruth Seggewiss (Würzburg, Germany), Dr. Satu Mustjoki (Helsinki, Finland), Dr. Katherine Matthews (formerly “Katherine Wynn”, Queensland, Australia), Ms. Emma Gostick (Abingdon, UK), Dr. Anna Kreutzman (Helsinki, Finland), Mrs. Morgan Marsden

(formerly “Morgan Jones”, Cardiff, UK) and all other co-authors on the publications listed in this thesis. For technical help, advice and resource provision, I thank Dr. Cheryl Stoddart, George Chkhenkeli, Sofiya Galkina, Mary Beth Moreno and José Rivera at the Division of Experimental Medicine, UCSF. I would also like to thank Dr. Ann Ager from the Institute of Infection & Immunity at Cardiff University School of Medicine for very helpful discussions and for advice on this thesis. I thank Prof. Marian Ludgate (Cardiff, UK) and Dr. Eddie Wang (Cardiff, UK) for taking the time to read my progress reports and for appraisals. I also thank my current co-workers and facility staff. Lastly, I thank my parents and my sister, who always have an interest in what I do and help me wherever they can, if there is anything that they can help me with.

Declaration

This work has not previously been accepted in substance for any degree and is not concurrently submitted in candidature for any degree.

Signed (candidate) Date 12th March 2013

Statement 1

This thesis is being submitted in partial fulfillment of the requirements for the degree of PhD.

Signed (candidate) Date 12th March 2013

Statement 2

This thesis is the result of my own independent work/investigation, except where stated otherwise. Other sources are acknowledged by explicit references.

Signed (candidate) Date 12th March 2013

Statement 3

I hereby give consent for my thesis, if accepted, to be available for photocopying and for inter-library loan, and for the title and summary to be made available to outside organizations.

Signed (candidate) Date 12th March 2013

Published or to-be published work incorporated in this thesis:

Ladell K, Hellerstein MK, Hazenberg MD, Fitch M, Mold J, Miller C, Cesar D, Emson C, McEvoy-Hein B, McCune JM. Continuous subcutaneous administration of peptide without adjuvant leads to aborted immune activation in DO11.10 TCR transgenic mice. (In preparation for submission to J Immunol; **chapter 3**).

Ladell K, Hellerstein MK, Boban D, Cesar D, Price DA, McCune JM. In Vivo Turnover of Human CD57+ or CD57- CD8+CD45RA-CCR7- Effector Memory T Cells in HIV Infection. Keystone Symposium on Imunologic Memory and Host Defense (B6), Keystone, Colorado, USA, 02/2009 (Abstract / Poster; **chapter 4**).

Jones M, **Ladell K**, Wynn KK, Stacey MA, Quigley MF, Gostick E, Price DA, Humphreys IR (2010) IL-10 restricts memory T cell inflation during cytomegalovirus infection. J Immunol 15;185(6):3583-92 (**chapter 5**).

Ladell K*, Kreutzman A*, Koechel C, Gostick E, Ekblom M, Stenke L, Melo T, Einsele H, Porkka K, Price DA*, Mustjoki S*, Seggewiss R* (2011) Expansion of highly differentiated $CD8^+$ T-cells or NK-cells in patients treated with dasatinib is associated with cytomegalovirus reactivation. [* Equal contribution.] Leukemia 25(10):1587-97 (**chapter 6**).

Other publications published since I enrolled for a PhD *(in chronological order)*:

Chattopadhyay PK, Melenhorst JJ, **Ladell K**, Gostick E, Scheinberg P, Barrett AJ, Wooldridge L, Roederer M, Sewell AK, Price DA (2008) Techniques to improve the direct *ex vivo* detection of low frequency antigen-specific $CD8^+$ T cells with peptide-major histocompatibility complex class I tetramers. Cytometry A 73(11):1001-09.

Lissina A, **Ladell K**, Skowera A, Clement M, Edwards E, Seggewiss R, van den Berg HA, Gostick E, Gallagher K, Jones E, Godkin AJ, Peakman M, Price DA, Sewell AK*, Wooldridge L* (2009) Protein kinase inhibitors substantially improve the physical detection of T-cells with peptide-MHC multimers. [*Equal contribution]. J Immunol Methods 340(1):11-24.

Melenhorst JJ, Scheinberg P, Chattopadhyay PK, Gostick E, **Ladell K**, Roederer M, Hensel NF, Douek DC, Barrett AJ, Price DA (2009) High avidity myeloid leukemia-associated antigen-specific $CD8^+$ T cells preferentially reside in the bone marrow. Blood 113(10):2238-44.

Venturi V, Chin HY, Asher TE, **Ladell K**, Scheinberg P, Bornstein E, van Bockel D, Kelleher AD, Douek DC, Price DA, Davenport MP (2008) TCR β-chain sharing in human $CD8^+$ T cell responses to cytomegalovirus and Epstein-Barr virus. J Immunol 181(11):7853-62.

Wooldridge L, Clement M, Lissina A, Edwards ESJ, **Ladell K**, Ekeruche J, Hewitt RE, Laugel B, Gostick E, Cole DK, Debets R, Berrevoets C, Miles JJ, Burrows SR, Price DA, Sewell AK (2010) MHC class I molecules with superenhanced CD8 binding properties bypass the requirement for cognate TCR recognition and nonspecifically activate CTLs. J Immunol 184(7):3357-66.

Van Tendeloo VF*, Van de Velde A*, Van Driessche* A, Cools N*, Anguille S, **Ladell K**, Gostick E, Vermeulen K, Pieters K, Nijs G, Stein B, Smits EL, Schroyens WA, Gadisseur AP, Vrelust I, Jorens PG, Goossens H, de Vries IJ, Price DA, Oji Y, Oka Y, Sugiyama H, Berneman ZN (2010) Induction of complete and molecular remissions in acute myeloid leukemia by Wilms' tumor 1 antigen-targeted dendritic cell vaccination. [*Equal contribution]. Proc Natl Acad Sci USA 107(31):13824-9.

Cole DK, Edwards ES, Wynn KK, Clement M, Miles JJ, **Ladell K**, Ekeruche J, Gostick E, Adams KJ, Skowera A, Peakman M, Wooldridge L, Price DA, Sewell AK (2010) Modification of MHC anchor residues generates heteroclitic peptides that alter TCR binding and T cell recognition. J Immunol 185(4):2600-10.

Subramanya S, Armant M, Salkowitz JR, Nyakeriga AM, Haridas V, Hasan M, Bansal A, Goepfert PA, Wynn KK, **Ladell K**, Price DA, N M, Kan-Mitchell J, Shankar P (2010) Enhanced Induction of HIV-specific Cytotoxic T Lymphocytes by Dendritic Cell-targeted Delivery of SOCS-1 siRNA. Mol Ther 18(11):2028-37.

Harris LD, Klatt NR, Vinton C, Briant JA, Tabb B, **Ladell K**, Lifson J, Estes JD, Price DA, Hirsch VM, Brenchley JM (2010) Mechanisms underlying γδ T cell subset perturbations in SIV-infected Asian rhesus macaques. Blood 116(20):4148-57.

van Bockel DJ, Price DA, Munier ML, Venturi V, Asher TE, **Ladell K**, Greenaway HY, Zaunders J, Douek DC, Cooper DA, Davenport MP, Kelleher AD (2010) Persistent Survival of Prevalent Clonotypes within an Immunodominant HIV Gag-Specific $CD8^+$ T Cell Response. J Immunol 186(1):359-71.

Hindley JP, Ferreira C, Jones E, Lauder SN, **Ladell K**, Wynn KK, Betts GJ, Singh Y, Price DA, Godkin AJ, Dyson J, Gallimore A (2011) Analysis of the T cell receptor repertoires of tumor-infiltrating conventional and regulatory T cells reveals no evidence for conversion in carcinogen-induced tumors. Cancer Res 71(3):736-46.

Clement M, **Ladell K**, Ekeruche-Makinde J, Miles JJ, Edwards ES, Dolton G, Williams T, Schauenburg AJ, Cole DK, Lauder SN, Gallimore AM, Godkin AJ, Burrows SR, Price DA, Sewell AK, Wooldridge L (2011) Anti-CD8 antibodies can trigger $CD8^+$ T cell effector function in the absence of TCR engagement and improve peptide-MHCI tetramer staining. J Immunol 15;187(2):654-63.

Cole DK*, Gallagher K*, Lemercier B*, Holland CJ, Junaid S, Hindley JP, Wynn KK, Gostick E, Sewell AK, Gallimore AM, **Ladell K**, Price DA, Gougeon M-L, Godkin A (2012) Modification of the carboxy-terminal flanking region of a universal influenza epitope alters $CD4^+$ T-cell repertoire selection. [* Equal contribution]. Nat Commun 3:665.

Liddy N*, Bossi G*, Adams KJ*, Lissina A, Mahon TM, Hassan NJ, Gavarret J, Bianchi FC, Pumphrey NJ, **Ladell K**, Gostick E, Sewell AK, Lissin NM, Harwood NE, Molloy PE, Li Y, Cameron BJ, Sami M, Baston EE, Todorov PT, Paston SJ, Dennis RE, Dunn SM, Ashfield R, Johnson A, McGrath Y, Price DA, Vuidepot A, Williams DD, Sutton DH, Jakobsen BK (2012) Monoclonal TCR-redirected tumour cell killing. [* Equal contribution]. Nat Med 18(6):980-7.

Ekeruche-Makinde J*, Clement M*, Cole DK*, Edwards ES, **Ladell K**, Miles JJ, Matthews KK, Fuller

A, Lloyd KA, Madura F, Dolton GM, Pentier J, Lissina A, Gostick E, Baxter TK, Baker BM, Rizkallah PJ, Price DA, Wooldridge L*, Sewell AK* (2012) T-Cell Receptor optimized peptide skewing of the T-cell repertoire can enhance antigen targeting. [*Equal contribution]. J Biol Chem 287(44):37269-81.

Hindley JP*, Jones E*, Smart K, Bridgeman H, Lauder SN, Ondondo B, Cutting S, **Ladell K**, Wynn KK, Withers D, Price DA, Ager A, Godkin AJ, Gallimore AM (2012) T cell trafficking facilitated by high endothelial venules is required for tumor control after regulatory T cell depletion. [*Equal contribution]. Cancer Res 72(21):5473-82.

Humphreys IR, Clement M, Marsden M, **Ladell K**, McLaren JE, Smart K, Hindley JP, Bridgeman HM, van den Berg HA, Price DA, Ager A, Wooldridge L, Godkin A, Gallimore AM (2012) Avidity of influenza-specific memory $CD8^+$ T-cell populations decays over time compromising antiviral immunity. Eur J Immunol 42(12):3235-42.

McCully ML, **Ladell K**, Hakobyan S, Mansel RE, Price DA, Moser B (2012) Epidermis instructs skin homing receptor expression in human T cells. Blood 120(23):4591-8.

Antrobus RD, Lillie PJ, Berthoud TK, Spencer AJ, McLaren JE, **Ladell K**, Lambe T, Milicic A, Price DA, Hill AV, Gilbert SC (2012) A T Cell-Inducing Influenza Vaccine for the Elderly: Safety and Immunogenicity of MVA-NP+M1 in Adults Aged over 50 years. PLoS One 7(10):e48322.

Chattopadhyay PK, Chelimo K, Embury PB, Mulama DH, Sumba PO, Gostick E, **Ladell K**, Brodie TM, Vulule J, Roederer M, Moormann AM, Price DA (2013) Holoendemic Malaria Exposure is Associated with Altered Epstein-Barr Virus-Specific $CD8^+$ T-Cell Differentiation. J Virol 87(3):1779-88.

Koning D, Costa AI, Hoof I, Miles JJ, Nanlohy NM, **Ladell K**, Matthews KK, Venturi V, Schellens IM, Borghans JA, Kesmir C, Price DA, van Baarle D (2013) $CD8^+$ TCR Repertoire Formation Is Guided Primarily by the Peptide Component of the Antigenic Complex. J Immunol 190(3):931-9.

Ladell K*, Hashimoto M*, Iglesias MC*, Wilmann PG*, McLaren JE, Gras S, Chikata T, Kuse N, Fastenackels S, Gostick E, Bridgeman JS, Venturi V, Arkoub ZA, Agut H, van Bockel DJ, Almeida JR, Douek DC, Venet A, Takiguchi M*, Rossjohn J*, Price DA*, Appay V* (2013) A molecular basis for the control of pre-immune escape variants by HIV-specific $CD8^+$ T-cells. [* Equal contribution]. Immunity 38(3):425-36

Table of Contents

List of Figures

List of Tables

Abbreviations

AAD, amino-actinomycin D

Ab, antibody

α, anti- or alpha, e.g. anti-CD3 or, TNF-α, respectively

Ag(s), antigen(s)

AICD, activation-induced cell death

APC(s), antigen presenting cell(s)

B cell receptor (BCR)

BC, blast crisis

BMMC(s), bone marrow mononuclear cells

BrdU, bromodeoxyuridine

C, constant

CCgR; complete cytogenetic response

CCL, C-C motif chemokine ligand ("C" here stands for cystein)

CCRC, Clinical and Translational Science Institute Clinical Research Center

CD, cluster of differentiation

cDNA, copy DNA

CDRs, complementarity-determining regions

CFA, complete Freund's adjuvant

CHR, complete haematological response

CML, chronic myeloid leukaemia

CMR, complete molecular response

CMV, cytomegalovirus

CP, chronic phase

CTLA-4, cytotoxic T lymphocyte antigen-4

CXCL, C-X-C motif chemokine ligand ("C" here stands for cystein)

DCs, dendritic cells

Deuterated water (^2H_2O) or deuterated (^2H-)glucose

Dg, diagnosis

DMSO, dimethyl sulfoxide

DN, double negative

DNA, deoxyribonucleic acid

DNNS, de novo nucleotide synthesis pathway

DNPS, de novo purine/pyrimidine synthesis pathway

DP, double positive

EBV, Epstein-Barr virus

FACS, fluorescence activated cell sorting

FBS, fetal bovine serum

fLuc, firefly luciferase
gB, glycoprotein B
GC, gas chromatography
GM-CSF, granulocyte macrophage-colony stimulating factor
GNG, gluconeogenesis/glycolysis
HA, hemagglutinin
HCMV, human cytomegalovirus
HIV, human immunodeficiency virus
HLA, human leukocyte antigen
[^{3}H], tritiated
IDO, indoleamine 2,3-dioxygenase
IE, immediate early
IFA, incomplete Freund's adjuvant
IFN, interferon
Ig, immunoglobulin
IL, interleukin
IL-10R / IL-2R, IL-10 receptor / IL-2 receptor
IP-10/CXCL 10, IFN-γ-inducible protein-10
i.p., intraperitoneally
i.v., intravenously
KLRG-1, killer cell lectin-like receptor subfamily G member 1
LAG, lymphocyte activation gene
LGL(s), large granular lymphocyte(s)
LN(s), lymph node(s)
LPS, lipopolysacccharide (LPS)
mAB(s), monocolonal Ab(s)
MCMV, murine cytomegalovirus
MCP-1/CCL2, monocyte chemoattractant protein-1
MFI, median fluorescence intensity
MHC, major histocompatibility complex
MIG/CXCL9, monokine induced by IFN-γ
MIP, macrophage inflammatory protein
MMR, major molecular response
MS, mass spectometry
N/D, not detected
ND, not done
NK, natural killer
NS, no symptoms

OVA, ovalbumin

OVAp, $OVA_{323-339}$ peptide

PBMC(s), peripheral blood mononuclear cell(s)

PBS, phosphate buffered saline

PCR, polymerase chain reaction

PD-1, programmed death-1

PFBHA, O-(2,3,4,5,6-pentafluorobenzyl)-hydroxylamine hydrochloride

PFTA, pentafluoro tri-acetate

Ph^+ ALL, Philadelphia chromosome-positive acute lymphoblastic leukaemia

pHLA, peptide/HLA

PMA, phorbol 12-myristate 13-acetate

pMHC, peptide-major histocompatibility complex

qPCR, quantitative polymerase chain reaction

RLU, relative light units

RNA, ribonucleic acid

RR, ribonucleotide reductase

RT, reverse transcriptase

s.c., subcutaneous

SD, standard deviation

SEM, standard error of the mean

SPCD4, single positive 4

SPL, spleen

TCR, T cell receptor

TCRA and *TCRB,* α-chain and β-chain encoding TCR genes, respectively

TCRBV, TCRB variable

TCRBJ, TCRB joining

T_{CM}, central memory T (cells)

T_E, effector T (cells)

T_{EM}, effector memory T (cells)

T_{EMRA}, highly differentiated $CD45RA^+CD28^-CCR7^-$ effector memory T (cell)

Tg, transgenic

TGF, transforming growth factor

Th, T helper

THY, Thymus

T_M, memory T (cell)

T_N , naive T (cell)

TNF, tumour necrosis factor

TNFR, TNF-receptor

$T_{REG,}$ regulatory T (cell)
UCSF, University of California at San Francisco
UK, United Kingdom
USA, United States of America
vIL-10, viral IL-10 ortholog
VL, vial load
Wt, wild type
zeo, zeocin

CHAPTER

1

Introduction

1.1 The immune system

The immune system is constructed from many different components, including organs, tissues, vessels, cells and molecular mediators, such as antibodies, chemokines and cytokines, all of which interact to provide holistic protection against external and internal threats. Appropriate immune responses control infections and protect against cancer. Inappropriate immune responses lead to autoimmunity and allergy. A fine balance between aggression and tolerance is therefore central to effective immune function at the system level, especially in the presence of chronic antigenic stimulation. The presented work addresses key aspects of the immune response under such conditions.

The main organs of the immune system are the thymus, the lymph nodes, the spleen, the small and large intestine and, to some extent, the liver. Epithelial surfaces such as the skin and mucosae form a physical barrier that protects the host from invading pathogens. The epithelium and dermis of the skin, as well as the mucosa that lines the intestine, the mouth, the nasal cavity and the genital tract are colonized by immune cells that are ready to attack anything recognized as foreign and pathogenic. The main cell types of the immune system are macrophages, neutrophils, eosinophilic and basophilic granulocytes, natural killer (NK) cells, monocytes, dendritic cells, B and T lymphocytes. Classically, the immune system is divided into two arms at the functional level, termed innate (natural) and adaptive (acquired) immunity (Medzhitov and Janeway 2000).

Innate immunity provides a first line of defence against host attack. Innate receptors or "pattern recognition receptors", such as Toll-like-receptors, recognize highly conserved structures expressed by many different pathogens (Medzhitov and Janeway 2000). Recognition of such structures can occur by receptors expressed on the cell surface or by intracellular receptors after phagocytosis. Phagocytic cells, such as macrophages and neutrophils, eosinophilic and basophilic granulocytes, and

NK cells are classical examples of innate immune cells. Monocytes may be precursors to antigen (Ag) presenting cells (APCs) and are associated with innate and adaptive immune responses. Many species have complement systems, including non-mammals like plants, fish and some invertebrates (Janeway, Travers et al. 2005). Complement is the main humoral component of the innate immune response (Rus, Cudrici et al. 2005). Components of the complement system assist in the killing of pathogens by antibodies. They also function as peptide mediators of inflammation and can recruit phagocytic cells, opsonize pathogens and assist in the removal of immune complexes, or form a membrane attack complex that can lyse cells or pathogens.

Adaptive immune responses are mainly executed by Ag-presenting cells, B and T lymphocytes. B lymphocytes and their descendants, plasma cells, mediate the humoral immune response, whereas T lymphocytes mediate the cellular immune response. B cells recognize Ag through the B cell receptor (BCR). The BCR is membrane-bound immunoglobulin (Ig), and Igs of the same specificity are secreted as antibody by terminally differentiated B cells, termed plasma cells. Antibodies bind pathogens or their toxic products in the extracellular spaces of the body. The antibody molecule specifically binds Ags from pathogens and marks them for destruction by complement activation or for uptake and destruction by phagocytic cells. Neutralizing antibodies can interfere with the binding of pathogens to receptors and block their uptake into cells, or neutralize bacterial toxins (Mayer and Nyland 2006). T cells recognize specific Ag through the T cell receptor (TCR). The TCR does not bind Ag directly, but instead recognizes short peptide sequences of proteins from pathogens that are bound to major histocompatibility complex (MHC) molecules on the surface of Ag-presenting cells (APCs). This adds an extra dimension to Ag recognition by T cells, termed MHC restriction. In humans, MHC molecules are called human leukocyte Ag (HLA) molecules. They are glycoproteins that show an enormous degree of variation at the population level (Janeway, Travers et al. 2005). Both the BCR and the TCR have common structural features that can accommodate great variability in Ag specificity.

1.1.1 T lymphocytes

T lymphocytes can be divided into subsets according to their phenotype and function. The phenotype of a T cell not only suggests what role it plays in immune responses, but also indicates whether it has come into contact with a foreign or self-derived inciting Ag. A key distinction is based on whether an αβTCR or a γδTCR is expressed. The focus here will be on $CD4^+$ and $CD8^+$ T cells that express αβTCRs. Beyond the primary distinction between $CD4^+$ and $CD8^+$ T cells, which is based on distinct Ag recognition properties, coreceptor usage and function, many other subsets have been demonstrated or proposed. For example, human $CD4^+$ and $CD8^+$ T cells can be divided phenotypically and functionally into naive, memory, effector memory or terminally differentiated effector T cells (Appay, van Lier et al. 2008). This categorization suggests that human T cells progress with division along a linear differentiation pathway. Although this is very likely, it has not yet been proven beyond all doubt. The terminally differentiated phenotype is less prevalent or even absent in $CD4^+$ T cell populations. In general, $CD8^+$ T cells are perceived to act as licensed killers and include cytotoxic $CD8^+$ T cells, NKT cells and anti-viral and immunomodulatory cytokine-producing $CD8^+$ T cells. Another proposed subset describes suppressor $CD8^+$ T cells. $CD4^+$ T cells are generally thought to provide helper functions to B cells and also contain regulatory T cells that play a role in tolerance. Originally, $CD4^+$ T cells were subdivided into two T helper (Th) subsets, Th1 or Th2, depending on the variety of cytokines that they made and their roles in immune responses (Tada, Takemori et al. 1978). Broadly speaking, Th1 cells play a role in the cellular immune response by creating a proinflammatory environment, providing help to macrophages, other APCs and cytotoxic $CD8^+$ T cells. In contrast, Th2 cells play a role in the humoral immune response by providing help to B cells and determining antibody class switching. More recently, new subsets of Th cells have been described, including T follicular helper cells (Chtanova, Tangye et al. 2004), Th17 (Harrington, Mangan et al. 2006), Th22 (Eyerich, Eyerich et al. 2009) and Th9 cells (Veldhoen, Uyttenhove et al. 2008). Another subset in the CD4 lineage comprises regulatory T cells (T_{REG}). Two subtypes of T_{REG} cells have been described, natural T_{REG} that originate in the thymus (Sakaguchi 2004) and peripheral T_{REG} that are induced by conversion of conventional $CD4^+$ T cells in the periphery (Apostolou and von Boehmer 2004).

1.1.2. T cell activation

T cell activation occurs via the CD3-TCR complex (Figure 1). The CD3-TCR complex interacts with peptide antigen presented by MHC. CD4 and CD8 serve as coreceprtors to augment antigen recognition (Janeway 1992; Gao, Rao et al. 2002). During T cell priming, costimulation via further cell surface molecules is usually required. Such costimulatory molecules include CD28, ICOS, CTLA-4, and adhesion molecules (Bridgeman, Sewell et al. 2012). Costimulation serves to tune the response elicited by activation of the CD3-TCR complex. As an example, CD28 co-ligation significantly enhances the response and prolongs or sustains an immune response (Smith-Garvin, Koretzky et al. 2009). CTLA-4 and CD28 share the ligands CD80 and CD86 and can counter each other in the regulation of downstream effects (Smith-Garvin, Koretzky et al. 2009). The activation requirements are different for $CD4^+$ and $CD8^+$ T cells. One important aspect that contributes to this difference is the fact that peptide MHC (pMHC)I-specific TCRs bind with stronger affinities (mean KD = 32 μM) than pMHCII-specific TCRs (mean KD = 92 μM) (Bridgeman, Sewell et al. 2012). Weak or antagonistic TCR ligation results in the rapid phosphorylation of a protein-tyrosine phosphatase, which then dephosphorylates the active site of Lck resulting in cessation of the TCR signal (Stefanova, Hemmer et al. 2003). Therefore, it is not unexpected that to stimulate resting $CD4^+$ T cells, signals must be transmitted through both the TCR and costimulatory receptors (Davis, Boniface et al. 1998). A number of adaptor proteins also play important roles in negatively regulating TCR signals, some of which mediate downregulation of the TCR following stimulation with antigenic peptides (Naramura, Jang et al. 2002). This dampening of TCR activation is important during the resolution of an immune response as well as for the maintenance of self-tolerance.

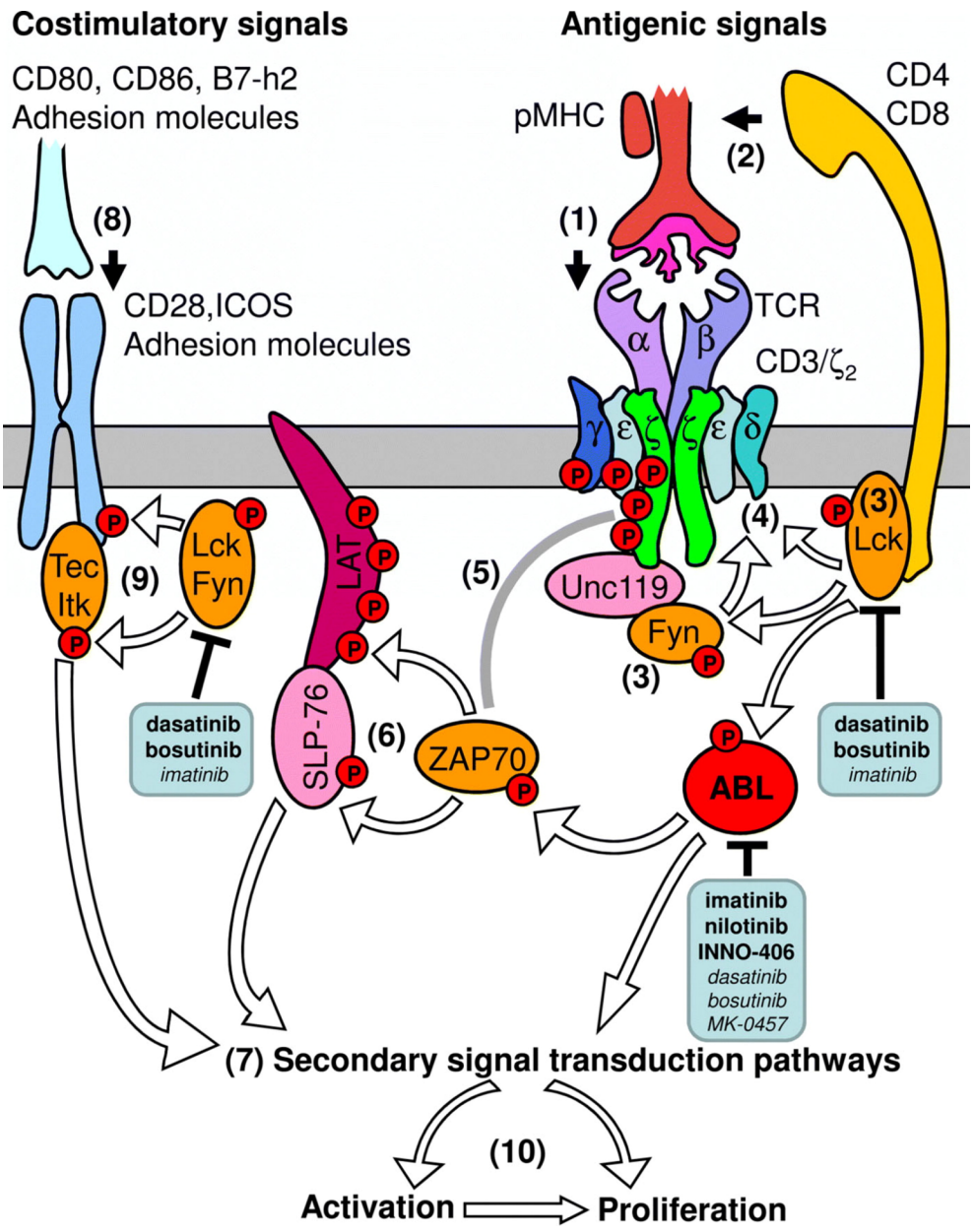

Figure 1. T cell activation via the CD3-TCR complex. Following engagement of the TCR-CD3 Ag receptor with peptide (p)MHC (1) and subsequent recruitment of the CD4/CD8 co-receptor (2), the Src tyrosine kinases Lck and Fyn are activated and recruited to the TCR-CD3 complex (3). Activated kinases then phosphorylate the tyrosine residues within the ITAM motifs of the CD3 complex (4). Phosphorylated ITAM in the CD3 ζ chain recruit ZAP-70 (5), which subsequently phosphorylates LAT and SLP-76 (6). SLP-76 and LAT mediate TCR recruitment of downstream signal transduction components, and thus activation of secondary signal transduction pathways (7). Co-stimulatory signals

mediated by ligation of CD28, ICOS and adhesion molecules with their respective ligands are necessary for complete T cell activation (8). Following ligation, CD28 is tyrosine phosphorylated in a Lck/Fyn-dependent manner, thus allowing members of the Tec family of protein tyrosine kinases (Tec/Itk) to associate with the CD28 cytoplasmic tail. Tec/Itk are in turn activated by Lck/Fyn-dependent tyrosine phosphorylation (9). Co-stimulatory signals integrate with the secondary signals emanating from the TCR-CD3 complex (7), leading to transcriptional activation and T cell proliferation (10). The tyrosine kinase Abl (depicted in red) plays a role in this signalling cascade by phosphorylating ZAP-70 and thus effecting different downstream pathways of the latter. Tyrosine kinase inhibitors (boxed) may interfere with this signalling cascade by blocking specific tyrosine kinases as shown. Primary tyrosine kinase inhibitor actions are shown in bold, with secondary inhibition shown in italics. (Seggewiss, Price et al. 2008)

1.1.3. T cell tolerance

A key feature of the immune system is that it can react to non-self while tolerating self and benign foreign Ags. There are also mechanisms in place that dampen down the immune response when it has been activated by an infectious process. Immune tolerance is facilitated by central and peripheral mechanisms. The thymus is critical for central tolerance. In the thymus, cells that react strongly to self are eliminated by clonal deletion (Hogquist, Baldwin et al. 2005). Peripheral tolerance cannot be linked directly to a lymphoid organ, even though certain organs are enriched for suppressor and regulatory T cells, such as the mucosal surfaces that line the gut and the orifices of the body, which are constantly exposed to non-self Ags from potentially dangerous sources (Lan, Mackay et al. 2007; Hand and Belkaid). Murine $CD8^+$ suppressor T cells were first described in 1978 (Cantor, Hugenberger et al. 1978), following which their existence was doubted (Janeway 1988) and then resurrected (Chess and Jiang 2004; Hu, Ikizawa et al. 2004). Another subset of suppressor T cells that have extensively been studied in the recent years are $CD4^+$ T_{REG} cells (Sakaguchi, Sakaguchi et al. 1995; Sakaguchi 2004; Sakaguchi, Wing et al. 2009). In both mice and humans, T_{REG} cells are characterized by high

expression of CD25, the IL-2 receptor α chain, low expression of CD127, the IL-7 receptor α chain, and high intracellular expression of the forkhead box transcription factor FoxP3. Additional markers can be used for the identification of T_{REG} cells, but the three listed are the most commonly used. So-called natural T_{REG} cells originate in the thymus and are believed to have a relatively high avidity for Ag, yet still survive the deletion process. Peripheral T_{REG} cells may be induced from conventional T cells (Apostolou and von Boehmer 2004). However, this was demonstrated using TCR transgenic (tg) mice on a $RAG^{-/-}$ background, which lack naturally occurring T_{REG} cells (Curotto de Lafaille and Lafaille 2009). In tumours, peripheral T_{REG} cells do not share the same repertoire as non-T_{REG} $CD4^+$ T cells (Hindley, Ferreira et al.), which argues against peripheral conversion of non-T_{REG} $CD4^+$ T cells to T_{REG} cells. After stimulation with antigen *in vitro*, some $FoxP3^+$ and $FoxP3^-$ proliferating $CD4^+$ T cells share the same dominant clonotypes, which suggests that individual T cell clonotypes may diversify into $FoxP3^+$ and $FoxP3^-$ populations during Ag-driven immune responses. However, some dominant clonotypes appeared to be exclusive to $FoxP3^+$ proliferating $CD4^+$ T cells, suggesting that these cells expanded from pre-existing $FoxP3^+$ $CD4^+$ T cells (Melenhorst, Scheinberg et al. 2008). The latter cells may be naturally occurring T_{REG} cells rather than T_{REG} cells generated by conversion.

1.1.4. T_{REG}-mediated suppression

Very early on in the study of T_{REG} cells, an *in vitro* assay was established to measure their suppressive activity (Takahashi, Kuniyasu et al. 1998; Thornton and Shevach 1998). This assay measures the extent to which T_{REG} cells suppress proliferation of co-cultured $CD4^+$ or $CD8^+$ T cells in the presence of specific Ag or agents that stimulate a polyclonal T cell response, such as cross-linking anti-CD3 monoclonal antibody. It has also been shown *in vivo* in mice that T_{REG} cells control: (i) peripheral $CD4^+$ T cell numbers (Almeida, Legrand et al. 2002); (ii) homeostatic proliferation of peripheral $CD4^+$ T cells (Shen, Ding et al. 2005); and, (iii) the size of the peripheral activated/memory T cell compartment (Annacker, Burlen-Defranoux et al. 2000). Their suppressive effect on activated T cells *in vitro* is dependent on cell-to-cell contact (Nakamura, Kitani et al. 2001). T_{REG} cells may kill activated T cells by

a granzyme- or perforin-dependent mechanism (Gondek, Lu et al. 2005; Cao, Cai et al. 2007). Alternatively, they can deliver a negative signal to activated T cells by: (i) upregulating intracellular cyclic AMP, which inhibits T cell proliferation and IL-2 formation (Bopp, Becker et al. 2007); (ii) generating adenosine catalyzed by CD39 and CD73 expressed on their surface (Deaglio, Dwyer et al. 2007); or (iii) interacting with B7 (CD80 and CD86) expressed by activated T cells (Paust, Lu et al. 2004). T_{REG} cells may also have an effect on the function of APCs, which in their presence may down-regulate or fail to up-regulate the expression of CD80 and CD86, molecules that are important for proper T cell activation (Oderup, Cederbom et al. 2006), or express the enzyme indoleamine 2,3-dioxygenase (IDO), which modulates tryptophan catabolism and creates the cell-toxic metabolite kynurenine (Grohmann, Orabona et al. 2002). Lymphocyte activation gene 3 (LAG-3), a CD4-related molecule that binds MHC class II, is also expressed by T_{REG} cells and is important for their suppressive activity (Huang, Workman et al. 2004). In addition, T_{REG} cells can kill B cells, which also function as APCs (Zhao, Thornton et al. 2006). Under certain circumstances, soluble factors such as IL-10 or transforming growth factor (TGF)β also play a role as mediators of suppression (Asseman, Mauze et al. 1999; Read, Malmstrom et al. 2000; Suri-Payer and Cantor 2001), especially *in vivo*; however, neutralization of either of these factors does not prevent suppression *in vitro* (Takahashi, Kuniyasu et al. 1998; Thornton and Shevach 1998). IL-10-producing regulatory T cells have been termed Tr1 cells (Asseman and Powrie 1998) and TGFβ-producing regulatory cells have been called Th3 cells (Fukaura, Kent et al. 1996). Although controversial, TGFβ can also act in membrane-bound form (Nakamura, Kitani et al. 2001). TGFβ may contribute to the differentiation of naïve / conventional $CD4^+$ T cells into T_{REG} cells or T_{REG} cell-like cells, which has also been termed “infectious tolerance” (Yamagiwa, Gray et al. 2001; Jonuleit, Schmitt et al. 2002; Chen, Jin et al. 2003; Fahlen, Read et al. 2005; Marie, Letterio et al. 2005; Andersson, Tran et al. 2008). In the latter case, TGFβ can be provided by a non-T_{REG} cell source (Fahlen, Read et al. 2005). Other factors that play a role in the suppressive activity of T_{REG} cells include IL-35 (Collison, Workman et al. 2007), galectin-1 (Garin, Chu et al. 2007), heme oxygenase-1 and carbon monoxide (Lee, Gao et al. 2007). T_{REG} cells can also suppress via IL-2 consumption / cytokine-deprivation-induced apoptosis of effector $CD4^+$ T cells

(Pandiyan, Zheng et al. 2007). This mechanism seems to operate before any effect on activation or proliferation takes place.

1.1.5. *In vivo* T cell turnover and ways of studying it

T cell turnover refers to the rates of T cell proliferation and cell death. Theoretically, T cell turnover can be studied *ex vivo* by staining of T cells with markers of proliferation, apoptosis and cell death. However, *ex vivo* staining will only give a snapshot of T cell proliferation, apoptosis and cell death at one specific moment in time. In other words, one will only be able to determine an on or off signal that will not reveal anything about the lifespan or the rates of proliferation and death of the cell population of interest. *In vivo* labelling can be carried out to gain more accurate estimates of T cell lifespan, rates of proliferation and cell death. In humans, *in vivo* labelling can be conducted with non-toxic stable isotopes such as deuterium (Hellerstein and Neese 1992; Neese, Misell et al. 2002), to determine T cell lifespan, proliferation and death rates of cells. Deuterated water (^2H_2O) or deuterated (^2H-)glucose is administered orally or intravenously (i.v.) for different lengths of time depending on the question asked, then the cells of interest are isolated / sorted, the deoxyribonucleic acid (DNA) is extracted and derivatized, and label enrichment is measured by gas chromatography/mass spectrometry. Two recently published articles by Busch *et al.* (Busch, Neese et al. 2007) and Macallan *et al.* (Macallan, Asquith et al. 2009) outline the background of the methodology and provide detailed protocols for *in vivo* labelling with ^2H_2O or ^2H-glucose. In addition, a very comprehensive and detailed review about the different mathematical models used for the interpretation of *in vivo* labelling data, including bromodeoxyuridine (BrdU) labelling data, was recently published by Borghans *et al.* (Borghans and de Boer 2007). In contrast to BrdU and tritiated[^3H]-thymidine, ^2H_2O or ^2H-glucose label DNA through the *de novo* nucleoside synthesis pathway (Hellerstein 1999).

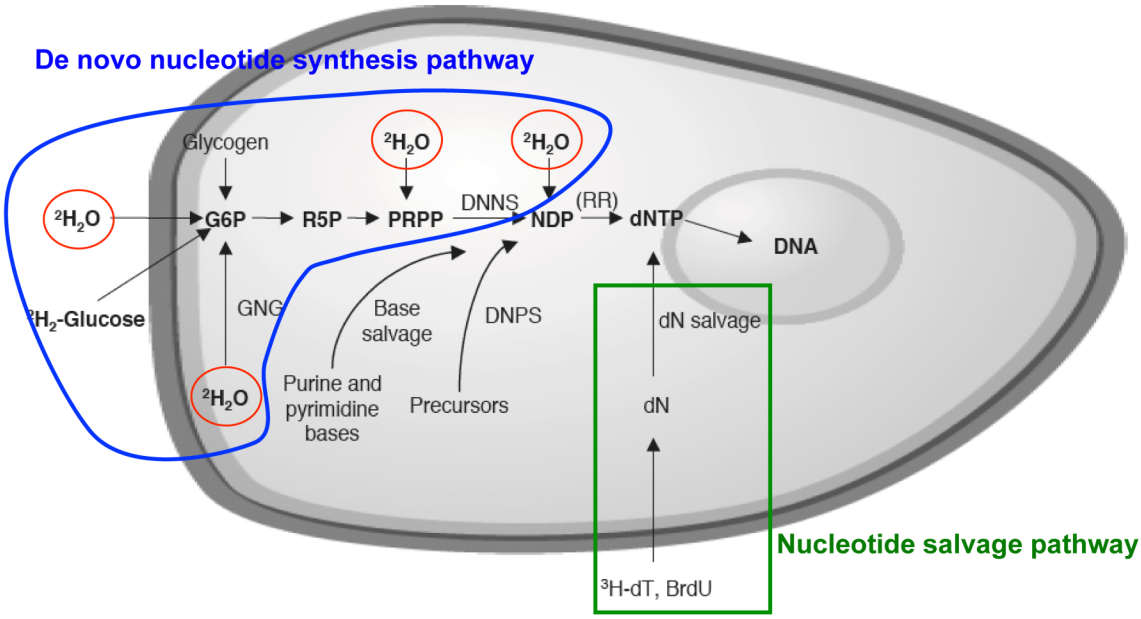

Figure 2. Labelling pathways for measuring DNA synthesis and cell proliferation. GNG, gluconeogenesis/glycolysis; RR, ribonucleotide reductase; DNPS, *de novo* purine/pyrimidine synthesis pathway; DNNS, *de novo* nucleotide synthesis pathway. Modified from Neese et al. and Turner et al. (Neese, Misell et al. 2002; Turner 2006).

This type of labelling allows the true quantification of DNA replication (Hellerstein and Neese 1992; Macallan, Fullerton et al. 1998) and is safe for use in humans (Hellerstein 1999). During DNA synthesis, deuterium is incorporated into both pyrimidines and purines, but purines are evaluated for label enrichment. The reason for this is that the efficiency of the *de novo* contribution to purine nucleosides is predictable and high in dividing cells (Macallan, Fullerton et al. 1998). Also, as shown in Fig. 2, the *de novo* pathway is relatively unaffected by extracellular nucleoside concentrations (Cohen, Barankiewicz et al. 1983; Reichard 1988; Macallan, Fullerton et al. 1998). Furthermore, stable isotope labelling is not influenced by post-labelling expansion. The reason for this is that after stable isotope labelling has been discontinued, labelled DNA strands will remain in the population, distributed among progeny. This is in contrast to what happens after BrDU labelling has been discontinued, as label in this case is diluted out and will not be detectable after approximately the third division. The latter two aspects, as well as the high toxicity of BrdU (Nakaguchi, Usui et al. 1971; Matsuoka, Nomura et al.

1990; Chaube and Murphy 1995), make deuterium labelling the favourable technique for studying cellular turnover. BrdU toxicities include both cytotoxic effects that can lead to skin lesions, anaemia, leukocytopenia, thrombocytopenia and inhibition of cell growth (the effect that I want to measure), as well teratogenic and mutagenic effects. The human body naturally contains deuterium and this is harmless. However, if a large fraction of body water (> 50%) were replaced with heavy water, then this would lead to cell dysfunction and death. When heavy water is used in labelling studies, the aim is to reach 1% deuterium enrichment of body water above background enrichment, which is safe. The only described side effect is tinnitus. After deuterium labelling, the labelled DNA strands remain in the population when cells divide, but they are distributed among the progeny cells. This means that each originally labelled parental DNA strand is counted as one strand, no matter whether it is found in only one cell or distributed among many daughter cells of the initially labelled cell. If cells change phenotype with cell division, labelled DNA strands will be found in other phenotypic compartments. A relative increase in label enrichment can therefore be found in a more differentiated phenotype, but this has to be paralleled by loss of label in a precursor of this more differentiated phenotype. The only way that label is truly lost from the studied cellular compartment is by permanent removal of labelled cells from the pool, which will be due to cell death unless the cells migrate to a tissue compartment that is not evaluated. Currently, *in vivo* labelling with stable isotopes is the best way to assess *in vivo* T cell proliferation and death rates in humans. BrDU labelling is not recommended for use in humans because of its toxicity and has several disadvantages over the deuterium labelling approach as mentioned above, although it can be used in animal models with the advantage that one can measure it directly *ex vivo* by flow cytometry.

1.1.6. CD57 expression & cellular senescence

Three cardinal features of cellular senescence (Latin: senescere meaning “to grow old“) have been described: (i) after repeated divisions, the proliferative capacity of a cell starts to dwindle and, eventually, ceases, for example due to shortening of telomerase if telomerase activity is not increased;

(ii) senescent cells develop resistance to apoptosis; and, (iii) senescent cells undergo multiple phenotypic and functional changes (Campisi 1996). CD57 expression has been proposed as a key marker of $CD8^+$ T cell senescence (Brenchley, Karandikar et al. 2003). However, recent studies have shown that most $CD57^+$ T cells do not express Programmed Death 1 (PD-1) (Petrovas, Chaon et al. 2009), a marker expressed by exhausted T cells (Day, Kaufmann et al. 2006; Freeman, Wherry et al. 2006; Petrovas, Casazza et al. 2006; Trautmann, Janbazian et al. 2006). T cell exhaustion is a state of T cell dysfunction that arises during chronic infection and cancer, defined by poor effector function, sustained expression of inhibitory receptors and a transcriptional state distinct from that of effector or memory T cells (Wherry, 2011). In addition, most $CD8^+CD57^+$ cells exhibit a highly differentiated $CD45RA^+CD28^-CCR7^-$ effector memory (T_{EMRA}) phenotype, and T_{EMRA} cells appear to have a long lifespan *in vivo* (Ladell, Hellerstein et al. 2008). Functionally, $CD57^+$ memory $CD8^+$ T cells exert protective effects associated with the progressive acquisition of cytolytic activity (Kern, Khatamzas et al. 1999; van Leeuwen, Gamadia et al. 2002; Le Priol, Puthier et al. 2006; Takata and Takiguchi 2006; Chong, Aicheler et al. 2008; Chattopadhyay, Betts et al. 2009). Furthermore, it has been reported that $CD57^+$ $CD8^{high}$ T cells are enriched for Ag-specific cells that exert a regulatory function, in that they are capable of down-modulating cytolytic activity (Mollet, Sadat-Sowti et al. 1998). T_{EMRA} cells, which incorporate the largest fraction of $CD57^+$ memory $CD8^+$ T cells, have also been associated with immune senescence (Nociari, Telford et al. 1999), but again this is controversial because many Ag-specific cells with anti-viral activity reside within this phenotypic compartment (Appay, van Lier et al. 2008). Furthermore, a larger proportion and absolute number of human immunodeficiency virus (HIV)-specific T_{EMRA} cells in early HIV infection has been linked to the control of HIV viremia and subsequent viral load set point, which predicts the rate of disease progression (Northfield, Loo et al. 2007). Such cells are also more frequently detectable in controlled compared to progressive HIV infection (Addo, Draenert et al. 2007). *Ex vivo*, using non-specific stimuli, $CD57^+$ memory $CD8^+$ T cells proliferate poorly, if at all, compared to other memory T cell subsets (Brenchley, Karandikar et al. 2003). However, it is not known whether these cells proliferate *in vivo*; a certain microenvironment or specific stimulus such as cognate Ag may be required for such proliferation to occur.

1.1.7. Detection of Ag-specific T cells

Ag-specific cells can be detected after *in vitro* stimulation with Ag by measuring functional response, such as cytokine secretion or production, cytotoxicity and proliferation (Klenerman, Cerundolo et al. 2002). Ag-specific cells can also be detected physically using soluble recombinant peptide-major histocompatibility complex (pMHC) (Garboczi, Hung et al. 1992) multimers (Altman, Moss et al. 1996), such as tetramers, pentamers, octamers or dextramers, attached to fluorochromes (Casalegno-Garduno, Schmitt et al.). This technology is based on the fact that $CD4^+$ T cells recognize peptide Ag in the context of MHC/HLA class II and $CD8^+$ T cells recognize peptide Ag in the context of MHC/HLA class I. Ags that are presented on APC are fragments of proteins, peptides that are generated by proteolysis. These peptides are loaded onto the MHC/HLA and the pMHC/pHLA complex is expressed on the cell surface of APCs. MHC class I molecules present degradation products derived from intracellular (endogenous) proteins in the cytosol. MHC class II molecules present fragments derived from extracellular (exogenous) proteins that are located in an intracellular compartment. The specificity of T cells is determined by the clonotypically expressed TCR, which binds cognate pMHC primarily via six highly variable complementarity-determining regions (CDRs) (Wooldridge, Lissina et al. 2009). The TCR/pMHC interaction is very weak (KD = 0.1 to > 500 μM (Bridgeman, Sewell et al. 2012), which is why multimeric forms of soluble pMHC molecules are required to visualize T cells that bear cognate Ag-specific TCRs. Schematic representations of monomeric and tetrameric pMHC complexes are shown in Fig. 3.

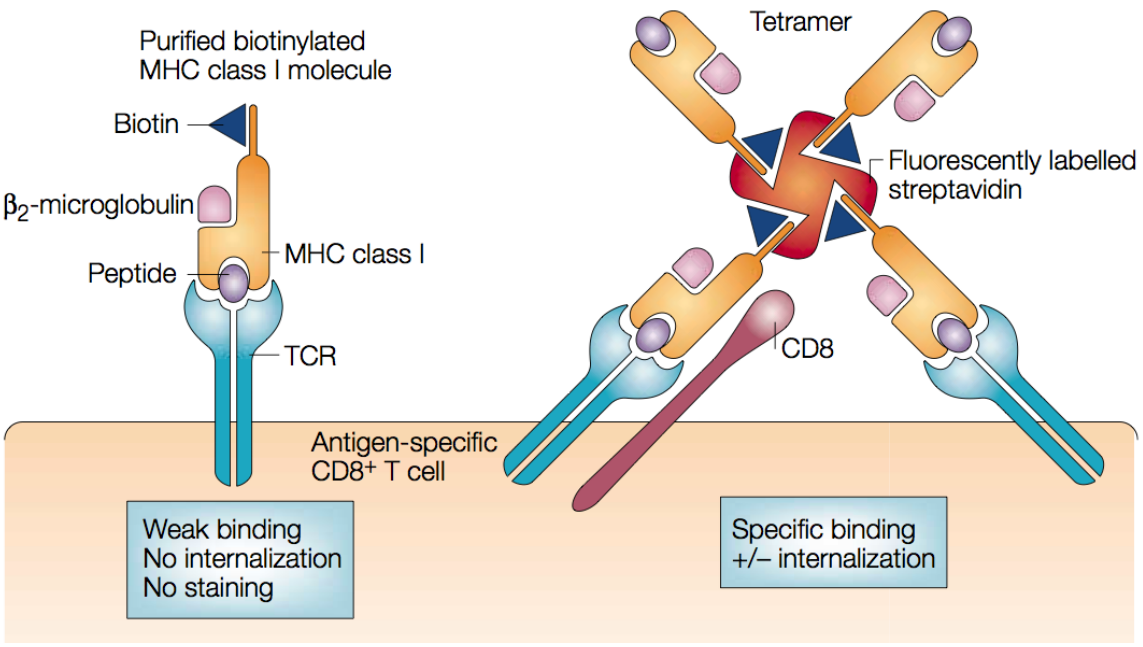

Figure 3. Schematics of a monomeric and tetrameric pMHC (Klenerman, Cerundolo et al. 2002).

1.2. TCR tg mice

TCR tg mice bear genes for TCRs of defined specificity (Scott, Bluthmann et al. 1989). They have been used to study T cell development, mechanisms of T cell tolerance and to establish basic principles of T cell biology (von Boehmer, Teh et al. 1989; von Boehmer and Kisielow 1990; Robey, Fowlkes et al. 1991; Teh, Garvin et al. 1991; Wells, Gahm et al. 1991; Miller 1992; Hogquist, Baldwin et al. 2005; Shen, Ding et al. 2005). Such mice have been extensively used to study central and peripheral T cell tolerance. In 1994, it was found that after *in vivo* peptide stimulation, TCR tg T cells respond differently *in vitro* to peptide stimulation compared to T cells from normal mice. This observation lead to the proposal that high Ag-specific precursor frequencies were non-physiological and that it would be better to transfer smaller numbers of TCR tg T cells into syngeneic (closely related, immunologically compatible) recipient or "host" mice (Kearney, Pape et al. 1994). As shown in Fig. 4B, T cells from non-immunized TCR tg mice proliferated vigorously in response to the cognate ovalbumin (OVA) 323–339 peptide *in vitro*, in contrast to T cells from non-immunized BALB/c mice (Fig. 4A). Kearney *et al.* also reported that draining lymph node T cells from "intact" TCR tg mice

showed no evidence of enhanced responsiveness following subcutaneous (s.c.) injection of ovalbumin 323–339 in complete Freund's adjuvant (CFA) and it was stated that they were tolerized much less efficiently compared to the corresponding T cells from normal mice when injected intraperitoneally (i.p.) with ovalbumin 323–339 in incomplete Freund's adjuvant (IFA) followed one week later by s.c. injection with ovalbumin 323–339 in CFA (compare Figures 4A and 4B).

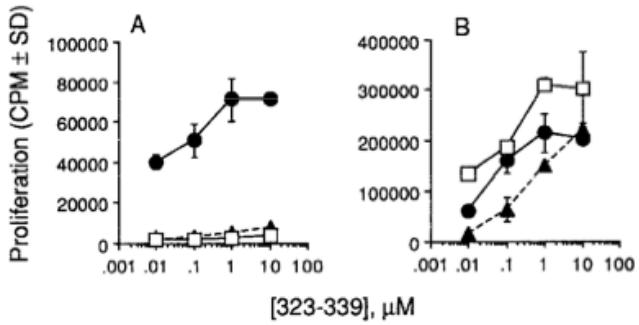

Figure 4. TCR tg mice respond differently to peptide injection compared to normal mice. Intraperetoneal injection of peptide in IFA induces T cell tolerance. Normal BALB/c mice (A) or TCR tg mice (B) were not injected (open squares); were injected s.c. with ovalbumin peptide in CFA (125 pg in [A], 200 ng in [B]) (closed circles); or were injected i.p. with ovalbumin peptide in IFA (300 ng), and then eight days later with ovalbumin peptide s.c. in CFA (125 ng in [A], 200 ng in [B]) (closed triangles: dashed lines). Seven days after the s.c. injection, brachial, axillary, and inguinal lymph node cells (4 x 10^5 in [A] and 5 x 10^4 in [B]) were cultured with irradiated (3,000 rads) BALB/c splenocytes and the indicated peptide concentrations for 4 (A) or 3 (B) days. T cell proliferative responses were measured by [^{3}H]thymidine incorporation. Results represent the mean cpm values + standard deviation (SD) of duplicate or triplicate determinations derived from single experiments. Similar results were obtained in at least two other independent experiments performed using normal BALB/c mice. [^{3}H]thymidine incorporation in the absence of ovalbumin 323–339 was generally less than 2,000 cpm and never greater than 6,000 cpm. (Kearney, Pape et al. 1994) This figure is of low resolution as only the pdf of this publication was available and it was taken from this pdf.

However, Martin and Bevan (Martin and Bevan 1997) have shown that adoptive transfer of small

numbers of mature TCR tg T cells into non-transgenic recipient mice followed by injection with cognate antigen led to the death of endogenous thymocytes that were not specific for that Ag. Therefore, many investigators have favoured the use of TCR tg mice that co-express the cognate Ag as an endogenous self-Ag for the modelling of negative selection of thymocytes by clonal deletion (Hogquist, Baldwin et al. 2005). The H-Y model is a classic example (Kisielow, Bluthmann et al. 1988). In this model, the TCR transgenic cells express a TCR that is specific for the male Ag H-Y. In female mice, these cells are positively selected in the thymus, whereas they are deleted in male mice. One major caveat to the use of TCR transgenic mice for the study of thymic selection is that deletion of TCR transgenic cells occurs early, at the double negative to double positive stage, in some TCR transgenic mouse strains (cortical deletion) and late, at the single positive stage, in others (medullary deletion) (Hogquist, Baldwin et al. 2005). One of the factors that determines when clonal deletion occurs is Ag location; late deletion is observed if Ag is present only in the medulla and early deletion is observed if Ag is also present or just present in the cortex (Hogquist, Baldwin et al. 2005). However, other factors, such as the affinity of the TCR for its cognate ligand (Sant'Angelo and Janeway 2002), also influence the timing of deletion. Thus, even when Ag is broadly expressed throughout the thymus, deletion happens early in some TCR transgenic mouse strains and late in others (Hogquist, Baldwin et al. 2005). Recently, a more physiological mouse model was developed to test whether early deletion occurs in normal mice. In this model, deletion was clearly induced late, at the single positive stage (Baldwin, Sandau et al. 2005). Doubts were raised, however, due to the fact that the temporal separation of *TCRA* and *TCRB* (α-chain and β-chain encoding genes, respectively) rearrangement dictates that Ag receptors are not formed until the double positive stage of thymocyte development (Hogquist, Baldwin et al. 2005). Data from other studies, including a landmark paper from the Kappler & Marrack group, also indicate that early deletion is a non-physiological aspect of TCR transgenic mice (Kappler, Roehm et al. 1987; Surh and Sprent 1994; Cho, Edmondson et al. 2003; Zhan, Purton et al. 2003). Recently, various TCR transgenic mouse strains have also been used to study mechanisms of peripheral T cell tolerance, including regulation by T_{REG} cells (Apostolou and von Boehmer 2004; Shen, Ding et al. 2005; Killebrew, Perdue et al. 2011).

1.3. Specific Aims

In this thesis, antigen-specific T cell responses were investigated under conditions of chronic antigenic stimulation to inform our understanding of this process.

- To examine the *in vivo* turnover (rates of proliferation and cell death) of antigen-specific and phenotypically defined T cell populations during chronic antigenic stimulation in TCR tg mice stimulated continuously with antigen in the presence or absence of adjuvant.

- To examine the *in vivo* turnover of phenotypically defined $CD8^+$ T cell populations in HIV-infected humans.

- To examine memory $CD8^+$ T cell expansions in MCMV infected mice and patients with dasatinib induced large granular lymphocyte (LGL) expansions.

CHAPTER

2

Materials & Methods

2.1 *Mice & ethics.* Data shown in **chapter 3** were from male and female OVA TCR tg mice (DO11.10) (Murphy, Heimberger et al. 1990), 6-12 weeks of age at the beginning of each experiment, purchased from The Jackson Laboratory (Bar Harbor, ME, USA) and held in the mouse facility at the University of California San Francisco (UCSF). Because these mice were not bred on a $RAG^{-/-}$ background, they have a variable fraction (2% - 32%) of non-OVA-specific $CD4^+$ T cells dependent on age and location, with lower fractions in younger mice than in older mice and lower fractions in peripheral lymph nodes (5% - 10% of $CD4^+$ T cells) than in the spleen (7% - 15% of $CD4^+$ T cells). Experiments with these mice were conducted in San Francisco, California, USA. Most of the data shown are from a large experiment carried out during a collaborative visit to San Francisco in 2010. All procedures involving these mice were approved by the University of California at San Francisco (UCSF) Institutional Animal Care and Use Committee.

For data shown in **chapter 5**, $IL\text{-}10^{-/-}$ mice were purchased from Jackson Laboratory and bred at Cardiff University School of Medicine, Cardiff, UK; wild-type C57BL/6 mice were purchased from Harlan UK. All experiments were conducted according to UK Home Office guidelines. Specifically, these experiments were performed under a Home Office project license granted to Ian Humphreys (these experiments were done in collaboration with him and his laboratory) in the Home Office-designated facility at Heath Park, Cardiff University.

2.2 *Procedures carried out on mice, infections of mice and treatments.* DO11.10 TCR tg mice were studied longitudinally for up to 7 weeks. Blood was acquired at varying time points by phlebotomy of the saphenous vein. Surgery was performed under general anesthesia, using ketamine/xylazine (Wyeth, Madison, NJ, USA and Lloyd Labs Inc., Iowa, USA). Mice were given buprenorphine (Reckitt

& Colman Pharmaceuticals Inc. Richmond, VA, USA) for pain relief after surgery. Alzet® mini-osmotic pumps (Durect Corporation, Cupertino, CA, USA) containing either the cognate $OVA_{323-339}$ peptide (ISQAVHAAHAEINEAGR, Biopeptide, CA, USA; OVAp) in phosphate buffered saline (PBS; Life Technologies, Carlsbad, CA, USA) or OVAp together with murine recombinant IL-1β (PeproTech Inc., NJ, USA) in PBS or sterile PBS alone (referred to below as "unstimulated DO11.10 mice") were placed s.c. between the scapulae of DO11.10 mice. Both 14-day (Model 1002) and 28-day (Model 2004) pumps were used, each releasing 0.2-0.25 μl/hour of PBS or a solution containing 0.25 - 1.25 μg/μl OVAp in PBS (for all data shown, the concentration of OVAp was 1.25 μg/μl and the total amount of peptide released per day was 6.6-7 μg) or 1.25 μg/μl OVAp in PBS together with IL-1β (10 μg of IL-1β / pump model 1002 and 20 μg of IL-1β / pump model 2004; both pump models released approx. 0.6 μg IL-1β / day). Pumps were equilibrated in sterile PBS according to the manufacturer's instructions for up to 48 hours (the duration of equilibration depended on the pump model) prior to implantation. For cross-sectional analyses of lymphoid tissue, mice were sacrificed by CO_2 asphyxiation followed by cervical dislocation. Thymus (THY), spleen (SPL), and inguinal, brachial and axillary lymph nodes (LNs) were harvested and passed through mesh filters in sterile PBS with 2% fetal bovine serum (FBS) to obtain a single cell suspension. The absolute number of cells per organ was determined using a Coulter Counter (Beckman Coulter, Fullerton, CA, USA).

MCMV Smith strain (American Type Culture Collection, ATCC) was prepared in BALB/c salivary glands and titered on 3T3 cells as described previously (Banks, Rickert et al. 2005). Mice were infected i.p. with 5×10^4 PFU MCMV. In some experiments, wild-type mice were injected on the days stated in the figure legends with 250 μg of either rat IgG (Chemicon International, Temecula, Ca, USA) or αIL-10Rα (clone 1B1.3A, BioXCell, West Lebanon, NH, USA).

2.3 *Human subjects.* Subjects from whom data in **chapter 4** were generated were recruited by advertisement. Written informed consent was obtained from all subjects. Ethical approval was either obtained by the University of California at San Francisco Committee on Human Research, San

Francisco, USA or at St. George's Hospital in London, UK. $^{2}H_2O$ enrichment data referred to in this thesis are from one HIV-negative and four antiretroviral-untreated HIV-infected subjects. ^{2}H-glucose enrichment data shown in this thesis are from two healthy subjects. Some characteristics of the study subjects are shown in Table 2. Except for one subject, all of the labelled HIV-infected subjects were naïve to antiretroviral treatment. Additional immunophenotyping was carried out on these subjects. Subjects were excluded if, at any time within the three month period before enrolment, they had either used a medication (such as glucocorticoids or other immunosuppressive drugs) or been diagnosed with a disease (such as lymphoproliferative diseases or cancer) that might affect T cell turnover. All the labelled subjects came in for a screening visit, at which time they had to fill out a questionnaire and blood was drawn to determine their eligibility to participate in the study. Changes in the relative proportion of $CD8^+$ T cell subpopulations were discerned by obtaining a complete blood count and a T cell phenotyping flow cytometric panel at each sort date. Both $CD8^+$ T cell counts and the relative composition of $CD8^+$ T cell subpopulations were found to be stable for individual subjects during the time period of study.

For the data shown in **chapter 6**, frozen peripheral blood mononuclear cells (PBMCs), bone marrow mononuclear cells (BMMCs), and plasma from CML or Ph^+ ALL patients on dasatinib therapy were analyzed, together with PBMC and plasma samples from healthy controls (Table 3 in **chapter 6**) (Mustjoki, Ekblom et al. 2009; Kreutzman, Juvonen et al. 2010). Measurements of plasma CMV DNA viral load were performed on the basis of clinical indications using a quantitative polymerase chain reaction (qPCR) assay with a detection limit of 250 copies/ml plasma. Dasatinib patients were grouped according to the presence or absence of LGL expansions, defined as an increased absolute lymphocyte count $>3.6x10^9$/l with morphological characteristics of LGLs. Written informed consent was obtained from all patients and healthy controls. The study was conducted in accordance with the principles of the Helsinki declaration and was approved by the Helsinki University Central Hospital Ethics Committee.

2.4 *Assessment of in vivo T cell turnover*. To measure the proliferation and death rates of OVAp-stimulated T cells *in vivo* (data shown in **chapter 3**), OVAp was administered s.c. with or without IL-1β to DO11.10 TCR tg mice. Control mice received PBS. All DO11.10 mice received a loading dose of ^2H_2O (Cambridge Isotope Laboratories Inc., Andover, MA, USA) i.p. to reach 5% body water enrichment (the amount injected was calculated for each individual mouse using the body weight and assuming that body water is 70% of body weight) immediately after pump implantation followed by 8% ^2H_2O orally (ad libitum; to reach 5% body water enrichment) for a total of 3 days. At days 3, 6, 12 and 20 after pump implantation, three mice per group from each of the three groups were sacrificed. Lymph nodes and spleens were collected and single cell suspensions were prepared. Cells were then counted and stained with fluorescently-labelled antibodies (please see section entitled "Flow cytometry and intracellular cytokine staining" below). Naive (T_N: $CD62L^{high}$ $CD44^{low}$) and memory (T_M: $CD62L^{low}CD44^{high}$) OVA-specific $CD4^+$ T cells were sort-purified so that ^2H-labelling in DNA could then be measured by mass spectrometry.

In an independent experiment, s.c. OVAp-stimulated or unstimulated (PBS) DO11.10 mice received a special mouse diet (PMI Nutrition International LLC, St Louis, MO, USA) containing 20% [6,6-$^2H_2$]glucose (Cambridge Isotope Laboratories Inc., Andover, MA, USA) for the 3 days immediately following pump implantation. Mice in the OVAp-stimulated and -unstimulated groups consumed similar amounts of the diet and had similar body weights (range 16.5 – 19.6 grams, Table 1). The 3-day administration protocol of [6,6-$^2H_2$]glucose was designed to pulse-label C-H bonds in the deoxyribose moiety of replicating DNA in dividing cells, as described previously (Macallan, Fullerton et al. 1998) and shown schematically in the Introduction (Fig. 2). Blood glucose enrichments fall rapidly after dietary [6,6-$^2H_2$]glucose label is removed (data not shown) and re-utilization of labelled ^2H-deoxyribose for new DNA synthesis in purine deoxyribonucleotides is minimal (Macallan, Fullerton et al. 1998; McCune, Hanley et al. 2000). Accordingly, this labelling protocol results in a pulse-chase incorporation of label into replicating DNA *in vivo* and allows accurate measurement of the lifespan of labelled cells. At days 3, 7, 12, 15, and 20 after pump implantation, three mice per group from each of the three groups were sacrificed. Naïve (T_N: $CD62L^{high}$ $CD44^{low}$) and memory (T_M: $CD62L^{low}CD44^{high}$) OVA-

specific $CD4^+$ T cells from spleens and individually pooled peripheral lymph nodes were sort-purified so that ^2H-labelling in DNA could then be measured by mass spectrometry.

2.5 *Labelling protocol for human subjects.* All subjects enrolled for labelling (data shown in **chapter 4**) were seen either at the Clinical and Translational Science Institute Clinical Research Center (CCRC) at San Francisco General Hospital, San Francisco, California, USA, or at St. George's Hospital, London, UK. After enrolment, subjects were provided with a sufficient number of 50 ml vials of 70% ^2H_2O (Cambridge Isotope Laboratories Inc., Andover, MA, USA) for a seven-week labelling protocol. Subjects drank three 50 ml vials of 70% ^2H_2O per day for the first week of labelling followed by two 50 ml vials of 70% ^2H_2O per day for the next six weeks. The first blood draw for cell sorting was obtained during the last week of ^2H_2O labelling and further blood draws were obtained at week 10 after the start of labelling, week 14 and week 18. Short-term ^2H-glucose labelling was carried out at St. George's Hospital, London, UK. B cells were positively selected by magnetic cell sorting in London and the leftover CD19-negative fraction was frozen and stored in 90% PBS containing 10% dimethyl sulfoxide (DMSO) before being shipped to Cardiff for sorting of $CD57^+$ and CD57-negative memory phenotype $CD8^+$ T cells by flow cytometry. Blood samples for sorting were collected on days 4, 10, and 21 after deuterated glucose labelling.

2.6 *Flow cytometry and intracellular cytokine staining.* For data shown in **chapter 3**, cells from heparinized blood, lymph nodes, spleen, and thymus were stained for fluorescence activated cell sorting (FACS) analyses using combinations of the following antibodies: αCD4-Alexa700 (clone L3T4), αCD4-allophycocyanin-Cy7 (clone L3T4), αCD25-PE (IL-2R alpha chain, p55; clone 7D4), αCD25-allophycocyanin-Cy7 (IL-2R alpha chain, p55; clone PC61), αCD38-PE (clone 90), αAnnexin V-FITC, αKi67-FITC (clone B56), and mouse BD FcBlock™ (purified rat-anti-mouse CD16/CD32) (all of the above from BD Pharmingen, San Jose, CA, USA), αCD8-Pacific Blue (clone 5H10) and α-mouse DO11.10 TCR-allophycocyanin (clone KJ1-26) (both from Caltag Laboratories, Burlingame, CA, USA),

αFoxP3-PE (clone FJK-16s), αCD62L-PE-Cy7 (clone MEL-14) and αCD44-PE-Cy5.5 (clone IM7) (all of the above from eBioscience, San Diego, CA, USA). The Live/DEAD® fixable Aqua Dead Cell Stain Kit for 405 nm excitation (Life Technologies) was used in conjunction with Annexin V to discriminate between live, apoptotic, and dead cells, and also in multi-colour flow cytometric panels for exclusion of dead cells. TruCount tubes (BD Biosciences, San Jose, CA, USA) were used with slight modifications to the manufacturer's instructions to measure absolute peripheral blood T cell numbers. The modifications were necessary as more antibody conjugates than described in the manufacturer's instructions were used for staining the whole blood in TruCount tubes. Cells for sorting were not fixed. Otherwise, cells were fixed after staining with either BD Lysing solution for TruCount analysis or with PBS containing 2% FBS and 1% paraformaldehyde after either surface staining alone or surface and intracellular staining. For intracellular staining, cells were permeabilized with BD^{TM} Phosflow Perm/Wash buffer 1 (BD Biosciences), a buffer containing saponin that does not fix the cells. Using this buffer, the incubation time for the intracellular FoxP3 staining could be reduced to 1 hour instead of overnight. Events for data shown in **chapter 3** were analyzed and/or sort-purified using a BD FACS LSR II, a Digital Vantage, or a custom-built BD FACSAria (BD Biosciences). Data were analyzed with FlowJo software (Tree Star Inc., Ashland, OR, USA).

For data shown in **chapter 4**, fresh human PBMCs (on average, 1 x 10^8 and 1.7 x 10^8 PBMCs from 80 ml of blood from HIV-negative and HIV-infected subjects, respectively) were obtained by density gradient centrifugation using Ficoll-Hypaque (Sigma-Aldrich, St. Louis, MO, USA). The frozen CD19-negative cells (the leftover fraction after magnetic bead positive selection of CD19$^+$ cells) from London were defrosted in Cardiff prior to staining. Cells were stained with the following antibodies purchased from BD Pharmingen (BD Pharmingen, San Jose, CA, USA): αCD3-Alexa700 or αCD3-allophycocyanin-Cy7, αCD8-Pacific Blue or αCD8-PE-Cy7, αCCR7-PE-Cy7, αCD28-allophycocyanin, αIL-7 receptor(R)-PE, and αCD57-FITC. Additional antibodies used for staining were αCD45RA-ECD or αCD45RO-ECD and αCD27-PE-Cy5 (Beckman Coulter), and αIL-18R1-FITC (Serotec Inc., Raleigh, NC, USA). Live/DEAD® fixable aqua or Live/DEAD® fixable violet (Amine-reactive dye) (Life

Technologies) were used for the exclusion of dead cells. As many cells as possible from the relevant $CD3^+CD8^+$ T cell subpopulations, comprising at least one sample of 20,000 cells from each subpopulation and duplicates to quadruplicates of 10,000-100,000 cells, if feasible, were sorted after ^{2}H-glucose labelling. The minimum number of cells was 48,862 and the maximum cell number was 458,376; higher numbers could be sorted from the CD57-negative subset. Cells were sorted on a triple-laser BD FACS Digital Vantage or a customized quadruple-laser BD FACSAria or FACSAria II (all from BD Biosciences), based on the presence or absence of CD45RA or CD45RO, CCR7, CD28, and/or CD57 expression or based on expression or lack of expression of CD57 on memory phenotype T cells. Gates for the T cell subpopulations were set based on fluorescence minus one (FMO) controls.

To evaluate MCMV-specific $CD8^+$ T cell responses (**chapter 5**), splenocytes and lung leukocytes were isolated from infected mice and incubated at 5 x 10^6 cells/ml for 5 hours at 37 °C with 2 μg/ml MCMV-derived peptides (GenScript, Piscataway, NJ, USA) in the presence of either 0.7 μg/ml monensin and αCD107a-FITC (both BD Pharmingen; IFN-γ and CD107a detection) or 2 μg/ml brefeldin A (Sigma-Aldrich; IFN-γ, tumour necrosis factor (TNF), and IL-2 detection). The optimal length peptides used in this study were as follows: 1) SSPPMFRVP (origin, M38; restriction, H-2Kb); 2) HGIRNASFI (origin, M45; restriction, H-2Db); 3) TVYGFCLL (origin, m139; restriction, H-2Kb); and 4) RALEYKNL (origin, immediate-early 3 [IE3]; restriction, H-2Kb) (Munks, Cho et al. 2006). Cells were then washed and incubated with Fc block (eBioscience). After incubation with peptide or medium alone as a control, cells were surface stained with αCD8a-allophycocyanin-H7 (BD Pharmingen). All cells were then fixed with 3% formalin, permeabilized with saponin buffer (PBS, 2% FCS, 0.05% sodium azide, and 0.5% saponin), and stained with the relevant combinations of αTNF-PE-Cy7, αIL-2-Pacific blue, and αIFN-γ-FITC (all eBioscience). To calculate percentage of virus-specific effector function, spontaneous degranulation or cytokine production in medium controls were subtracted from peptide-induced mobilization or expression, respectively.

To identify MCMV-specific $CD4^+$ T cells, splenocytes and lung leukocytes were incubated for 5–16

hours at 37 ºC with 2 μg/ml brefeldin A (Sigma-Aldrich) and 3 mg/ml MCMV-derived peptides (Genscript) restricted by MHC class II as follows: 1) GYLYIYPSAGNSFDL (origin, m09); 2) NHLYETPISATAMVI (origin, M25); 3) TRPYRYPRVCDASLS (origin, m139); and 4) RSRYLTAAAVTAVLQ (origin, m142) (Arens, Wang et al. 2008). To identify IL-10 expression by B cells and macrophages, splenocytes were stimulated for 5 hours at 37 ºC with either 10 mg/ml lipopolysaccharide (LPS; macrophages) or 10 mg/ml LPS, 50 ng/ml phorbol 12-myristate 13-acetate (PMA), and 500 ng/ml ionomycin (B cells; all reagents from Sigma-Aldrich). Cells were then incubated with Fc block and surface stained with either αCD4-Pacific Blue (BD Pharmingen), αCD19-FITC or αCD11b-PE-Cy7 prior to permeabilization and intracellular staining with αIFN-g-FITC (CD4 analysis only) and αIL-10-allophycocyanin (all eBioscience). The percent virus-specific cytokine production by $CD4^+$ T cells was calculated as described for $CD8^+$ T cells.

To assess APC accumulation, unstimulated splenocytes and lung leukocytes were incubated with Fc block and then stained with αCD11b-allophycocyanin-Cy7 (BD Pharmingen), αCD11c-PE-Cy7 (BD Pharmingen), αMHC class II-PE-Cy5 (eBioscience), αF4/80-Pacific Blue (BioLegend, San Diego, CA), αGr1-FITC (BioLegend), and α7/4-PE (Serotec, Oxford, UK).

To examine the expression of surface molecules by MCMV-specific $CD8^+$ T cells, 1 x 10^6 splenocytes were incubated with Live/Dead Fixable Aqua (Life Technologies), followed by Fc block, then stained with H-2Kb tetramers loaded with M38, m139, or IE3 peptides. Cells were then stained with αCD3-PerCP-Cy5.5 (BD Pharmingen), αCD8-allophycocyanin-H7 (BD Pharmingen), and either αCD44-FITC (BioLegend), αCD62L-PE-Cy7 (Abcam plc, Cambridge, UK), and αCD122-PE (eBioscience) or α-killer cell lectin-like receptor subfamily G member 1 (KLRG-1)-FITC (Southern Biotechnology Associates, Birmingham, AL, USA), αCD27-PE (eBioscience), and αCD127- Pacific Blue (eBioscience).

Data shown in **chapter 5** were acquired on either a BD FACSCanto II or a 4-laser modified BD FACSAria II cell sorter equipped for the detection of 18 fluorescent parameters (BD Immunocytometry Systems, San Jose, CA). Electronic compensation was performed in all cases using Ab capture beads stained separately with the individual monoclonal antibodies (mAbs) used in each experimental panel.

A minimum of 30,000 events was acquired in each case, and data were analyzed using FlowJo software (Tree Star Inc.).

For the data shown in **chapter 5**, total numbers of different cell populations were calculated by multiplying the total number of viable splenic or pulmonary leukocytes (assessed by trypan blue exclusion) by percent positive cells, as detected by flow cytometry. Total numbers of virus-specific T cells were calculated by: total T cell number ($CD4^+$ or $CD8^+$) x percent peptide-specific IFN-g^+ cells (calculated as described above). Total numbers of virus-specific TNF^+ or $CD107a^+$ T cells were calculated similarly.

Live/Dead Fixable Aqua or Violet dyes (Life Technologies) were used to exclude dead cells from the analysis of the samples described in **chapter 6**; αCD14 and αCD19 mAbs (Life Technologies), both conjugated to Pacific Blue, were used to exclude monocytes and B cells, respectively. The following mAbs were used for polychromatic phenotypic analyses: αCD3-allophycocyanin-H7 (BD Biosciences), αCD4-Cy5.5PE (Life Technologies), αCD8-Cy7PE and αCD57-FITC (BD Pharmingen), αCD8-QDot 705 (Life Technologies), αCD27-Cy5PE, αCD45RO-ECD, αCD69-allophycocyanin, αCD127-PE (Beckman Coulter), and biotinylated αPD-1 (R&D Systems). For visualization of $PD\text{-}1^+$ events, a secondary stain was performed with streptavidin-Pacific Blue (Life Technologies). In some experiments, Annexin V-FITC (BD Pharmingen) was used for the identification of apoptotic cells directly *ex vivo*; in other experiments, αCD16-PE (BD) and αCD56-allophycocyanin (Miltenyi Biotec, Bergisch Gladbach, Germany) were used. Stained samples for polychromatic analyses were acquired and recorded using a customized BD FACSAria II flow cytometer (BD Biosciences) equipped for the simultaneous detection of 18 fluorescent parameters; data were analyzed using FlowJo software (Tree Star Inc.). For experiments limited to a maximum of 4 fluorescent parameters, samples were acquired and recorded using a BD FACSCalibur flow cytometer (BD Biosciences); data were analyzed using CellQuest software (BD). All cell sorts for data shown in **chapter 6** were conducted to a purity of >98% using the BD FACSAria II flow cytometer mentioned above.

2.7 *Peptide/HLA-A*0201 tetrameric complexes.* Fluorochrome-labelled tetrameric peptide/HLA-A*0201 (pHLA-A*0201) complexes were produced and used as described elsewhere (Price, Brenchley et al. 2005). ExtrAvidin-R-PE (Sigma-Aldrich), streptavidin-allophycocyanin (Prozyme, Hayward, CA, USA) or streptavidin-QDot 705 (Life Technologies) were used for tetramerization.

2.8 *Measurement and analysis of ^{2}H enrichment in T cell DNA.* The stable isotope/FACS/mass spectrometric method for measuring T cell proliferation has been described in detail elsewhere (Hellerstein 1999; McCune, Hanley et al. 2000; Neese, Siler et al. 2001). Additional precautions and controls required for working with low cell count samples are outlined in Busch *et al.* (Busch, Neese et al. 2007). DNA from subsets of cells sorted in the context of the study described in **chapter 3** was extracted using the QiaAmp Micro DNA extraction kit (Qiagen, Valencia, CA, USA) and was hydrolyzed as described (Hellerstein 1999; McCune, Hanley et al. 2000; Neese, Siler et al. 2001; Busch, Neese et al. 2007). For the data shown in **chapter 4**, instead of using a DNA extraction kit, sorted cell pellets were resuspended in 200 ml PBS, boiled for 10 min to release DNA from chromatin, and rapidly chilled. For DNA hydrolysis, 50 ml 5x concentrated hydrolysis cocktail was added, containing sodium acetate buffer, pH 5, zinc sulfate, nuclease S1, and acid phosphatase (Busch, Cesar et al. 2004), and the mixture was incubated at 37 °C for 1-16 hours. Samples were transferred to screw-capped glass hydrolysis tubes**.** Aqueous O-(2,3,4,5,6-pentafluorobenzyl)-hydroxylamine hydrochloride (PFBHA) solution (1 mg/ml, 100 µl) was added, followed by 75 µl glacial acetic acid, and the mixtures incubated at 100ºC for 30 min. After cooling to room temperature, 1 ml of acetic anhydride was added to each sample, followed by 100 µl of N-methylimidazole with rapid mixing. The reaction was allowed to proceed for 15-20 min. After cooling, 2 ml water were added, and the reactions were extracted twice with 750 µl dichloromethane. The organic layers were pooled, dried over sodium sulphate, evaporated to dryness, reconstituted in 50 ml ethyl acetate, and transferred to gas chromatography (GC) vials for analysis. In addition to controls employed routinely in the stable isotope/FACS/mass spectometry (MS) method (Hellerstein 1999; McCune, Hanley et al. 2000; Neese,

Misell et al. 2002), additional sets of blanks and standards were included in each run. DNA standards were approximately matched to the range of cell counts in the experimental samples, assuming about 6 pg DNA per human diploid nucleus. Labelled cell samples and DNA standards of known ^{2}H enrichment were diluted and run with each preparation to verify the stability of measured enrichments at low sample abundance, and reagent blanks were used to assess contamination by extraneous deoxyribose or DNA. Before analyzing samples with low cell counts, the entire procedure was checked several times, using only DNA standards, blanks, and titrated amounts of cells from an abundant source with known ^{2}H enrichment.

GC/MS analysis was performed using an Agilent (Palo Alto, California, USA) model 5973 MS with a 6890 GC and an autosampler in negative chemical ionization mode with methane as reagent gas. Samples were resolved on a 30-m DB-17 column or a DB-225 column (J&W Scientific, Agilent, Foster City, CA, USA) with helium as the carrier gas, and selected ion monitoring was used to quantify the fractional molar abundances of the parent ion [M – HF, = M0] (*m/z* 435) and the M1 mass isotopomer (*m/z* 436) of the pentafluoro tri-acetate (PFTA) derivative of dR. ^{2}H enrichment was calculated as EM1, the excess fractional abundance of the M1 mass isotopomer above baseline (as determined by analysis of the unlabelled deoxyribose derivative, with correction for analyte abundance effects) (McCune, Hanley et al. 2000). The EM1 value represents isotope enrichment from ^{2}H above natural abundance and is analogous to specific activity values with radioisotopes (Hellerstein 1999; Hellerstein and Neese 1999). Data were rejected if the signal to background ratio fell below 10, or if the M0 abundance fell below the abundance range that generated reliable EM1 values with the diluted, labelled standards. $^{2}H_2O$ enrichments in body water were calculated as described previously (McCune, Hanley et al. 2000; Hellerstein, Hoh et al. 2003) by comparison to standard curves generated by mixing 100% $^{2}H_2O$ with natural abundance H_2O in known proportions.

2.9 *Calculations of the fraction of labelled cells and the number of labelled cells per organ.* For the data shown in **chapter 3**, the fraction (f) of labelled cells present in each organ was measured as

described above. The absolute number of labelled cells per organ for every time point was calculated by multiplying the fraction of labelled cells by the total number of cells of that particular phenotype present in the organ as determined by counting all cells from the respective organ with a Coulter counter and determining the frequency of the respective T cell subset by flow cytometry.

2.10 *TCR clonotyping.* Clonotypic analysis of murine (**chapter 5**) or human (**chapter 6**) Ag-specific $CD8^+$ T cell populations was conducted as described previously with minor modifications (Douek, Betts et al. 2002; Price, West et al. 2004). Briefly, tetramer-labelled murine $CD8^+$ T cells (median, 3200; range, 808–5,000) or human $CD8^+$ T cells (2,232-5,000 cells) were sorted viably into 1.5-ml microtubes (Sarstedt AG & Co., Nümbrecht, Germany) containing 100 ml ribonucleic acid (RNA)later (Applied Biosystems, Foster City, CA, USA), mRNA was extracted using a mRNA extraction kit that uses the magnetic separation technology developed by Miltenyi (Miltenyi Biotech) and unbiased amplification of all expressed TCRB gene products was conducted using a template-switch anchored reverse transcriptase (RT)-polymerase chain reaction (PCR) with a 3' TCRB constant (C) region primer for murine cells (5'-TGGCTCAAACAAGGAGACCT-3') or human cells (5'-TGCTTCTGATGGCTCAAACACAGCGACCT-3'). Amplicons were subcloned, sampled, sequenced, and analyzed as described previously (Price, Brenchley et al. 2005). The International ImMunoGeneTics Information System nomenclature is used throughout this thesis (Lefranc, Pommie et al. 2003).

2.11 *Viral genome detection.* For data shown in **chapter 5**, genomic DNA was isolated from spleen and lung tissue (Qiagen, Valencia, CA), and MCMV glycoprotein B (gB) was then assayed by quantitative PCR using a Mini Opticon (Bio-Rad, Hercules, CA) and Platinum SYBR green mastermix reagent (Life Technologies). One hundred-nanogram aliquots of DNA were used as templates for each reaction. The primer sequences used for detection of β-actin were 5'-GATGTCACGCACGATTTCC-3' and 5'-GGGCTATGCTCTCCCTCAC-3'; primers used for detection of

gB were 5'- GAAGATCCGCATGTCCTTCAG-3' and 5'-AATCCGTCCAACATCTTGTCG-3'. Genome copy numbers were calculated using a standard curve generated with the pARK25 MCMV plasmid (a gift from A. Redwood, University of Western Australia, Perth, Western Australia, Australia) with the limit of detection = 10 copies.

2.12 *gB and IL-10 gene expression.* For data shown in **chapter 5**, IL-10 and gB were assayed by quantitative RT-PCR using a Mini Opticon and Platinum SYBR green mastermix reagent (Invitrogen / Life Technologies). For IL-10 expression analysis, lung and spleen cells from mock or MCMV-infected mice were frozen on dry ice in TRIzol reagent (Life Technologies). Thawed samples were homogenized, and total cellular RNA was extracted and quantified. DNase-treated RNA was then used to synthesize copy DNA (cDNA) with a TaqMan reverse transcription kit (Applied Biosystems). The primer sequences used for detection of IL-10 were 5'-AGCATGGCCCAGAAATCAAG-3' and 5'-CGCATCCTGAGGGTCTTCA-3'. For gB expression analysis, RNA was isolated from lung and spleen tissue (Qiagen); cDNA was then synthesized as described above, and gB and actin were measured using the primers detailed above.

2.13 *Virus reactivation assay.* For data shown in **chapter 5,** virus-infected organs were divided into three parts and placed in separate wells in a 6-well plate containing 5 ml (spleen) or 3 ml (lung) D10 medium. Tissue was gently minced with the end of a 2 ml syringe, and in the case of lung pieces, an additional 2 ml D10 was then added. Tissue pieces were then cultured for 5 weeks; 4 ml supernatant was collected weekly and replaced with 5 ml fresh D10. Sonicated supernatant was then assayed for infectious virus by plaque assay as described previously (Banks, Rickert et al. 2005).

2.14 *Reagents used for experiments shown in **chapter 6**.* Dasatinib was synthesized according to the published procedure (Lombardo, Lee et al. 2004), dissolved in DMSO and purity tested as described previously (Seggewiss, Lore et al. 2005; Weichsel, Dix et al. 2008). All functional assays were

conducted in RPMI 1640 medium supplemented with 10% FBS, 2 mM L-glutamine, 100 U/ml penicillin and 100 µg/ml streptomycin (R10 medium). DMSO as a solvent control for dasatinib was included in all functional assays performed *ex vivo*. Interleukin-2 (IL-2; Proleukin™, Chiron) was applied when indicated at 2,000 IU/ml.

2.15 *Cytokine and chemokine determination by multiplex.* For data shown in **chapter 6**, plasma from patients with CML or Ph^+ ALL treated with dasatinib (n=23) and healthy controls (n=10) was analyzed for the following soluble factors using a Human Cytokine 25-plex Panel (Life Technologies) according to the manufacturer's instructions: IL-1β, IL-1RA, IL-2, IL-2R, IL-4, IL-5, IL-6, IL-7, IL-8, IL-10, IL-12, IL-13, IL-15, IL-17, TNF-α, IFN-α, granulocyte macrophage-colony stimulating factor (GM-CSF), macrophage inflammatory protein-1α (MIP-1α/CCL3), MIP-1β (CCL4), IFN-γ-inducible protein-10 (IP-10/CXCL10), monokine induced by IFN-γ (MIG/CXCL9), eotaxin (CCL11), RANTES (CCL5), monocyte chemoattractant protein-1 (MCP-1/CCL2) and IFN-γ. Measurement and analysis were performed using the Bio-Plex™ 200 System (BioRad).

2.16 *Apoptosis assay.* PBMCs ($1x10^6$ cells/ml; data shown in **chapter 6**) were either unstimulated or stimulated with 5 µg/ml OKT3 (Orthoclone™, Janssen-Cilag) and antibodies against the costimulatory molecules CD28 and CD49d (1µg/ml each; BD Pharmingen) for 4 days after overnight rest in R10 medium. Cells were then harvested and stained with Annexin V-PE (BD Pharmingen) and 7-amino-actinomycin D (7AAD; Sigma-Aldrich). Apoptotic cells were defined by flow cytometry as $7AAD^-$/Annexin V^+; late apoptotic/necrotic cells were defined as $7AAD^+$/Annexin V^+.

2.17 *NK cell expansion.* For data shown in **chapter 6,** polyclonal NK cells were generated as described previously (Valiante, Rengaraju et al. 1992). In brief, non-adherent PBMCs obtained from healthy controls after plastic adherence were co-cultured with the irradiated Epstein-Barr virus (EBV)-

transformed B cell line RPMI 8866, a kind gift from Dr. Jörg Wischhusen, at a ratio of 4:1 for 8-11 days in R10 medium. NK cells were defined as $CD3^-$, $CD16^+$ and/or $CD56^+$; purity was determined by flow cytometry using αCD3-PerCP (BioLegend) and αCD16/56-allophycocyanin (both Miltenyi Biotech). Experiments were performed when the purity of expanded NK cells exceeded 75%.

2.18 *Transfection of target cells.* For data shown in **chapter 6**, K562 cells, a kind gift from Dr. Ulrike Kämmerer, were transfected at 300 V with the firefly luciferase (fLuc):zeocin (zeo) mammalian expression vector consisting of an engineered fusion between the fLuc and zeo resistance genes under the control of the CMV immediate early (IE) promoter (InvivoGen, San Diego, CA, USA) cloned into the pcDNA3.1(+) plasmid backbone as described previously (Brown, Wright et al. 2005). The vector was a kind gift from Dr. Jörg Wischhusen. K562 $fLuc^+$ cells were cultivated in zeocin-containing R10 medium.

2.19 *NK cell cytotoxicity assay.* For the modified biophotonic luciferase assay (Brown, Wright et al. 2005) that was used to generate data shown in **chapter 6**, K562 $fLuc^+$ cells were applied as target cells at a concentration of $5x10^4$ cells/ml. Effector NK cell concentration was adjusted to $5x10^5$ cells/ml, based on the frequency of NK cells ($CD3^-$, $CD16^+$ and/or $CD56^+$). Untransfected K562 cells served as the negative control in all assays. NK cells and target cells were incubated at effector:target ratios of 10:1, 2.5:1 and 0.6:1. Assays were conducted for 4 hours in the presence of 10 or 50 nM dasatinib, as indicated, or DMSO as a solvent control. Each condition was measured in triplicate. Target cell lysis was monitored by a decrease in detected luminescence flux, measured in relative light units (RLU) using an Orion II Microplate luminometer (Berthold Detection Systems, Pforzheim, Germany).

2.20 *NK cell cytokine production and degranulation assay.* For data on NK cell cytokine production and NK degranulation shown in **chapter 6**, PBMCs were pre-treated either with DMSO or with 10 or 50 nM dasatinib for 1 h. The mAbs αCD107a-FITC and αCD107b-FITC (both BD Pharmingen) were then added and NK cells ($CD3^-$, $CD16^+$ and/or $CD56^+$) were stimulated with untreated and untransfected K562 cells in the presence of brefeldin A and GolgiStop™ (BD Biosciences). After 6 h, the cells were surface-stained with αCD3-PerCP (BioLegend) and αCD16/56-allophycocyanin (both Miltenyi Biotech), then fixed/permeabilized using Cytofix/Cytoperm (BD Biosciences) and stained intracellularly with αTNF-α-PE and αIFN-γ-PE (BD Pharmingen). Data were acquired using a 4-colour BD FACSCalibur flow cytometer (BD Biosciences) and analyzed with CellQuest software (BD Biosciences).

2.21 *Carboxyfluorescein diacetate succinimidyl ester (CFSE) proliferation assay.* For data shown in Figures 32 and 33 of **chapter 6**, PBMCs were suspended in PBS (PBS; $1x10^6$ cells/ml) and labelled with the vital dye CFSE (Molecular Probes/Life Technoologies) at a final concentration of 0.25 µM as described previously (Seggewiss, Lore et al. 2005; Weichsel, Dix et al. 2008). After overnight rest, CFSE-labelled cells were pre-incubated with dasatinib or DMSO as indicated for 1 h, then cultured for 4 days in the presence of 5 µg/ml OKT3 and αCD28/αCD49d (1 µg/ml each).

2.22 *CMV-specific $CD8^+$ T cell proliferation, cytokine production and degranulation assays.* For data shown in Figures 32 and 33 of **chapter 6**, PBMCs from HLA-A*02^+ and CMV IgG seropositive LGL patients, a non-LGL patient and healthy donors were labelled with CFSE and stimulated with the CMV $pp65_{495-503}$ peptide NLVPMVATV, which is restricted by HLA-A*02, at a concentration of 2 µM for 6 days in the presence of αCD28/αCD49d (1 µg/ml each). The cells were then harvested, stained with the CMV $pp65_{495-503}$/HLA-A*0201-allophycocyanin tetramer and αCD8-PerCP (BD Biosciences), and analyzed by flow cytometry as described previously (Seggewiss, Lore et al. 2005; Weichsel, Dix et al. 2008). Expression of the degranulation markers CD107a/b, together with intracellular cytokine

production, in the presence or absence of dasatinib was evaluated in 5 hour assays as described above for NK cells.

2.23 *Calculations of decay constants and half-lives for $CD3^+CD8^+CD45RA^-CCR7^-$ T cells that were either $CD57^+$ or $CD57^-$ after 7 weeks of ^2H_2O labeling.* As in previous studies (Hellerstein Nat Med 1999, McCune JCI 2000), ^2H_2O kinetic calculations were based on the precursor-product relationship. In this pulse/chase experiment, the loss of label enrichment in cellular DNA during the de-labeling phase was determined for each T cell subset. ^2H enrichment in cellular DNA at either sort 0 or sort 1 (week 7 during labeling or week 10, three weeks after the last dose of ^2H_2O), representing the baseline value (or pulse) before (sort 0) or after wash-out (sort 1) of ^2H_2O from body water pools, was used as the time zero value. The latter time point was chosen because body water ^2H_2O enrichments fall with a half-life of approximately 7 days, allowing the assessment of die-away kinetics without the confounding effects of continued label incorporation (Ladell, Hellerstein et al. 2008). Data from sort 0 were used for calculation, as the biggest difference between the two T cell subsets was observed between sort 0 and sort 1. The loss of label from cellular DNA of the two subsets was quantified between S0 and S1 as well as S1 and S2 (week 14). The decay constant (k) was calculated using the equation for exponential decay: k = -[ln(sort 1/ sort 0)]/Dt or k = -[ln(sort 2/sort 1)]/Dt, where Dt is the time between measurements (3 or 4 weeks, respetively). The half-life was calculated as $t_{1/2} = \ln(2)/k$. For these calculations single-pool, single-exponential kinetics of label die-away were assumed.

2.24 *Statistical analysis.* Statistical analysis was perfomed using GraphPad Prism software (GraphPad, La Jolla, CA, USA). For data shown in **chapter 3**, statistical differences between groups were determined using the two-way ANOVA for repeated measures (with Bonferroni post-tests) for more than two groups or the two-tailed non-parametric Mann-Whitney U Test or parametric two-tailed Student's t-test for comparison of two groups. For data shown in **chapter 4**, statistical significance was determined using the two sample equal variance two-tailed Student's t-test and the two-tailed non-

parametric Mann-Whitney U test. For data shown in **chapter 5**, statistical significance was determined using the paired two-tailed Student's t-test or the non-parametric Mann-Whitney U test. For data shown in **chapter 6**, statistical significance was determined using the non-parametric Kruskal-Wallis test, the paired two-tailed Student's t-test or one-way analysis of variance (ANOVA). Statistical significance was defined as $p<0.05$.

CHAPTER

3

Continuous subcutaneous administration of peptide without adjuvant leads to aborted immune activation and Ag-specific T cell depletion in DO11.10 TCR transgenic mice

3.1 Introduction

In several contexts, it would be desirable if T cell tolerance could either be broken or induced. It would be beneficial if T cell tolerance could be broken in tumours and it would likewise be beneficial to induce tolerance in transplant patients or patients with autoimmune diseases or allergies. It is a general concept that co-stimulation is required in addition to the peptide MHC-TCR interaction for proper T cell activation to occur (Chambers, Krummel et al. 1996) and that lack of co-stimulation leads to either a decreased response or even to the induction of T cell tolerance or anergy (also referred to as unresponsiveness to Ag or T cell dysfunction) (Chen 2004). It has also been suggested that the route of administration determines whether $CD4^+$ T cell activation or T cell tolerance is induced (Kearney, Pape et al. 1994).

In 1994, it was described that antigenic challenge with soluble cognate peptide given i.v. or i.p. resulted in tolerance whereas administration by the s.c. route resulted in immunity (Kearney, Pape et al. 1994). However, in this study, soluble cognate peptide Ag was given i.v. without adjuvant or i.p. in IFA, whereas s.c. it was given in CFA. Cognate peptide Ag was not given s.c. without adjuvant, thereby rendering the study incomplete. Since then, discrepant results have been reported with regard to whether s.c. administration of cognate peptide without adjuvant leads to T cell tolerance or immunity. In principle, Ag-specific T cell tolerance could occur upon intrathymic deletion or active suppression of Ag-specific T cell clones (central tolerance), and/or TCR-mediated signalling in T cells in the periphery leading to the induction of $CD4^+CD25^+FoxP3^+$ T_{REG} cells or Ag-specific induction of activation-induced cell death (AICD) or T cell anergy. In the latter instance, antigenic stimulation in the absence of “second signals” (for example, as delivered by internally driven inflammatory events or by

externally delivered adjuvants) can be preceded by limited initial expansion of Ag-specific cells and accompanied by the induction of T_{REG} cells (Read, Mauze et al. 1998; Knoechel, Lohr et al. 2006; Chappert, Leboeuf et al. 2008). Of note, in some contexts, *in vivo* $CD4^+$ T cell tolerance induction versus priming is independent of the rate and number of cell divisions (Adler, Huang et al. 2000). Furthermore, antigenic stimulation without "second signals" may negatively affect T cell trafficking to non-lymphoid tissues, a process that has been proposed to facilitate peripheral tolerance (Marelli-Berg, Okkenhaug et al. 2007).

In related experiments addressing these potential mechanisms, others have provided cognate Ag by varying routes of administration to $CD4^+$ TCR tg mice or syngeneic host mice that previously received TCR tg $CD4^+$ T cells (Kearney, Pape et al. 1994; Liblau, Tisch et al. 1996; Pape, Khoruts et al. 1997; Reinhardt, Khoruts et al. 2001). Administration of peptide by the i.p. or i.v. route was found to induce central and peripheral tolerance by apoptosis (Murphy, Heimberger et al. 1990), whereas s.c. administration of peptide with adjuvant prompted a functional immune response (Kearney, Pape et al. 1994; Liblau, Tisch et al. 1996). S.c. administration of peptide without adjuvant has recently been tested in Balb/c $CD4^+$ TCR-HA (influenza hemagglutinin HA-specific tg TCR) $Rag2^{-/-}$ mice (Apostolou and von Boehmer 2004), in DO11.10 $CD4^+$ TCR tg (ovalbumin-specific tg TCR) $Rag2^{-/-}$ mice (Dahlberg, Schartner et al. 2007), and in B10.BR $CD4^+$ TCR tg mice (transgenic for the 2B4 TCR that recognizes pigeon or moth cytochrome c) not on a Rag-deficient background (Switzer, Wallner et al. 1998). $CD4^+$ TCR tg mice on a Rag-deficient background characteristically do not have natural $CD25^+$ T_{REG} cells, as endogenous TCR α-chain expression is required to drive selection of this population in the thymus (Itoh, Takahashi et al. 1999). However, it has been shown that peripheral T_{REG} cells can be induced in Rag-deficient $CD4^+$ TCR tg mice by continuous delivery of peptide for 14 days using osmotic pumps implanted s.c. or by daily s.c. injections of peptide (Apostolou and von Boehmer 2004; Dahlberg, Schartner et al. 2007). In 2B4 TCR tg mice not on a Rag-deficient background, repeated s.c. injections of peptide without adjuvant led to a tolerant state of the Ag-specific T cells without substantial deletion, but continuous peptide administration for one week using s.c. implanted osmotic pumps containing the peptide did not tolerize 2B4 TCR tg $CD4^+$ T cells (Switzer, Wallner et al. 1998).

The interpretation of the data published in the studies outlined above is complicated by differences in experimental design, the use of different strains of mice, including mice on Rag-sufficient or Rag-deficient backgrounds, and adoptive T cell transfer into syngeneic (closely related, immunologically compatible) host mice.

A number of questions clearly remain unresolved regarding the tolerogenic effects of s.c. administration of peptide Ag without adjuvant. To revisit this subject, experiments were designed to further explore the mechanisms by which tolerance might be induced upon s.c. administration of peptide Ag in the absence of adjuvant.

3.2 Hypotheses

- Continuous administration of cognate peptide without adjuvant in $CD4^+$ DO11.10 TCR tg mice by s.c. delivery leads to immunological tolerance.
- Not all memory-phenotype T cell subsets are induced in $CD4^+$ DO11.10 TCR tg mice given peptide without adjuvant continuously by s.c. implanted mini-osmotic pump, but are inuduced in $CD4^+$ DO11.10 TCR tg that receive cognate peptide with adjuvant.
- *In vivo* naïve and memory effector T cell proliferation rates differ in $CD4^+$ DO11.10 TCR tg mice that continuously receive cognate peptide without or with adjuvant.

3.3 Specific Aims

- To determine whether continuous administration of cognate peptide without adjuvant leads to immunological tolerance or immunity in $CD4^+$ DO11.10 TCR tg mice.
- To determine whether memory phenotype T cells are induced in $CD4^+$ DO11.10 TCR tg mice that continuously receive cognate Ag without or with adjuvant.
- To determine whether continuous delivery of cognate Ag without or with adjuvant by s.c. administration is associated with thymic deletion, T cell redistribution, the induction of T_{REG}

cells, or T cell activation leading to T cell depletion / cell death.

- To determine whether the *in vivo* proliferative response of Ag-specific T cells and their subsets differs if cognate Ag is given without or with adjuvant.

3.4 Results

Subcutaneous antigenic stimulation with OVAp and IL-1β leads to distress and immune activation in TCR tg mice

To study the effect of s.c. peptide stimulation without or with adjuvant, mini-osmotic pumps containing either sterile PBS, $OVA_{323-339}$ peptide in sterile PBS (OVAp; 6.6 µg peptide released per day), or OVAp together with IL-1β (6.6 µg OVAp and 0.6 µg of IL-1β released per day) as adjuvant were implanted s.c. between the scapula of OVA DO11.10 TCR tg mice. OVA DO11.10 TCR tg mice were used instead of a TCR tg T cell adoptive transfer approach to ensure that sufficient numbers of T cell subsets could be sorted for assessment of label enrichment after *in vivo* stable isotope labelling. IL-1β was chosen as adjuvant because it induces robust and durable primary and secondary $CD4^+$ T cell responses (Ben-Sasson, Hu-Li et al. 2009), because it is a dominant and proximal mediator of the effects of classical adjuvants such as LPS (Lachman, Page et al. 1980), and because it is more acceptable to administer to mice on a continuous basis.

Within 24 hours after pump implantation, mice that received OVAp and IL-1β had scruffy fur and weight loss whereas those administered OVAp alone or PBS looked normal. Over the next 12 days, weight loss persisted in those receiving OVAp and IL-1β (Table 1). At that time, the pumps were discontinued (with evidence of proximal s.c. inflammation in the case of those delivering IL-1β) and the weight and condition of the mice improved over the next eight days.

Table 1. Weights of the mice in grams (medians and ranges are shown).

Group / Day	PBS	OVAp	OVAp and IL-1β
0	18.0 (17.0 – 19.6)	18.8 (16.5 – 19.6)	18.0 (16.6 – 19.6)
1	19.1 (17.3 – 20.5)	19.7 (16.9 – 21.4)	17.2 (15.8 – 19.3)* **
3	19.5 (18.1 – 20.6)	18.5 (18.3 – 20.4)	17.1 (15.8 – 18.0)
6	20.0 (19.5 – 20.3)	20.0 (19.6 – 20.2)	17.5 (15.8 – 18.7)*
12	19.6 (18.8 – 20.1)	20.4 (20.1 – 21.6)	17.8 (16.2 – 18.9)*
20	22.7 (19.8 – 22.8)	23.8 (20.5 – 23.8)	22.4 (19.9 – 22.5)

* $p < 0.05$ parametric Student's t-test, ** $p < 0.05$ non-parametric Mann Whitney U test, OVAp and IL-1β versus PBS or OVAp. For days 0 and 1, there were 13 mice per group; for days 3, 6 and 20, there were 3 mice per group; and, for day 12, there were 4 mice per group.

Subcutaneous antigenic stimulation without adjuvant leads to depletion of circulating and splenic OVA-specific $CD4^+$ T cells

Mice that received OVAp + IL-1β had significantly increased cellularity in the spleen and in pooled peripheral (brachial, axillary, and inguinal) LNs at days 6 and 12 (Fig. 5A and 5B), associated with splenomegaly that was most marked on day 12 (Fig. 6), but already apparent on day 6 as reflected by the cellularity of the spleen (Fig. 5A). Although mice receiving OVA alone showed increased LN cellularity at days 3 and 6, LN cellularity was normal by day 12 (Fig. 5B), and spleen cellularity and size remained normal throughout the time of investigation (Fig. 5A, Fig. 6).

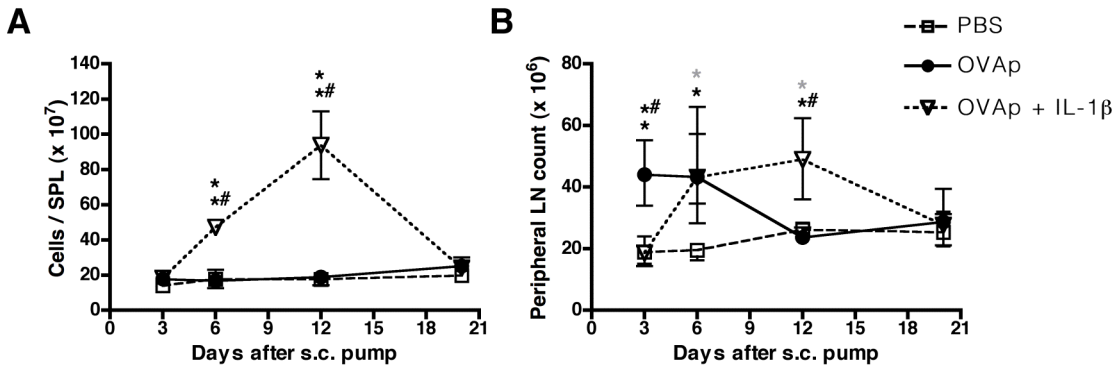

Figure 5. Continuous administration of OVAp with IL-1β as adjuvant leads to a significant increase in spleen and LN cellularity, whereas OVAp without adjuvant leads to significant increase in LN cellularity only. Mini-osmotic pumps containing either PBS, OVAp in PBS, or OVAp together with IL-1β were implanted s.c. between the scapulae of DO11.10 TCR tg mice and, at the indicated time points, the numbers of **(A)** SPL cells and **(B)** peripheral LN (brachial, axillary, inguinal) cells were assessed. Data shown are from three mice per group per time point and are representative of three similar experiments (seven experiments were carried out in total). Shown are means and ranges. * $p<0.05$ PBS versus OVAp, grey asterix $p<0.05$ PBS versus OVAp + IL-1β, and $*^{\#}$ $p<0.05$ OVAp versus OVAp + IL-1β (two-way ANOVA for comparison of more than two groups with Bonferroni post-tests to compare replicate means per time point).

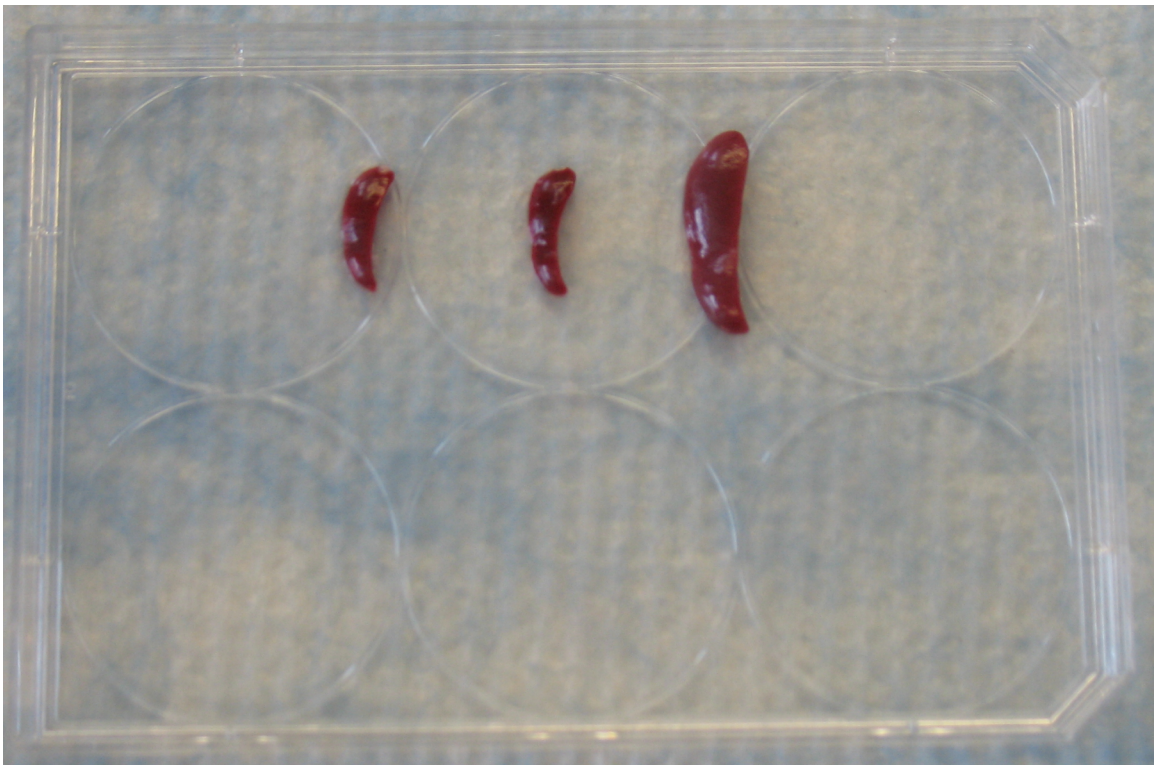

Figure 6. *In vivo* priming of mice with OVAp + IL-1β leads to splenomegaly. Mice were implanted with mini-osmotic pumps (as per the legend of Fig. 4). The spleens shown on the lid of a 6-well tissue culture plate were harvested on day 12 and are representative for those from mice that received PBS (left), OVAp (middle), and OVAp + IL-1β (right).

Flow cytometric evaluation of peripheral blood, spleen (representative flow data are shown in Fig. 7), and peripheral LNs revealed that OVAp stimulation without IL-1β resulted in a rapid and statistically significant decrease of OVA-specific $CD4^+$ T cells in the blood (Fig. 8A) and spleen (Fig. 8B), but not in LNs (Fig. 8C), of DO11.10 TCR tg mice. This loss was mainly due to a decrease in the number of OVA-specific $CD4^+$ ($CD62L^{high}CD44^{low}$) T_N cells (Figs. 8D and 8E, respectively). Even though OVA-specific $CD4^+$ T cells were increased at days 3 and 6 after administration of OVAp without IL-1β, there was a significant reduction of T_N cells in LNs at days 6 that continued until the last day (day 20) of evaluation (Fig. 8F). Administration of OVAp + IL-1β led to a similar decrease of OVA-specific $CD4^+$ T cells in the blood (Fig. 8A) and this was associated with a decrease in T_N cells in the blood, spleen and LNs (Fig. 8D, 8E and 8F). In the spleens of mice that received OVAp + IL-1β, in contrast to those that

received OVAp only, all effector/memory T cell subpopulations showed substantial and significant increases by days 6-12 (Figs. 8H, 8K, and 8M). This included OVA-specific effector-type $CD4^+$ T_E cells ($CD62L^{low}CD44^{low}$) (Thomas, Brown et al.) (Fig. 8H), classical "effector memory" $CD4^+$ T_{EM} cells ($CD44^{high}CD62L^{low}$) (Connor, Harvie et al.) (Fig. 8K), and "central memory" $CD4^+$ T_{CM} cells ($CD62L^{high}CD44^{high}$; Fig. 8M). OVA-specific $CD4^+$ T_E cells also increased in the blood of mice that received OVAp + IL-1β (Fig. 8G), but the number of OVA-specific $CD4^+$ T_{EM} cells or T_{CM} cells did not increase in the blood in either of the other two groups (data not shown).

As mentioned above, mice that received OVAp alone showed only an increase in the cellularity of the peripheral LNs at days 3 and 6 (Fig. 5B), accounted for by an increased number of OVA-specific $CD4^+$ T cells that were predominantly $CD4^+$ T_E cells at day 3 (Fig. 8I) and, to a lesser extent and only at day 6, T_{EM} cells (Fig. 8L). Of note, in the spleens of mice that received OVAp without adjuvant, increases in OVA-specific "memory/effector-phenotype" OVA-specific $CD4^+$ T cell subsets were very small and not sustained (Fig. 8H, 8K, and 8M). T_{CM} cells increased substantially only in spleens and LNs of mice that received OVAp + IL-1β (Fig. 8M and 8N).

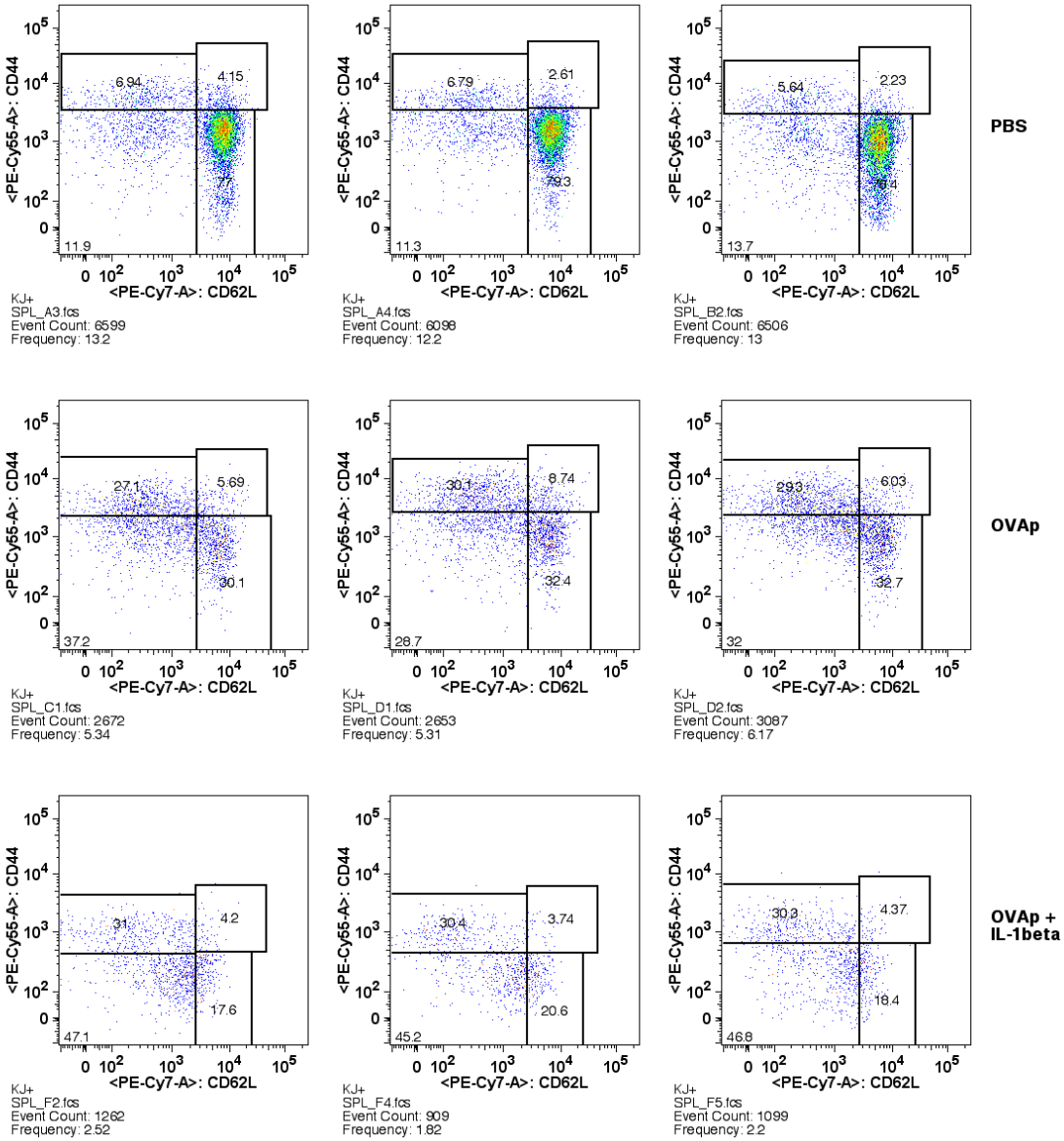

Figure 7. CD44 versus CD62L staining profiles of splenocytes from mice that received either PBS or OVAp in PBS or OVAp + IL-1β in PBS. Representative data shown are from day 6 after s.c. pump implantation. The sequence of gating was as follows: 1. Cells; 2. Singles to remove doublets; 3. Boolean gating to remove artefacts and aggregates; 4. Live cells; 5. $CD4^+$ cells; 6. $KJ1\text{-}26^+$ cells (= cells that express the transgenic TCR); 7. CD44 versus CD62L (depicted). $CD4^+KJ1\text{-}26^+$ T cells from the spleens of mice that received OVAp + IL-1β showed the lowest fluorescence for CD62L when compared to the other groups and gates were adjusted accordingly. The event counts refer to the number of $CD4^+KJ1\text{-}26^+$ events that are shown.

In sum, the major differences in cell composition of spleen and LNs in mice that received OVAp + IL-1β versus those that received PBS or OVAp alone were found in the OVA-specific $CD4^+$ T_{CM} cell subpopulation (which was numerically increased at days 6 and 12 in mice that received OVAp + IL-1β) (Fig. 8M and 8N, respectively) and in OVA-specific $CD4^+$ T_E cells (which increased also and to a greater extent early on in the peripheral LNs of mice that only received OVAp) (Fig. 8I). Although OVA-specific $CD4^+$ T_{CM} cell numbers were low in the blood of mice that received OVAp or OVAp + IL-1β (data not shown), a significant and large increase of this T cell subset was observed at days 6 and 12 also in the spleen and LNs of mice that received OVAp + IL-1β (Fig. 8M and 8N, respectively). These findings suggest that s.c. antigenic stimulation without adjuvant leads to depletion of circulating and splenic OVA-specific $CD4^+$ T cells, especially those with a T_N phenotype, and that this depletion cannot be readily attributed to maturation of T_N cells to memory/effector phenotype T cells or to redistribution of T cells to peripheral lymphoid compartments. Indeed, when peripheral $CD4^+$ T cells from blood, peripheral LNs, and spleen were considered in aggregate, mice that received OVAp without adjuvant showed a significant depletion of $CD4^+$ T cells by day 12 (Fig. 8J). Meanwhile, the presence of adjuvant led, as expected, to an increase in Ag-specific memory/effector $CD4^+$ T cell subsets accompanied by a reciprocal fractional decrease in the number of Ag-specific T_N cells, most likely due to maturation of these cells to memory/effector phenotypes.

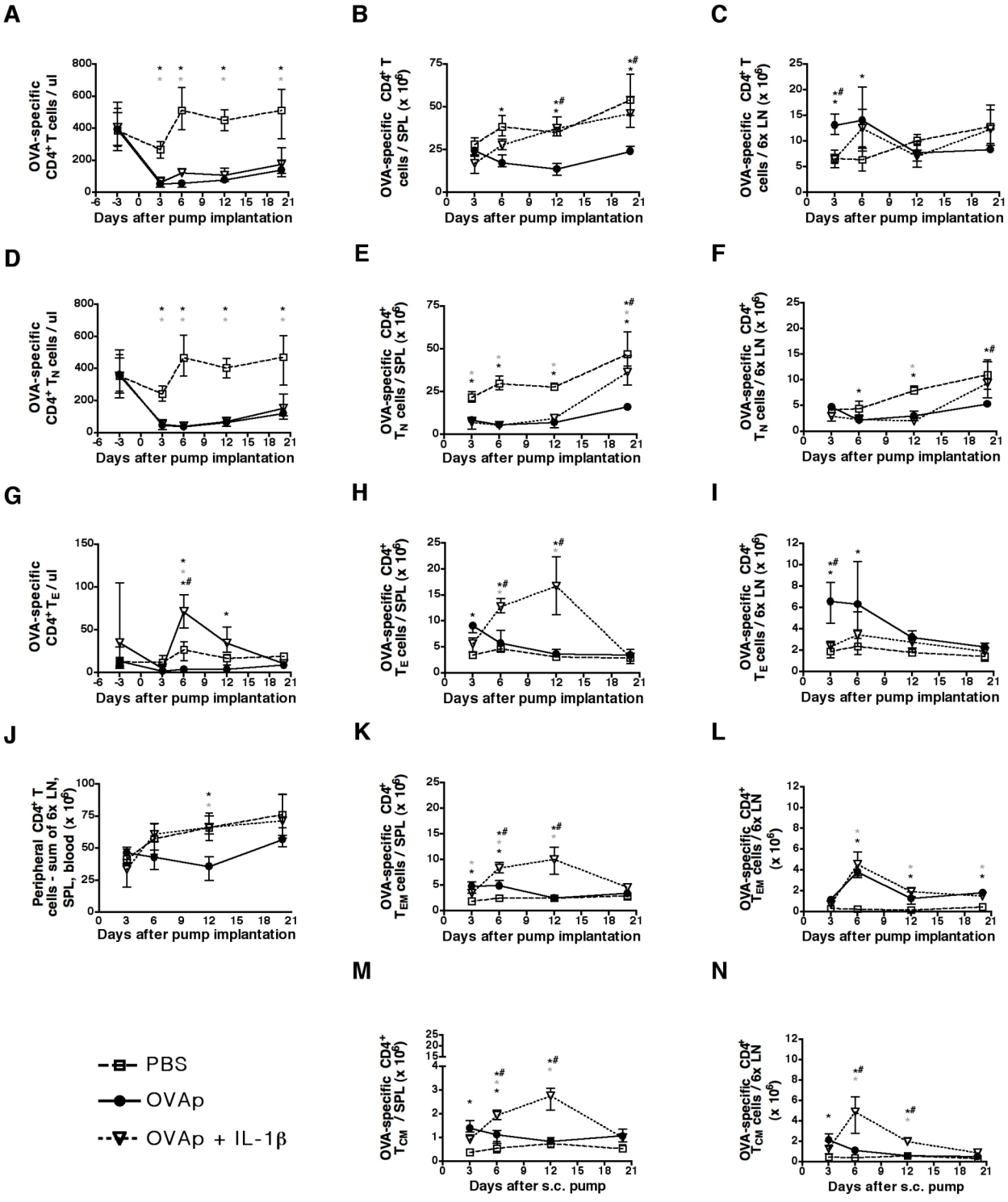

Figure 8. Continuous s.c. administration of OVAp results in a rapid decrease of OVA-specific, naive $CD4^+$ T cells in the periphery and this loss cannot be readily attributed to T cell maturation or redistribution to lymphoid compartments. Mice were implanted with mini-osmotic pumps (as per the legend of Fig. 5) and individual mice were bled as a function of time to measure the number of: OVA-

specific $CD4^+$ T cells **(A)** per μl of peripheral blood, **(B)** per SPL, or **(C)** per pooled (axillary, brachial and inguinal) lymph nodes. OVA-specific $CD4^+$ T_N cells, **(D)** per μl of peripheral blood, **(E)** per spleen, or **(F)** per pooled (axillary, brachial and inguinal) lymph nodes. OVA-specific $CD4^+$ T_E cells, **(G)** per μl of peripheral blood, **(H)** per spleen, or **(I)** per pooled (axillary, brachial and inguinal) lymph nodes. **(J)** The sum of total peripheral $CD4^+$ T cells (from blood, spleen and peripheral LN) was calculated and is shown. OVA-specific $CD4^+$ T_{EM} cells, **(K)** per spleen or **(L)** per pooled (axillary, brachial and inguinal) lymph nodes. OVA-specific $CD4^+$ T_{CM} cells, **(M)** per spleen or **(N)** per pooled (axillary, brachial and inguinal) LNs. Data shown are from the same experiment as shown in Fig. 5. Shown are means and ranges. * $p<0.05$ PBS versus OVAp, grey asterix $p<0.05$ PBS versus OVAp + IL-1β, and $*^{\#}$ $p<0.05$ OVAp versus OVAp + IL-1β (Student's t-test for data from PBMCs and two-way ANOVA for comparison of more than two groups with Bonferroni post-tests to compare replicate means per time point for organ counts).

Subcutaneous antigenic stimulation without adjuvant does not lead to thymic involution

Given the early and rapid drop of OVA-specific $CD4^+$ T_N cells in the periphery in mice that received either OVAp or OVAp + IL-1β, we explored the possibility that s.c. Ag stimulation without or with adjuvant might lead to thymic involution. At days 6 and 12 after pump implantation, OVAp + IL-1β-stimulated mice showed a significant loss of thymocytes (Fig. 9A), associated with depletion of $CD3^+CD4^+CD8^+$ (double positive, or DP) (Fig. 9B), $CD3^+CD4^+CD8^-$ (single positive CD4, or SPCD4) (Fig. 9C), and $CD3^-CD4^-CD8^-$ (double negative, or DN) (Fig. 9D) cells. Transient thymic involution was not, however, noted in those mice that received Ag in the absence of adjuvant.

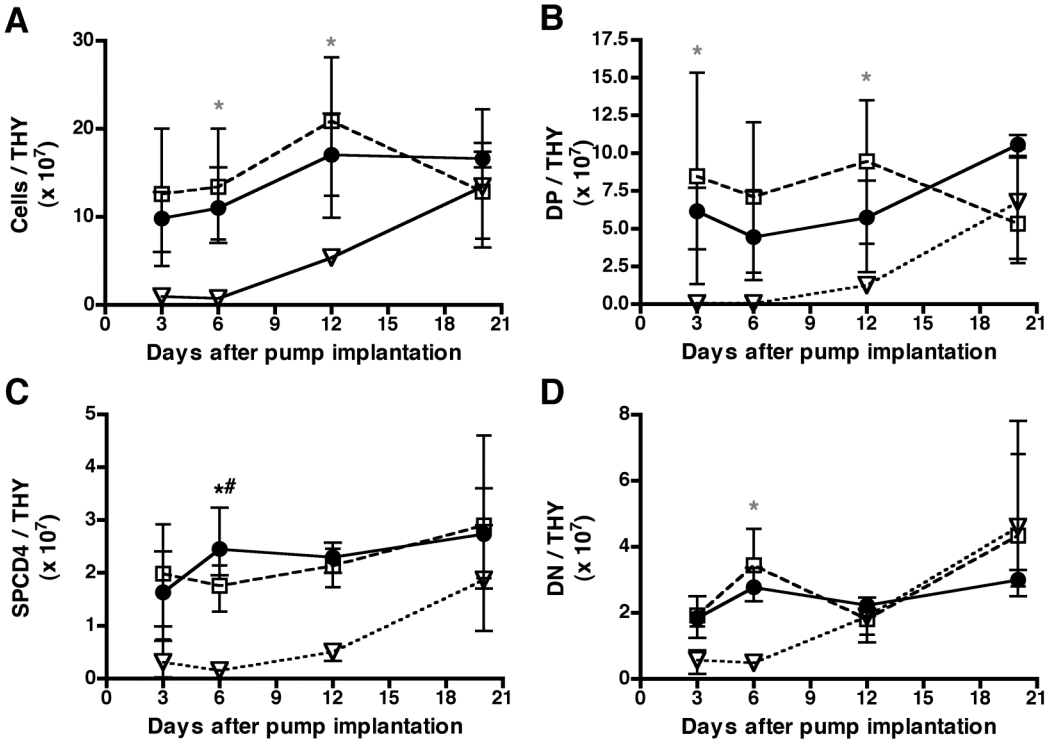

Figure 9. Loss of thymocytes early after s.c. OVAp with IL-1β administration. Mice were implanted with mini-osmotic pumps (as per the legend of Fig. 5) and, at four time points thereafter, thymi were removed from individual mice to count the number of: **(A)** total cells, **(B)** DP THY cells, **(C)** SPCD4 THY cells, and **(D)** DN THY cells. Open squares: PBS group; filled circles: OVAp group; open inverted triangles: OVAp + IL-1β group. Data shown are from the same experiment as shown in Fig. 5. Shown are means and ranges. * $p<0.05$ PBS versus OVAp, grey asterix $p<0.05$ PBS versus OVAp + IL-1β, and $*^{\#}$ $p<0.05$ OVAp versus OVAp + IL-1β (two-way ANOVA for comparison of more than two groups with Bonferroni post-tests to compare replicate means per time point).

Subcutaneous antigenic stimulation without adjuvant leads to a rapid increase in the proportion and absolute number of Ki67$^+$ CD4$^+$ T cells in peripheral LNs, but not in the spleen.

Since the rapid drop in peripheral T_N cell numbers in mice infused with OVAp alone could not be explained by thymic involution, we investigated the possibility that s.c. OVAp administration might instead induce clonal proliferation and maturation of Ag-specific T_N cells to effector/memory T cells, potentially resulting in depletion of the T_N compartment. In mice receiving OVAp without adjuvant, the percentage of OVA-specific CD4$^+$ T cells that expressed Ki67 was significantly increased in the LNs at

days 3 and 6 compared to mice that also received IL-1β (Fig. 10A). Compared to mice that received OVAp + IL-1β, those receiving OVAp alone showed a significant increase in the absolute number of $Ki67^+$ $CD4^+$ T_N, T_{EM}, T_E and T_{CM} T cells at days 3 and/or 6 (Figs. 10B, 10C, 10D and 10E). At days 6 and 12, however, the percent and absolute number of $Ki67^+$ OVA-specific $CD4^+$ T_N cells in the spleens of mice that received OVAp + IL-1β was significantly higher than in those that received either PBS or only OVAp (Fig. 10F and 10G). These data suggest that antigenic stimulation in the absence of adjuvant is associated with early rounds of T_N proliferation that do not ultimately lead to the generation of more mature T cells.

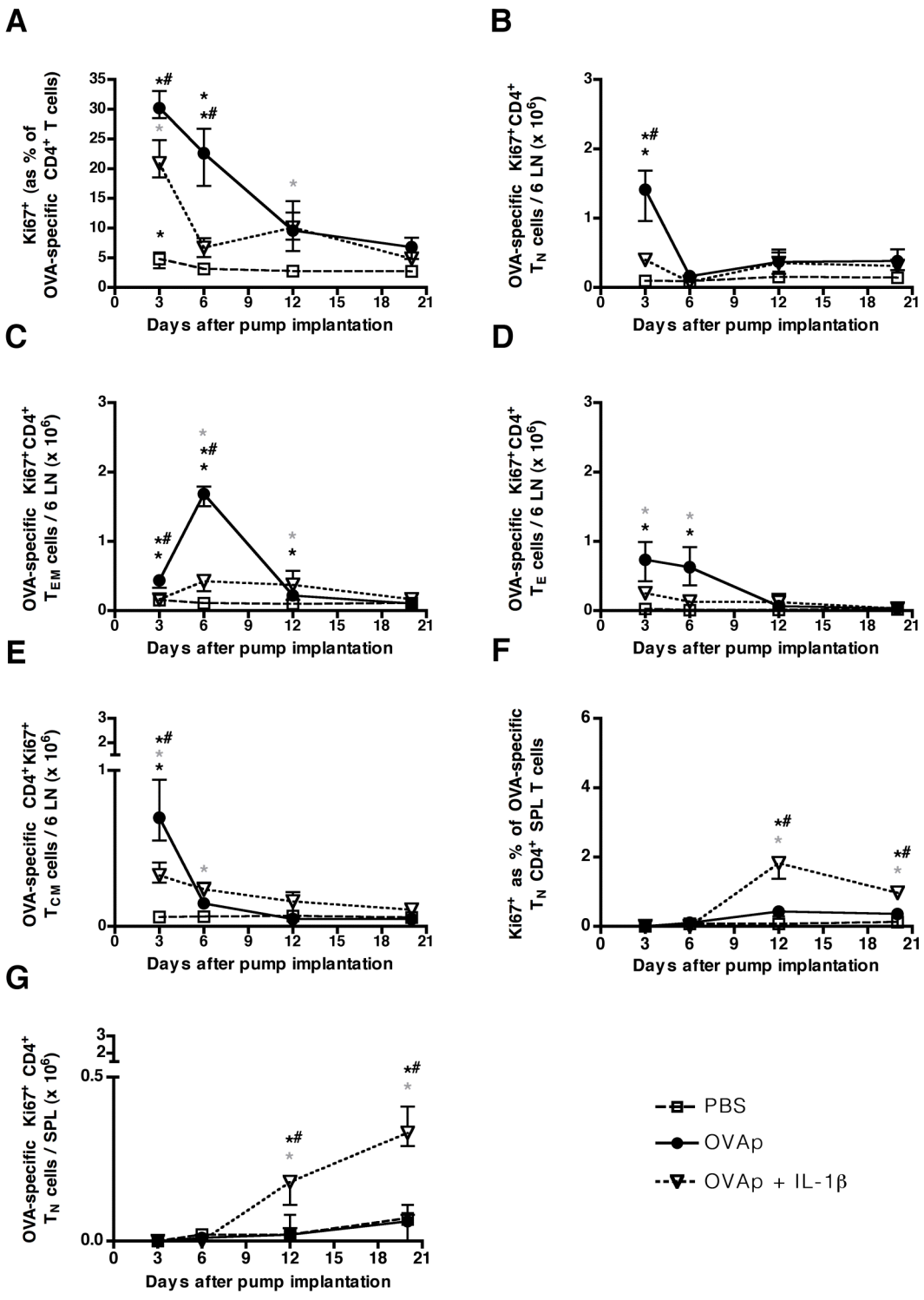

Figure 10. Proliferation profiles, as measured by expression of Ki67 in OVA-specific $CD4^+$ T cells in the LNs and spleen. Mice were implanted with mini-osmotic pumps (as per the legend of Fig. 5) and, at the indicated time points, peripheral LNs (including two brachial, two axillary, and two inguinal) were collected to determine **(A)** $Ki67^+$ cells as percentage of OVA-specific $CD4^+$ T cells or the absolute

numbers per 6 LNs of **(B)** Ki67$^+$ OVA-specific CD4$^+$ T_N cells, **(C)** Ki67$^+$ OVA-specific CD4$^+$ T_{EM} cells, **(D)** Ki67$^+$ OVA-specific CD4$^+$ T_E cells, or **(E)** Ki67$^+$ OVA-specific CD4$^+$ T_{CM} cells. **(F)** The percentage of Ki67$^+$ OVA-specific T_N cells in the spleen or **(G)** the absolute number of Ki67$^+$ OVA-specific T_N cells in the spleen are shown. Data shown are from the same experiment as shown in Fig. 5. Shown are means and ranges. * $p<0.05$ PBS versus OVAp, grey asterix $p<0.05$ PBS versus OVAp + IL-1β, and *# $p<0.05$ OVAp versus OVAp + IL-1β (two-way ANOVA for comparison of more than two groups with Bonferroni post-tests to compare replicate means per time point).

Subcutaneous antigenic stimulation without adjuvant leads to limited proliferation and rapid loss of dividing cells from the T cell pool

To explore further the proliferation and loss of OVA-specific CD4$^+$ T cell subsets in lymphoid compartments during s.c. administration of peptide without or with adjuvant, *in vivo* oral stable-isotope labelling was carried out in DO11.10 mice during the first 3 days after s.c. pump implantation. ^{2}H enrichment was analyzed at days 3, 6, 12 and 20 after pump implantation in the Ag-specific T_N and classical effector memory T_{EM} cells from peripheral LNs or spleen. In stimulated mice (mice that received OVAp or OVAp + IL1β), ^{2}H enrichments in T_N cells from the spleen appeared to be lower than in T_N cells from peripheral LNs at early time points. Also, ^{2}H enrichments were higher in T_{EM} cells than T_N cells in all groups of mice at early time points (compare Fig. 11A to 11C or Fig. 12A to 12C). T_{EM} ^{2}H enrichments appeared to be higher in LNs than spleen in mice that received OVAp + IL1β (for example at day 6, 8% versus 6% enrichment in T_{EM} cells from LNs versus spleen from OVAp + IL-1β mice; compare Fig. 11C and Fig. 12C).

In peripheral LNs, peak labelling of OVA-specific CD4$^+$ T_N cells was reached at day 12 in mice that received PBS, but ^{2}H enrichments were higher at days 3 or at days 3 and 6 in mice that received either OVAp alone or OVAp + IL-1β, respectively (Fig. 11A). Peak labelling of OVA-specific CD4$^+$ T_N cells from spleens was reached on day 12 in both OVAp-stimulated and unstimulated (PBS) DO11.10 mice (this was the case after either ^2H_2O labelling (Fig. 12A) or [6,6-$^2H_2$]glucose; data not shown).

However, peak labelling of OVA-specific $CD4^+$ T_N cells in spleens of mice that received OVAp + IL-1β was only reached at day 20 (Fig. 12A), likely due to early and rapid conversion of T_N cells into effector/memory T cells and/or due to trafficking of the primed T_N cells to non-lymphoid inflamed tissue / the effector site at the earlier time points. The delay in peak labelling of OVA-specific $CD4^+$ T_N cells from PBS-treated mice in both LNs and spleen possibly reflects the movement of cells labelled in the thymus to these peripheral lymphoid tissues.

In mice that received OVAp, the fraction and absolute number of labelled T_N cells was significantly increased in LNs at day 3 and, by day 6, the absolute number of labelled T_N cells dropped to the same level as in mice that received PBS (Fig. 11B). In contrast, in mice that received OVAp + IL-1β, the fraction and absolute number of labelled T_N cells remained significantly elevated at day 6 (Fig. 11E and 11B, respectively). Of note, the fraction of labelled cells or absolute numbers of labelled cells per organ can only be calculated during the period of label incorporation and not during delabelling, as the labelled cell population during delabelling is not representative of the whole cell population (Asquith, Debacq et al. 2002). In the spleen, ^2H enrichments and the fraction of labelled T_N cells were similar in all the three groups of mice (Fig. 12E). The absolute number of labelled T_N cells appeared to be higher at day 6 in mice that received PBS (Fig. 12B), because these mice in contrast to mice that received OVAp or OVAp + IL-1β did not loose T_N cells and their T_N cell number in the spleen increased slightly between days 3 and 6 (Fig. 8E).

In the LNs and spleen of mice that received OVAp or OVAp + IL-1β, OVA-specific $CD4^+$ T_{EM} cells showed peak labelling at day 6 and ^2H enrichments in this subset were highest at days 3 and 6 in T_{EM} cells from mice that received OVAp + IL-1β (Fig. 11C and Fig. 12C). The highest fractions and absolute numbers of labelled T_{EM} cells were observed at day 6 in the LNs and spleens of mice that received OVAp + IL-1β (Fig. 11F, 11D and 12F, 12D). ^2H enrichments in T_{EM} cells from both LNs and spleens of mice that received OVAp + IL-1β decreased after day 6 (Fig. 11C and 12C). However, ^2H

enrichments in T_{EM} cells from the LNs decreased only after day 12 in mice that received OVAp alone (Fig. 11C and 11G), indicating that T_{EM} cells were not lost from the peripheral LNs by cell death or trafficking or were replenished by conversion / differentiation of local or thymic precursors labelled previously. Alternatively, as the labelled population during delabelling is not representative of the whole population, this result could represent a proportionate loss of both labelled and unlabelled cells. This is likely because LN cellularity in mice that received OVAp decreased after day 6, as did the number of Ag-specific T_{EM} cells (Fig. 5B and Fig. 8L, respectively). Of note, even though the frequency of $Ki67^+$ OVA-specific $CD4^+$ T cells was highest at days 3 and 6 in mice that received OVAp (Fig. 10A), ^2H enrichments were highest in, especially, T_{EM} cells of OVAp + IL-1β mice at day 6 in both LNs (Fig. 11C) and spleen (Fig. 12C). In addition, and as mentioned above, T_{EM} cells that had incorporated label (new cells) were not as rapidly lost in LNs of OVAp only mice between days 6 and 12, but declined rapidly thereafter (Fig. 11G). It is possible that these cells survived for longer and failed to exit the LNs due to the lack of an appropriate signal two that would be necessary for "proper“ T cell activation and the migration of cells from the LNs to non-lymphoid tissue (reviewed in (Marelli-Berg, Okkenhaug et al. 2007)). The more rapid loss of new T_{EM} cells from LNs in OVAp mice after day 12 may be due to aborted activation.

In the spleen, newly divided OVA-specific $CD4^+$ T_{EM} cells lost label more steadily in all groups, although the early loss (between days 6 and 12) of labelled cells was greatest in mice that received OVAp + IL-1β (Fig. 12G). Mice that received OVAp + IL-1β lost OVA-specific T_{EM} cells more steadily and at earlier time points also in LNs (Fig. 11G). This kinetic analysis indicates that T cell turnover is highest in mice that receive peptide + adjuvant (OVAp + IL-1β). Together with the cell counts described above, these data show that cells divide after s.c. administration of OVAp, but that in contrast to administration of OVAp + IL-1β, proliferation is limited and does not lead to sustained peripheral T cell expansion, and cells are lost from the T cell pool. In other words, sustained rounds of cell proliferation that lead to expansion of the T cell pool are not observed in mice stimulated with

OVAp alone.

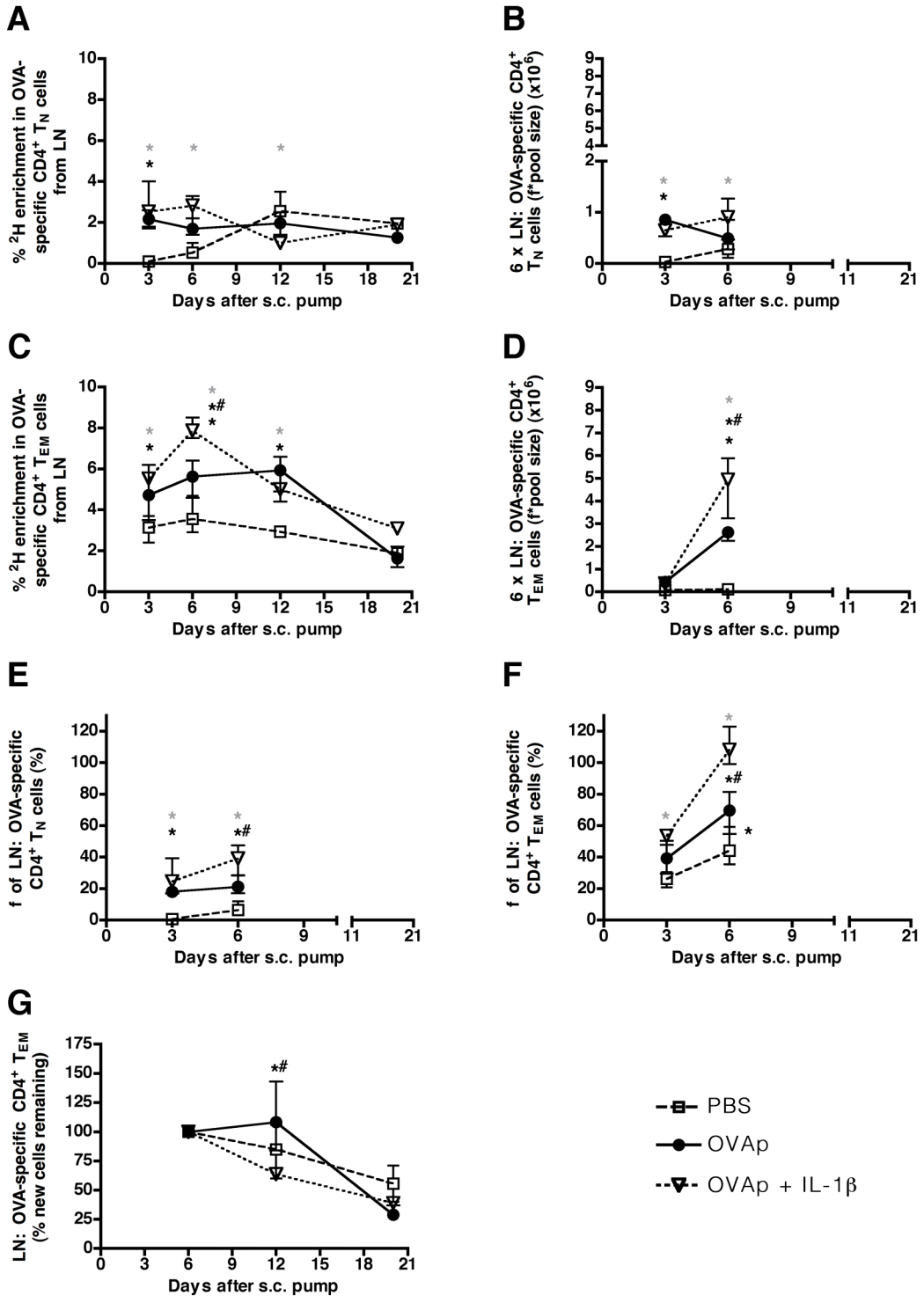

Figure 11. ^{2}H enrichment labelling profiles, as measured after *in vivo* $^{2}H_2O$ labelling of OVA-specific $CD4^+$ T cells in peripheral LNs following pump implantation. Mice were labelled orally with $^{2}H_2O$ provided in drinking water for the initial 72 hours that they carried s.c. mini-osmotic pumps delivering

PBS, OVAp or OVAp + IL-1β. The percentage of ^{2}H enrichment in DNA over time from OVA-specific $CD4^{+}$ **(A)** T_N or **(C)** T_{EM} cells from peripheral LNs of PBS, OVAp-, or OVAp + IL-1β-stimulated DO11.10 mice. The absolute numbers of labelled OVA-specific $CD4^{+}$ **(B)** T_N or **(D)** T_{EM} cells per 6 peripheral LNs (2 each of brachial, axillary and inguinal; the fraction of labelled cells was multiplied by the number of cells of the respective phenotype). The fraction of OVA-specific $CD4^{+}$ **(E)** T_N or **(F)** T_{EM} cells, and **(G)** the percentage of new OVA-specific $CD4^{+}$ T_{EM} cells remaining in LNs at the indicated times. Open squares: PBS group; filled circles: OVAp group; open inverted triangles: OVAp + IL-1β group. Data shown are from the same experiment as shown in Fig. 5. Shown are means and ranges. * $p<0.05$ PBS versus OVAp, grey asterix $p<0.05$ PBS versus OVAp + IL-1β, and $*^{\#}$ $p<0.05$ OVAp versus OVAp + IL-1β (two-way ANOVA for comparison of more than two groups with Bonferroni post-tests to compare replicate means per time point).

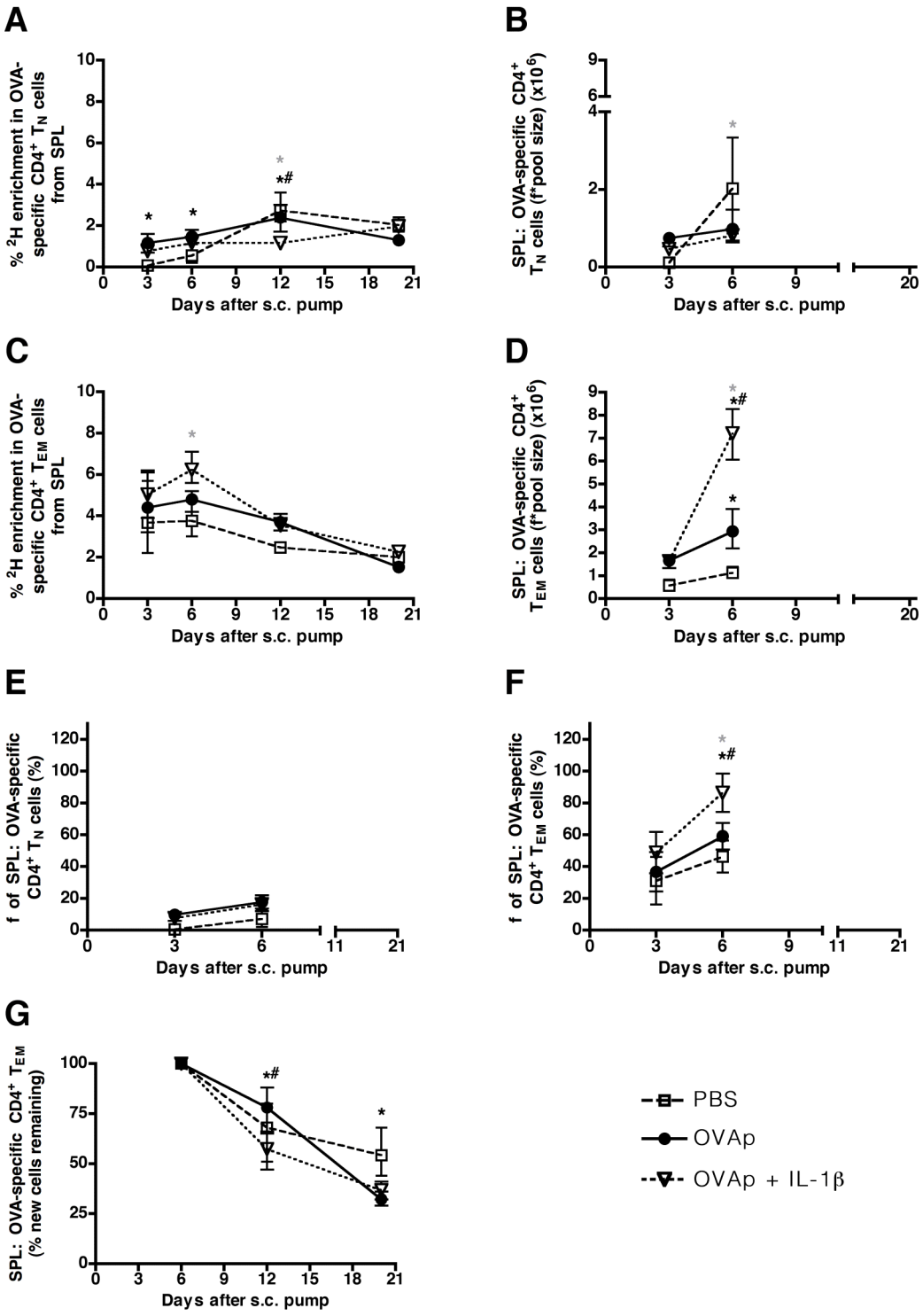

Figure 12. ^{2}H enrichment labelling profiles, as measured after *in vivo* $^{2}H_2O$ labelling of OVA-specific $CD4^+$ T cells in spleens following pump implantation. Mice were labelled orally with $^{2}H_2O$ provided in drinking water for the initial 72 hours that they carried s.c. mini-osmotic pumps delivering PBS, OVAp or OVAp and IL-1β. The percentage of ^{2}H enrichment in DNA over time from OVA-specific $CD4^+$ **(A)**

T_N or **(C)** T_{EM} SPL cells of PBS, OVAp-, or OVAp + IL-1β-stimulated DO11.10 mice. The absolute numbers of labelled OVA-specific $CD4^+$ **(B)** T_N or **(D)** T_{EM} per spleen (the fraction of labelled cells was multiplied by the number of cells of the respective phenotype). The fraction of OVA-specific $CD4^+$ **(E)** T_N or **(F)** T_{EM} cells, and **(G)** the percentage of new OVA-specific $CD4^+$ T_{EM} cells remaining in the spleen at the indicated times. Open squares: PBS group; filled circles: OVAp group; open inverted triangles: OVAp + IL-1β group. Data shown are from the same experiment as shown in Fig. 5. Shown are means and ranges. * $p<0.05$ PBS versus OVAp, grey asterix $p<0.05$ PBS versus OVAp + IL-1β, and $*^{\#}$ $p<0.05$ OVAp versus OVAp + IL-1β (two-way ANOVA for comparison of more than two groups with Bonferroni post-tests to compare replicate means per time point).

Subcutaneous antigenic stimulation without adjuvant leads to a rapid increase in the proportion and absolute number of $CD4^+$ T_{REG} cells in peripheral LNs.

Since $CD4^+$ T_{REG} can negatively impact upon T_N cell proliferation (Annacker, Pimenta-Araujo et al. 2001; Almeida, Legrand et al. 2002; Dahlberg, Schartner et al. 2007), they might be responsible for the relative suppression of T cell proliferation when OVA is provided in the absence of adjuvant. Indeed, an early and sustained increase in the fraction (Fig. 13A) and absolute number (Fig. 13B) of OVA-specific $CD4^+FoxP3^+$ T_{REG} cells was observed in LNs after the initiation of antigenic stimulation. A very early (day 3) fractional increase of $CD4^+$ $FoxP3^+$ T_{REG} cells was also observed in spleen (Fig. 13E). In a different experiment where an OVAp + IL-1β group of mice was not included, a large fraction of proliferating $Ki67^+$ OVA-specific $FoxP3^+CD4^+$ T_{REG} cells was observed in the peripheral LNs of OVAp-stimulated mice and was sustained through day 10 (Fig. 13C), during which time the frequency of $Ki67^+FoxP3^-$ OVA-specific $CD4^+$ T cells was returning to normal (Fig. 13D). Examples of flow cytometric data depicting FoxP3 against Ki67 expression in OVA-specific $CD4^+$ T cell populations are shown for representative mice from each group (Fig. 14). Of note, in mice that received OVAp without adjuvant, both the fraction and absolute number of T_{REG} cells in LNs remained elevated for more than 30 days when 4-week s.c. mini-osmotic pumps were implanted (data not shown). These findings suggest that, in mice given OVA without adjuvant compared to those receiving adjuvant, the induction of Ag-specific $FoxP3^+CD4^+$ T_{REG} cells is greater and more sustained.

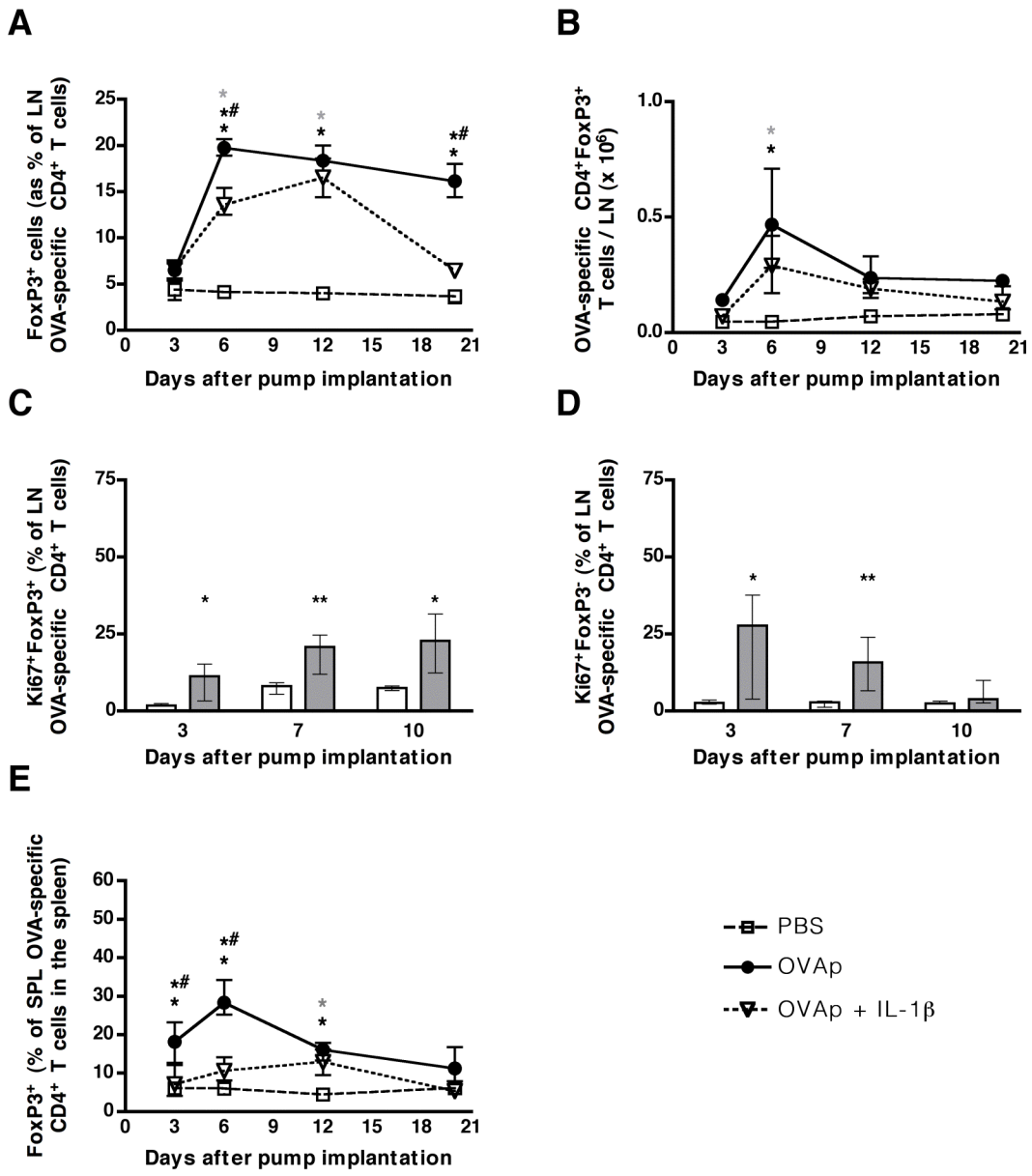

Figure 13. Early and sustained increases in LN FoxP3$^+$CD4$^+$ T_{REG} cells are observed after administration of s.c. OVAp in the absence of adjuvant. **(A)** The frequency of FoxP3$^+$CD4$^+$ T cells in peripheral LNs increased significantly early after pump implantation and remained high thereafter in OVAp only mice. **(B)** Although the frequency of FoxP3$^+$CD4$^+$ T cells remained high, their absolute number decreased to almost normal levels between days 6 and 12. **(C)** Bar graphs showing the percentage of OVA-specific CD4$^+$ T cells that are Ki67$^+$FoxP3$^+$ over time. **(D)** Bar graphs showing the percentage of OVA-specific CD4$^+$ T cells that are Ki67$^+$FoxP3$^-$ over time. **(E)** The percentage of OVA-specific CD4$^+$ T cells in the spleen positive for FoxP3. Open squares or white columns: PBS group; filled circles or grey columns: OVAp group; open inverted triangles: OVAp + IL-1β group. Data shown in **(A)**, **(B)** and **(E)** are from the same experiment as shown in Fig. 5. Data shown in **(C)** and **(D)** are

from 5 mice per group per time point, except for day 10 where the PBS group consisted of 4 mice. Shown in **(A)**, **(B)** and **(E)** are means and ranges and in **(C)** and **(D)** median values and IQRs. The latter data are representative of 2 similar experiments. * $p<0.05$ PBS versus OVAp, grey asterix $p<0.05$ PBS versus OVAp + IL-1β, and $*^{\#}$ $p<0.05$ OVAp versus OVAp + IL-1β (two-way ANOVA for comparison of more than two groups with Bonferroni post-tests to compare replicate means per time point or two-tailed non-parametric Mann-Whitney U Test for comparisons between two groups; ** $p<0.01$).

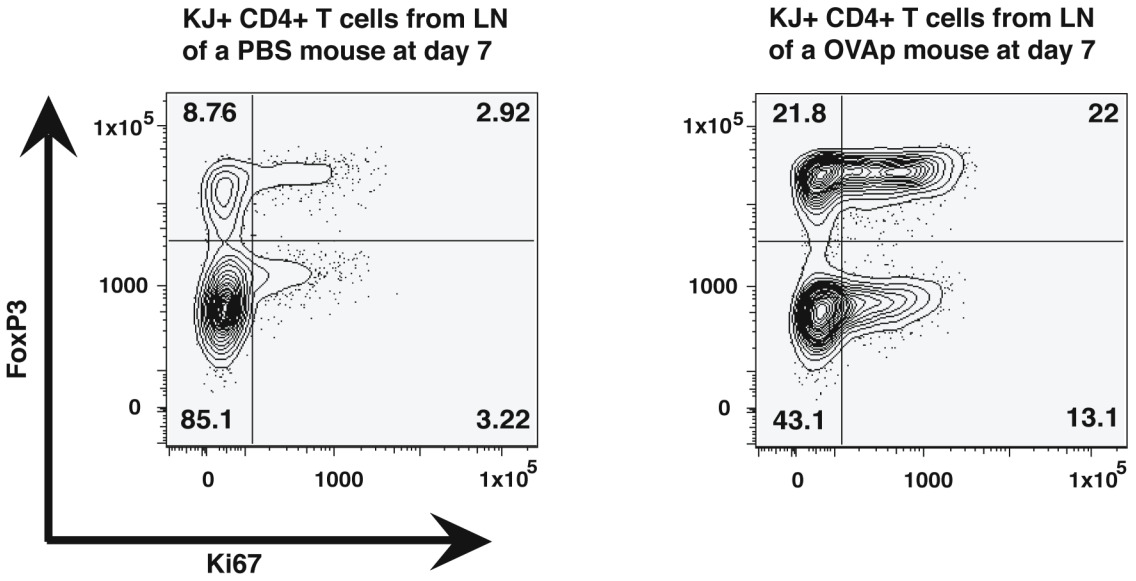

Figure 14. Representative flow cytometry plots showing the percentages of OVA-specific $CD4^+$ T cells from PBS or OVAp only mice that express or do not express Ki67 and/or FoxP3 at day 7 after pump implantation. The gating depicted here was used to calculate the data shown as bar graphs in Fig. 13C and 13D.

3.5 Discussion

The data in this chapter show that immunological tolerance through "aborted" immune activation rather than immunity is established in DO11.10 $CD4^+$ TCR tg mice after and during s.c. administration of peptide without adjuvant. Ag-specific $CD4^+$ T cells in mice that receive OVAp without adjuvant are initially primed, but both priming and peripheral expansion of Ag-specific T cells appear to be limited and confined to the peripheral LNs. This could potentially be due to a lack of T cell trafficking (Marelli-

Berg, Okkenhaug et al. 2007), perhaps related to differential regulation of activation marker expression (Shiow, Rosen et al. 2006) when peptide is given without or with adjuvant. Conversion of T_N to memory/effector phenotype T cell subsets was also limited and not sustained, and T_{REG} cells were induced and increased both numerically and relatively in peripheral LNs as well as relatively in PBMCs and spleen in mice that received peptide without adjuvant. In addition, a significant transient depletion of $CD4^+$ T cells was observed in mice that received peptide only and this might have contributed to immunological tolerance. The data described here also show that cognate Ag given with adjuvant leads to the systemic induction and expansion of all memory/effector phenotype T cell subsets studied (at the expense of naïve T cells) in $CD4^+$ TCR tg mice and that this immunological response is accompanied by typical symptoms such as scruffy fur and weight loss suggestive of a state of heightened immune activation. Furthermore, pumps were discontinued due to inflammation at the pump release site only in mice that received peptide with adjuvant.

The significant loss of Ag-specific $CD4^+$ T cells, especially T_N cells, in the peripheral blood of stimulated mice warranted further investigation. Thymic deletion of Ag-specific T cells could, at least in part, have been responsible for the peripheral loss of OVA-specific T_N cells, at least if the peptide or peptide-loaded APCs reached the thymus (Bonasio, Scimone et al. 2006). In the original paper using DO11.10 mice, for example, three relatively high dose i.p. injections of $OVA_{323-339}$ peptide induced thymic deletion by apoptosis (Murphy, Heimberger et al. 1990). In the current study, no significant differences were observed in the number of total, DP, $SPCD4^+$, or DN thymocytes in mice that received PBS versus those that received peptide without adjuvant. Also, even though mice that received peptide with adjuvant presented with transient thymic involution, which could have been due to a stress reaction associated with the observed weight loss (Table 1) (Hogquist, Baldwin et al. 2005) and/or due to direct effects of IL-1β (Morrissey, Charrier et al. 1988), their overall peripheral $CD4^+$ T cell numbers remained stable. Thus, it seems unlikely that the rapid loss of peripheral Ag-specific $CD4^+$ T cells in mice that received peptide without adjuvant was due to thymic deletion.

The rapid drop in OVA-specific $CD4^+$ T_N cells in the peripheral blood could instead have been due to

their redistribution to lymphoid tissues or the skin as the effector site, or to their increased differentiation into more mature T cell phenotypes. However, the increase in cellularity observed in the LNs of OVAp-stimulated mice was small, transient and insufficient to account for the massive decline of $CD4^+$ T_N cell numbers in the peripheral blood and spleen. This in contrast to mice that received OVAp + IL-1β where redistribution of differentiated $CD4^+$ T cells can explain the decrease in T_N cell numbers. More detailed examination of the increase in LN cellularity in OVAp-stimulated mice revealed that it was due in part to a small but significant numerical increase of T_E and T_{EM} cell subsets. It is known that both T_E and T_{EM} subsets show substantially lower capacity for further expansion than T_{CM} cells (Thomas, Brown et al. 2010), and a marked and sustained T_{CM} cell increase was only observed in the LNs and spleens of mice stimulated with OVAp + IL-1β. These observations suggest that effector memory T cells are generated by s.c. peptide administration without adjuvant in the LNs of TCR tg mice, but that such cells fail to differentiate into T_{CM} cells or populate the periphery in the absence of adjuvant. In addition, the small changes observed in LN cellularity and composition, and the fact that the skin at the pump release site remained intact in TCR tg mice that received peptide without adjuvant, suggest that peripheral T cell depletion in mice that received OVAp without adjuvant is not likely due to redistribution.

Low naïve T cell numbers in the periphery could also be explained by an expansion of $CD4^+$ T_{REG} cells, as these cells can inhibit proliferation of T cells (Annacker, Pimenta-Araujo et al. 2001; Almeida, Legrand et al. 2002; Dahlberg, Schartner et al. 2007). Indeed, the loss of OVA-specific $CD4^+$ T cells from the blood and spleen was accompanied by a fractional increase of T_{REG} cells in the blood and spleen as well as a fractional and numerical increase of T_{REG} cells in peripheral LNs. This finding supports the notion that $OVA_{323-339}$ peptide has high agonist activity and may convert some naïve T cells into T_{REG} cells (Apostolou and von Boehmer 2004; Kretschmer, Apostolou et al. 2005; Polansky, Kretschmer et al. 2008; Daniel, Weigmann et al.) or preferentially select T_{REG} cells in the thymus (Jordan, Boesteanu et al. 2001). Of note, while proliferation of FoxP3-negative Ag-specific $CD4^+$ T cells returned to normal by day 10, proliferation of $FoxP3^+$ Ag-specific $CD4^+$ T cells remained elevated, which may indicate that the latter were maintained in high numbers due to continuous turnover. Thus,

to the extent that $CD4^+$ T_{REG} cells may play a role in naïve T cell homeostasis (Annacker, Pimenta-Araujo et al. 2001; Almeida, Legrand et al. 2002), the $CD4^+$ T cell depletion observed after administration of peptide without adjuvant may, at least in part, be attributable to their induction.

Finally, the possibility was explored that the T cell depletion observed in these experiments might be due to one or more forms of Ag-induced T cell activation: "functional" activation leading to the expansion of Ag-specific $CD4^+$ T cells followed by AICD (Green, Droin et al. 2003) and "aborted" activation that would be accompanied by a more limited number of rounds of cell division before AICD. It has been proposed that AICD might also contribute to the establishment of peripheral tolerance (Kabelitz and Janssen 1997). We carried out *in vivo* stable isotope labelling in mice that received OVAp without adjuvant, OVAp with IL-1β or PBS continuously by s.c. mini-osmotic pump. As expected, ^2H enrichment was higher in classical effector memory T_{EM} than T_N phenotype T cells (Tough and Sprent 1994). Interestingly, similar to T_N phenotype T cells from human peripheral blood (Hellerstein, Hoh et al. 2003), ^2H enrichments increased over time in T_N cells from peripheral LNs and spleen of control mice that received only PBS. This increase possibly reflects the movement of cells labelled in the thymus to these peripheral lymphoid tissues. In both LNs and spleen, the rate of proliferation and loss of Ag-specific $CD4^+$ T_{EM} cells was highest in mice that received OVAp together with IL-1β, even though Ki67 expression at the same time points was lower than in mice that received OVAp alone. This may indicate that most of the cell division in mice that received OVAp + IL-1β had already occurred before day 3, the earliest time point at which cells were examined for Ki67 expression or label enrichment, and that peak labelling of T_{EM} cells from OVAp + IL-1β mice was mostly due to conversion of labelled T_N cells. Interestingly, Ki67 expression was close to absent in T cells derived from the spleens of mice from all groups, but Ki67 expression was detected in LNs, even though cells in the spleen showed similar label enrichment to those from peripheral LNs. In theory, one could explain this result if cells were labelled before they populated the spleen. T_N and T_{EM} cells in the LNs of mice that received OVAp only showed high Ki67 expression, but also incorporated more label at early time points than T_N and T_{EM} cells in LNs of mice that received PBS, indicating that cells

were dividing. In contrast to mice that received OVAp + IL-1β, label was not lost as rapidly from LN-derived T_{EM} cells from mice that received OVAp without IL-1β. This could have been due to cells being stuck in cell cycle (Ki67 could still be expressed in this case, as it is expressed in all stages of the cell cycle except for G_0 (Scholzen and Gerdes 2000)) and lack of trafficking of labelled T cells to other peripheral lympoid tissues such as the spleen or the skin as the effector site. This could explain, at least in part, why splenomegaly was observed in mice that received OVAp + IL-1β, but not in those that received OVAp alone. This finding would also be in line with "aborted T cell activation", as it would indicate that sustained rounds of cell proliferation leading to expansion of the T cell pool were not induced by peptide alone. Lymphopenia-induced proliferation (Martin, Bourgeois et al. 2003; Neujahr, Chen et al. 2006; Voehringer, Liang et al. 2008) in mice that received OVAp without adjuvant probably did not account for the proliferation profile observed in these mice, as peripheral $CD4^+$ T cell depletion was not yet significant at days 3 and 6, the days when Ki67 expression was highest. T_{REG} cells have been shown to have high proliferation rates (Vukmanovic-Stejic, Zhang et al. 2006) and often display a memory phenotype (Rallon, Lopez et al. 2009). Therefore, it is also possible that proliferation of T_{REG} cells contributed to a great extent to the label enrichments observed in T_{EM} cells from mice that received OVAp without adjuvant. In support of this, at early time points, 40% of $CD25^{high}FoxP3^+$ T_{REG} cells in LNs of mice that received peptide only expressed Ki67, which was approximatey twice as high as in mice that received peptide with adjuvant (data not shown). Given these data, we can most conservatively conclude that functional T cell activation leading to T cell expansion did not occur after stimulation of mice with peptide only. Instead, continued s.c. infusion of OVAp was associated with cells in the LNs that entered cell cycle, then most likely retained label and remained $Ki67^+$, but did not divide or exit the LNs, and eventually underwent cell death possibly due to lack of survival signals and / or degradation of the peptide in the pumps. Of note, in the original article where the DO11.10 tg TCR model was described, *in vitro* Ag sensitivity of the transgenic T cells appeared to be greatest for $OVA_{323-339}$ rather than the other altered peptide ligands tested, but proliferation tailed off with higher doses of this peptide (Murphy, Heimberger et al. 1990). Having speculated that the peptide concentration could have dropped due to degradation of the peptide in the pumps, we assessed

stability of the peptide under different conditions and found that OVAp in PBS was most stable when kept sterile in the fridge for 20 days and less stable when kept sterile at 37 ºC (Fig. 15).

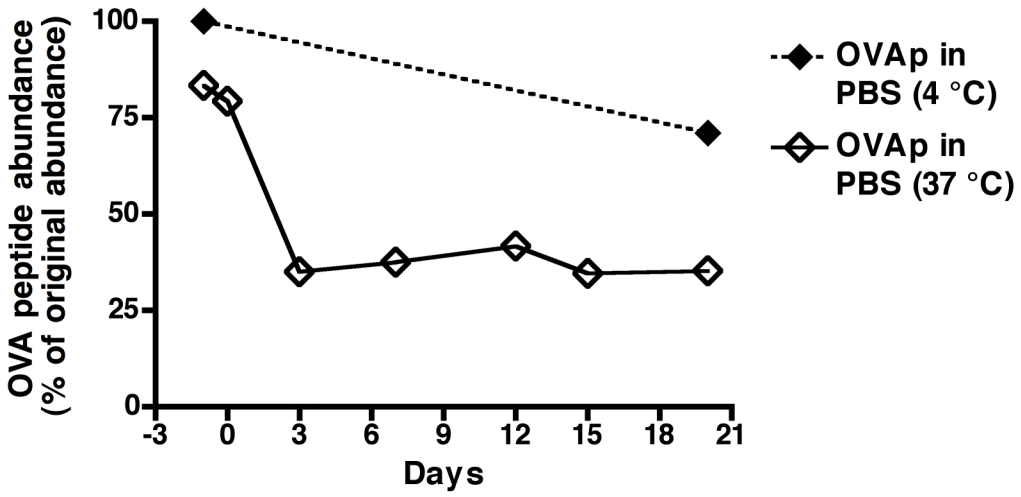

Figure 15. OVAp in PBS is most stable when kept sterile at 4 ºC and degrades to some extent when kept sterile at 37 ºC, especially during the first 3 days. Peptide concentrations were measured using MS by the company (Biopeptide, CA, USA) that synthesized the peptide. The percentage of original abundance was calculated.

The peptide concentration appeared to be much lower in the remaining pump content removed from pumps that were implanted s.c. in mice (data not shown). The latter was very likely skewed due to measurement errors when very small volumes are analyzed and due to the fact that the pump content was not sterile anymore after the pumps were explanted and opened to retrieve the content, which could have resulted in increased degradation of the peptide during transit before analysis at the company that synthesized the peptide.

The results described here are in line with the finding from a previous study that continuous s.c. administration of Ag using osmotic pumps to TCR tg mice on a Rag-deficient background led to the induction of Ag-specific suppressor T cells (Apostolou and von Boehmer 2004). These data are also consistent with studies demonstrating that serial s.c. administration of peptide in a non-inflammatory

context leads to the induction of T_{REG} cells (Dahlberg, Schartner et al. 2007). However, these results are dissimilar to those of Switzer *et al.*, who reported that Ag-specific tolerance did not develop in 2B4 TCR tg mice given peptide without adjuvant by s.c. osmotic pumps (Switzer, Wallner et al. 1998). There may be several reasons for this discrepancy, the most important being that Switzer *et al.* administered a much higher dose of peptide and only examined *ex vivo* responsiveness of Ag-specific $CD4^+$ T cells, as opposed to the kinetics of cell division *in vivo*.

In summary, this study shows that continuous s.c. administration of peptide without adjuvant leads to the induction of a form of immunological tolerance that could be called aborted activation, with the predominant mechanisms at play being very limited memory T cell expansion, transient peripheral deletion, lack of T_{CM} cell generation, possible insufficient egress of T cells from the peripheral LNs, and the induction of T_{REG} cells. These findings suggest that continuous s.c. administration of peptide without adjuvant can lead to persistent immunologic tolerance *in vivo*. In addition, this study shows that a systemic expansion of memory/effector-phenotype T cells (at the expense of T_N cells) is observed when peptide is given with adjuvant even in TCR tg mice with a non-physiological and extremely high Ag-specific precursor frequency.

CHAPTER

4

In vivo turnover of human CD57$^+$ and CD57$^-$ memory CD8$^+$ T cells in HIV-infected subjects and healthy volunteers

4.1 Introduction

A better understanding of the human memory T cell compartment is needed to advance the development of protective T cell vaccines. In HIV infection, increasing evidence suggests that qualitative rather than quantitative measures of Ag-specific T cell responses provide the key to antiviral efficacy (Gea-Banacloche, Migueles et al. 2000; Betts, Nason et al. 2006; Appay, van Lier et al. 2008). An important prerequisite for long-term immunological T cell memory appears to be a long lifespan or the potential for long-term self-renewal within a subset of memory T cells. Recent evidence indicates that increased rates of clonal senescence and succession in immunodominant HIV-specific CD8$^+$ T cell populations are associated with progressive loss of immune control in HIV infection (Almeida, Price et al. 2007). Replicative senescence and loss of dominant clonotypes can have disastrous effects on the immune system (Davenport, Fazou et al. 2002). Although CD57 expression has been associated with CD8$^+$ T cell senescence (Brenchley, Karandikar et al. 2003), a recent study found that most CD57$^+$ T cells do not express PD-1 (Petrovas, Chaon et al. 2009), a marker expressed by exhausted T cells (Day, Kaufmann et al. 2006; Freeman, Wherry et al. 2006; Petrovas, Casazza et al. 2006; Trautmann, Janbazian et al. 2006). Most CD57$^+$ cells display the highly differentiated RA$^+$CD28$^-$CCR7$^-$ CD8$^+$ effector memory RA revertant (T_{EMRA}) phenotype, and T_{EMRA} cells appear to have a long lifespan (Ladell, Hellerstein et al. 2008). It has also been shown that CD57$^+$ memory CD8$^+$ T cells exert protective effects associated with the progressive acquisition of cytolytic activity (Kern, Khatamzas et al. 1999; van Leeuwen, Gamadia et al. 2002; Le Priol, Puthier et al. 2006; Chong, Aicheler et al. 2008; Chattopadhyay, Betts et al. 2009). Furthermore, it has been reported that CD57$^+$ CD8^{high} T cells are enriched for Ag-specific cells that exert a

regulatory function, in that they are capable of down-modulating cytolytic activity (Mollet, Sadat-Sowti et al. 1998). The highest fraction of $CD57^+$ cells is found within the T_{EMRA} phenotype. T_{EMRA} cells have also been associated with immune senescence (Nociari, Telford et al. 1999), but this again is controversial because many Ag-specific cells with anti-viral activity reside within this phenotypic compartment (Appay, van Lier et al. 2008). Furthermore, a larger proportion and absolute number of HIV-specific T_{EMRA} cells in early HIV infection has been linked to the control of HIV viremia and, indeed, predicted the subsequent viral load set point (Northfield, Loo et al. 2007); such cells are also more frequently detectable in controlled compared to progressive HIV infection (Addo, Draenert et al. 2007). *Ex vivo*, using non-specific stimuli, $CD57^+$ memory $CD8^+$ T cells appear to proliferate much less than other memory T cell subsets (Brenchley, Karandikar et al. 2003). However, it is not known whether these cells proliferate *in vivo*. They may require a certain microenvironment or specific stimuli, such as cognate Ag. Here, as a first step towards learning more about this subset of T cells, the lifespan and proliferation rates of $CD57^+$ memory $CD8^+$ T cells were investigated *in vivo* in humans with or without chronic viral infections using non-toxic ^2H-glucose or ^2H_2O labelling.

4.2 Hypothesis

$CD57^+$ memory $CD8^+$ T cells proliferate less than $CD57^-$ memory $CD8^+$ T cells.

4.3 Specific Aim

To study *in vivo* the turnover (rates of proliferation and cell death) of $CD57^+$ memory $CD8^+$ T cells and $CD57^-$ memory $CD8^+$ T cells.

4.4 Results

After 7 weeks of $^{2}H_2O$ labelling, high fractions of $CD3^+CD8^+CD45RA^-CCR7^-$ T cells that were either $CD57^+$ or $CD57^-$ incorporated deuterium. However, the $CD57^-$ cells appeared to loose label more rapidly than the $CD57^+$ cells after labelling was discontinued (Fig. 16A and 16B). Half-lives were calculated between sort 0 and sort 1 (when label enrichments differed the most between T cell populations) using the formula for exponential decay for $CD3^+CD8^+CD45RA^-CCR7^-CD57^-$ T cells from all four HIV-infected individuals (half-life in days, 31 (open triangles), 32 (inverted open triangles), 33 (open squares), 84 (open circles)) and for $CD3^+CD8^+CD45RA^-CCR7^-CD57^+$ T cells from three HIV-infected individuals, as for one individuals the label enrichment at sort 0 was not available (half-life in days, 342 (open triangles), 167 (open squares), 696 (open circles)). For such small sample sizes, non-parametric statistical tests are not powerful and paramtetric statistical test are not robust. Therefore, both, the two-tailed Student's t-test and the two-tailed Mann Whitney U Test were carried out to determine whether the above stated half-lives are significantly different. The half-lives of $CD3^+CD8^+CD45RA^-CCR7^-CD57^-$ T cells were significantly lower than those of $CD3^+CD8^+CD45RA^-CCR7^-CD57^+$ T cells when the Student's t-test was used ($p=0.042$). There was no significant difference when the Mann Whitney U Test was used ($p=0.057$). The formula for exponential decay should not really be used for half-life calculations between sorts 0 and 1, as sort 0 was done during the last week of labelleing and sort 1 was done three weeks after labelling was stopped and this time frame is considered the ^{2}H wash-out phase (body water during this time may still be enriched with ^{2}H). Half-lives calculated between subsequent sorts (e.g. between sorts 1 and 2) were not significantly different. The reasoning behind initially studying $CD3^+CD8^+CD45RA^-CCR7^-CD57^+$ or $CD3^+CD8^+CD45RA^-CCR7^-CD57^-$ T cells was that T_{EMRA} phenotype T cells would contribute substantially to the labelled population if they were included, because almost all of the cells with this phenotype express CD57, and T_{EMRA} labelling data has already been published (Ladell, Hellerstein et al. 2008). In two healthy subjects who received short-term oral ^{2}H-glucose labelling and in whom the whole memory $CD8^+$ T cell compartment was divided into $CD57^+$ and $CD57^-$ cells, deuterium incorporation in $CD57^+$ memory phenotype $CD8^+$ T cells was low (Fig. 17 and Fig. 18). In one of the

two healthy subjects, deuterium incorporation was higher in $CD57^-$ memory phenotype $CD8^+$ T cells at days 4 and 10 (Fig. 17); in the other subject, deuterium enrichment appeared ("appeared, as the replicate values for this time point were variable) to be higher in $CD57^-$ memory phenotype $CD8^+$ T cells at day 4 (Fig. 18). In both healthy subjects, deuterium enrichment in $CD57^+$ memory phenotype $CD8^+$ T cells appeared to rise at the latest time point (21 days post-labelling). The characteristics of study subjects are shown in Table 2.

Table 2. Characteristics of study subjects.

Group	Symbol	Age	VL (copies / ml)	Years HIV-infected	CD4 count / μl of blood	CD8 count / μl of blood	^2H_2O labeling (weeks)	^2H-glucose labeling (hours)	CMV Ig
HIV-negative	Black diamond	27	-	-	586	376	7	ND	-
	#	ND	-	-[$]	1377	769	ND	10	ND
	#	ND	-	-[$]	1060	357	ND	10	ND
HIV-infected (not on HAART)	Inverted open triangles	40	2,059	NA	852	3388	7	ND	+
	Open Circles	38	30,851	NA	431	1646	7	ND	+
	Open Squares	36	448,343	NA	349	2445	7	ND	+
	Open triangles	53	74,199	NA	330	1397	7	ND	+

Stated in the relevant Figure legends. VL, viral load; [$] low risk, as assessed by risk assessment; ND, not done.

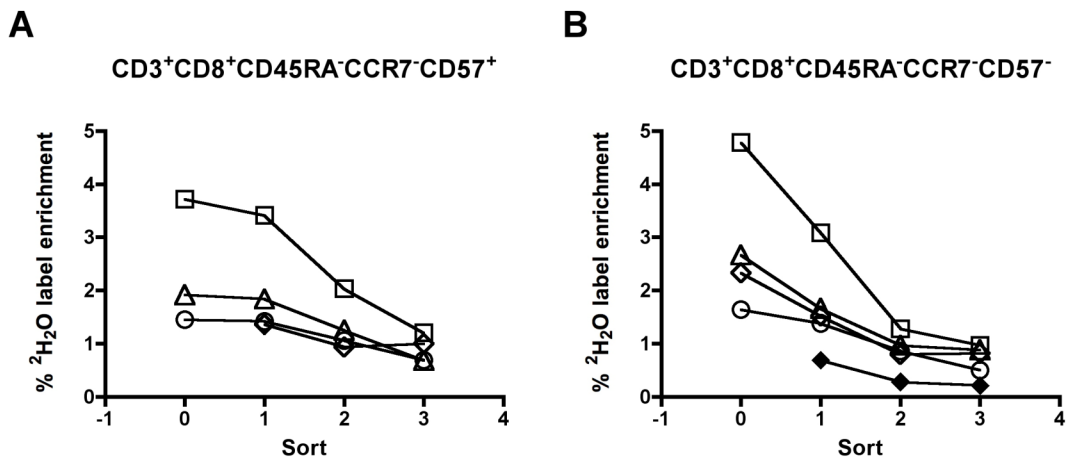

Figure 16. Raw labelling data from 4 HIV-infected subjects (open symbols) and 1 HIV non-infected subject (closed symbols) labelled for 7 weeks with deuterated (^2H_2O) water. Sort 0 was performed during the last week of labelling to determine maximum label enrichment in the two distinct T cell subsets. Sort 1 was performed 3 weeks after labelling was discontinued, as label remains present in the body water for this length of time. Sorts 2 and 3 were performed at successive one-month intervals. Cells were sorted on a BD FACS Digital Vantage or a BD FACS Aria I. DNA was extracted, hydrolyzed and derivatized, and label enrichment was assessed by gas chromatography mass spectrometry.

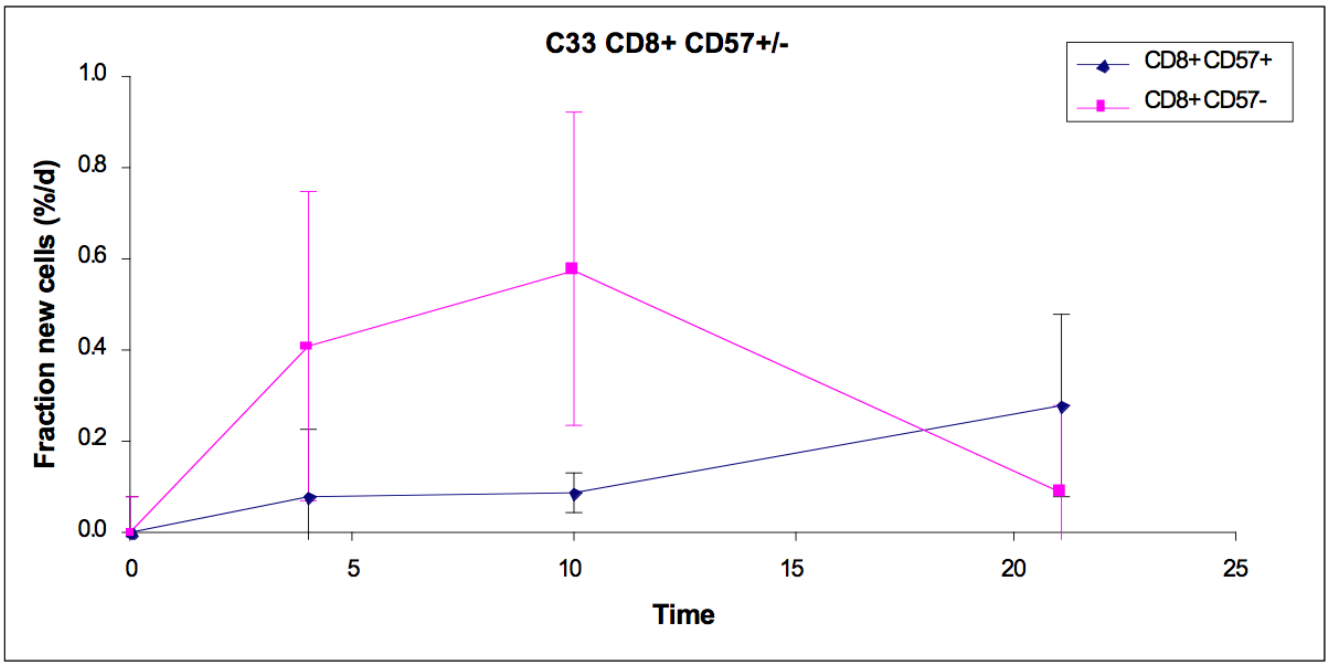

Figure 17. Label incorporation in memory phenotype $CD8^+CD57^+$ (filled blue diamonds) or memory

phenotype $CD8^+CD57^-$ (filled pink squares) T cells from healthy subject C33 labelled for 10 hours orally with ^{2}H-glucose. Sort samples were collected on days 4, 10 and 21. Cells were sorted on a customized 20-parameter BD FACSAria II. DNA was extracted, hydrolyzed and derivatized, and label enrichment was assessed by gas chromatography mass spectrometry.

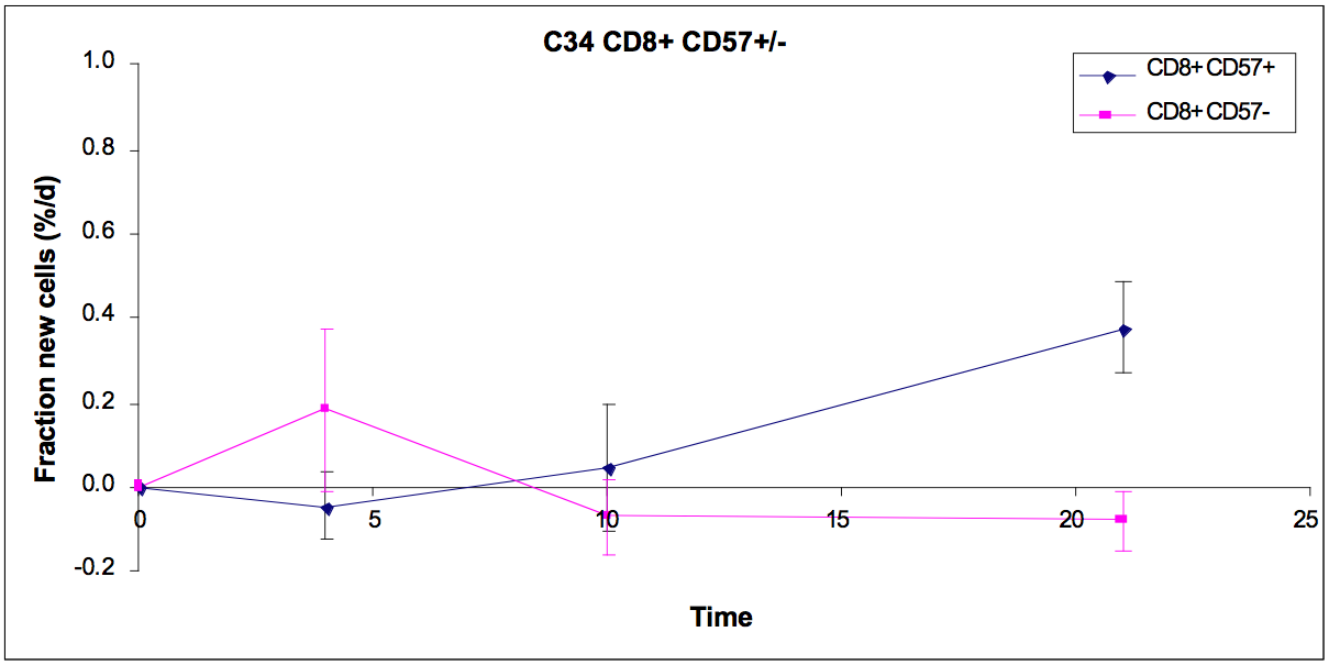

Figure 18. Label incorporation in memory phenotype $CD8^+CD57^+$ (filled blue diamonds) or memory phenotype $CD8^+CD57^-$ (filled pink squares) T cells from healthy subject C34 labelled for 10 hours orally with ^{2}H-glucose. Sort samples were collected on days 4, 10 and 21. Cells were sorted on a customized 20-parameter BD FACSAria II. DNA was extracted, hydrolyzed and derivatized, and label enrichment was assessed by gas chromatography mass spectrometry.

4.5 Discussion

Stable isotope labelling with ^{2}H-glucose or ^2H_2O in humans is a very sophisticated technique for the measurement of lymphocyte turnover *in vivo* (Macallan, Fullerton et al. 1998; Neese, Misell et al. 2002). Importantly, this type of labelling is non-toxic and can be carried out safely in humans over long periods of time without side effects (Neese, Misell et al. 2002). In combination with fluorescence activated cell sorting (FACS) and mass spectrometric (MS) analysis, *in vivo* studies with this

labelling technique have shown that the turnover of bulk $CD8^+$ T cells is increased in HIV-infected individuals and that this increase in turnover takes place mainly in memory/effector $CD8^+$ T cell subpopulations (Mohri, Perelson et al. 2001; Hellerstein, Hoh et al. 2003). More recently, as described above, it was shown that central memory $CD8^+$ T cells are preferentially lost and that more differentiated CD45RA-expressing effector $CD8^+$ T cells accumulate in HIV-infected subjects (Ladell, Hellerstein et al. 2008). Until recently, analytic limitations (for example cell numbers below detection limits and low isotope enrichments) have made it difficult to measure directly the lifespan of Ag-specific T cell subpopulations. However, recent refinements to the stable isotope/FACS/MS method now allow reliable measurements from fewer than 50,000 cells (Busch, Neese et al. 2007; Ladell, Hellerstein et al. 2008).

The preliminary data from a pilot long-term *in vivo* ^2H_2O labelling study carried out in HIV-infected subjects showed that high fractions of $CD8^+$ $CD45RA^-CCR7^-$ T cells that were either $CD57^+$ or $CD57^-$ incorporated deuterium after labelling for 7 weeks and that the $CD8^+$ $CD45RA^-CCR7^-CD57^-$ cells appeared to loose label more rapidly compared to the $CD8^+$ $CD45RA^-CCR7^-CD57^+$ cells after labelling was discontinued. Although these findings may be interpreted in different ways, some features of the data suggest that the $CD8^+$ $CD45RA^-CCR7^-CD57^-$ cells may be precursors of the $CD57^+$ cells. Possible interpretations of the data include: (i) high label enrichment at the end of the 7-week ^2H_2O labelling period could be due either to a high rate of proliferation in the two T cell phenotypes or to labelled cells from an earlier differentiation phenotype entering these phenotypes; (ii) the higher label enrichment at the end of the labelling period (sort 0 in Fig. 16) in the $CD57^-$ cells may indicate that they proliferate more than the $CD57^+$ cells; and, (iii) stable label in $CD57^+$ cells during the wash-out phase (= during the three weeks after labelling was stopped) may indicate that remaining label in the circulation is still being incorporated or that previously labelled cells from an earlier differentiation state enter this phenotype. Alternatively, label could be stably retained because the labelled cells do not divide or die during this short period of time. This latter possibility may be the most likely, as the “true” de-labelling curves (the curves excluding data from sort 0, as body water would have still been enriched with deuterium between sort 0 and sort 1 (during the wash-out

phase) of the $CD57^+$ cells appear to be slightly less steep than those of the $CD57^-$ cells.

Levels of deuterium incorporation in $CD57^+$ memory phenotype $CD8^+$ T cells were low in the two healthy subjects labelled short-term with ^2H-glucose, which suggests slow turnover of these cells. In one of the two subjects, deuterium incorporation was higher in $CD57^-$ memory phenotype $CD8^+$ T cells at both days 4 and 10, which is in line with higher turnover rates for these cells compared to their $CD57^+$ counterparts. However, deuterium incorporation was also low in $CD57^-$ memory phenotype $CD8^+$ T cells from the other subject (Fig. 18), and this may be a hint that short-term ^2H-glucose labelling is not the ideal approach to study turnover of these T cell subsets (longer labelling might be necessary to get more reliable results). Interestingly, enrichment in $CD57^+$ memory phenotype $CD8^+$ T cells appeared to rise at the latest time point studied (21 days post-labelling), which would be consistent with phenotype transition from $CD57^-$ to $CD57^+$, although other explanations are also possible. Other explanations for increased enrichment in a cell population at a later time point include the movement of cells with a particular phenotype from one compartment to another, e.g. from lymphoid or extravascular tissue into the peripheal blood, or the death of unlabeled cells, which would make enrichment of the remaining cells appear higher artificially. These data are preliminary. Taken together, however, it appears to be the case that $CD57^+$ memory phenotype $CD8^+$ T cells indeed show low/slow turnover and that this population is either fed by a "younger“ pool of memory phenotype $CD8^+$ T cells or that $CD57^+$ memory phenotype $CD8^+$ T have a longer lifespan than their CD57-negative counterparts.

CHAPTER

5

Interleukin-10 maintains latent murine cytomegalovirus infection by restricting the expansion and function of memory CD8$^+$ T cells

5.1 Introduction

Human cytomegalovirus (HCMV) is a β-herpesvirus that infects approximately 70% of the human population. Although primary HCMV infection is typically asymptomatic, it causes multi-organ disease in unborn children and immune compromised seronegative adults (Sweet 1999). HCMV also establishes a latent infection that is generally well contained by healthy hosts. However, in individuals with impaired immune function, such as transplant recipients receiving immunosuppressive drugs, latent virus can reactivate and induce severe clinical disease (Riddell 1995; Fishman, Emery et al. 2007). Furthermore, indirect effects such as acute and chronic graft rejection can be triggered by these events (Fishman, Emery et al. 2007).

CD8$^+$ T cells are critical mediators of antiviral immune responses to HCMV. Viral reactivation in immunosuppressed individuals is associated with a numerical and functional impairment of virus-specific CD8$^+$ T cells (Quinnan, Kirmani et al. 1982; Reusser, Riddell et al. 1991), and adoptive transfer of CD8$^+$ T cells affords protection from virus reactivation and viremia (Riddell, Watanabe et al. 1992; Walter, Greenberg et al. 1995; Einsele, Roosnek et al. 2002; Cobbold, Khan et al. 2005). In addition, using the murine CMV (MCMV) model of infection, it has been shown that adoptive transfer of CD8$^+$ T cells protects immunosuppressed hosts from infection (Reddehase, Weiland et al. 1985; Reddehase, Mutter et al. 1987; Reddehase, Jonjic et al. 1988; Podlech, Holtappels et al. 1998). Critically, MCMV reactivation from latency is also controlled by CD8$^+$ T cells (Polic, Hengel et al. 1998).

CMV-specific CD8$^+$ T cells expand to unusually high frequencies in immune competent humans and mice (Gillespie, Wills et al. 2000; Sylwester, Mitchell et al. 2005), a phenomenon that has been termed

"memory inflation" (Karrer, Sierro et al. 2003). During MCMV infection, the memory $CD8^+$ T cell pool consists of "stable" memory T cells that are present at low numbers and "inflationary" memory T cell populations that expand to high frequencies as infection progresses (Holtappels, Pahl-Seibert et al. 2000; Karrer, Sierro et al. 2003; Munks, Cho et al. 2006). Inflation of memory T cells is Ag-dependent (Snyder, Cho et al. 2008), and phenotypic analysis suggests that these cells are highly differentiated and have recently been exposed to Ag (Holtappels, Pahl-Seibert et al. 2000; Appay, Dunbar et al. 2002; van Leeuwen, Gamadia et al. 2002; Sierro, Rothkopf et al. 2005; Munks, Cho et al. 2006); thus, it appears that periodic viral reactivation events drive the expansion of these cells. However, it is unclear whether immunological factors also regulate this process.

IL-10 is an immune regulatory cytokine that suppresses T cell responses primarily via effects mediated on APCs; specifically, IL-10 inhibits the expression of pro-inflammatory cytokines and chemokines, MHC class II and costimulatory molecules by APCs (Moore, O'Garra et al. 1993; O'Garra, Barrat et al. 2008). During viral infections, IL-10 has paradoxical functions. In models of acute influenza (Sun, Beilke et al. 2009) and herpes simplex infection (Sarangi, Sehrawat et al. 2008), IL-10 limits immunopathology. In contrast, IL-10 antagonizes protective immunity following high dose influenza challenge (McKinstry, Strutt et al. 2009) and MCMV persistence in the salivary glands (Humphreys, de Trez et al. 2007). Moreover, IL-10 induction during chronic lymphocytic choriomeningitis virus infection promotes functional dysregulation of T cells and lymphopenia, thereby enabling prolonged viral replication (Brooks, Trifilo et al. 2006; Ejrnaes, Filippi et al. 2006). The expression of a functional IL-10 ortholog (vIL-10) by HCMV indicates the importance of IL-10 in the suppression of HCMV-specific immunity (Kotenko, Saccani et al. 2000; Slobedman, Barry et al. 2009). Intriguingly, in vitro experiments have demonstrated vIL-10 gene expression during latent HCMV infection (Jenkins, Abendroth et al. 2004) and suggest that vIL-10 may inhibit memory CD4 T cell recognition of latently infected cells (Cheung, Gottlieb et al. 2009). To date, however, nothing is known regarding the role of IL-10 in the regulation of CMV-specific memory T cell responses in vivo.

5.2 Hypotheses

- The anti-inflammatory cytokine IL-10 reduces memory T cell inflation during MCMV infection.
- The anti-inflammatory cytokine IL-10 inhibits memory T cells during chronic/latent MCMV infection.

5.3 Specific Aims

- To study the effect of IL-10 on memory T cell inflation during MCMV infection.
- To determine the effect of IL-10 on the functional and phenotypic characteristics of memory $CD8^+$ T cells, including Ag-specific memory $CD8^+$ T cells, using two approaches: (i) MCMV-infected knockout ($IL\text{-}10^{-/-}$) mice; and, (ii) IL-10 receptor blockade.

5.4 Results

IL-10 limits memory $CD8^+$ T cell expansion during MCMV infection

In our C57BL/6 mouse model of MCMV infection, productive replication (data not shown) and late viral gene expression (Fig. 19A) were undetectable in the spleen and lung by 60 days post-infection. In contrast, viral DNA was present in both organs and virus could reactivate ex vivo in cultures of spleen and lung isolated as late as 110 days post-infection (Fig. 19B), thereby suggesting that MCMV persisted in these organs primarily in the form of latent virus.

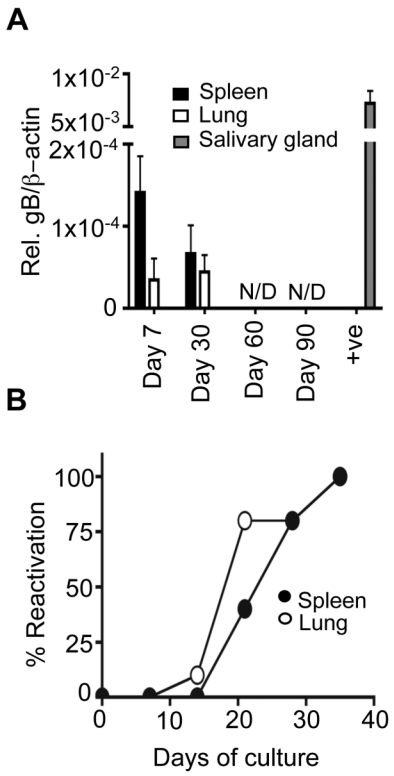

Figure 19. MCMV latency is established by day 60 post-infection. **(A)** RNA was extracted from the spleen and lung, and gB (glycoprotein B) expression was measured by quantitative RT-PCR at days 7 (n=3), 30 (n=5), 60 (n=4) and 90 (n=4) post-MCMV infection. The positive control comprised RNA extracted from salivary glands at day 7 post-infection. Results are expressed as mean +/- SEM. N/D, not detected. **(B)** Spleens (filled circles) and lungs (open circles) from MCMV-infected mice at day 100 post-infection were mashed and incubated for 35 days. Every 7 days, the presence of replicating virus was detected by plaque assay. Results are shown as % organ pieces with viral reactivation from 5 mice per group. The data in this figure and this figure were produced by co-investigators.

Despite the absence of detectable MCMV replication from day 60, expression of IL-10 in the spleen (but not lung) was increased compared with uninfected mice (Fig. 20A). Flow cytometric analyses revealed IL-10 protein production by splenic IFN-γ^+IL-17$^-$ MCMV-specific CD4$^+$ T cells after peptide stimulation directly ex vivo (Fig. 20B). The frequency of IL-10-producing cells within MCMV-specific CD4$^+$ T cell populations was substantially higher than that observed in IFN-γ^- CD4$^+$ T cells (3.7-8.3%, mean = 6.3 versus 0.08-0.3%, mean = 0.19%; $p < 0.01$). Splenic B cells (CD19$^+$) and monocytes/macrophages (CD11b$^+$) derived from mice 90 days post-infection were also capable of

producing IL-10 following ex vivo non-specific stimulation; in the case of $CD11b^+$ cells, but not $CD19^+$ cells, this MCMV-associated IL-10 production was significantly increased compared to cells derived from naïve mice (Fig. 20C).

The hypothesis was that IL-10 acts to inhibit systemic and mucosal antiviral T cell responses during MCMV infection. To test this, the accumulation of both "stable" memory $CD8^+$ T cells specific for a peptide derived from the M45 protein that is immunodominant during acute infection and "inflationary" memory $CD8^+$ T cells specific for peptides derived from the M38, m139 and IE3 proteins (Munks, Cho et al. 2006) were measured in both wild-type C57BL/6 and IL-$10^{-/-}$ mice. Expression of these viral proteins in infected cells is thought to occur during productive replication rather than viral latency (Munks, Cho et al. 2006; Munks, Gold et al. 2006). During acute infection, there were comparable numbers of MCMV-specific $CD8^+$ T cells in the lungs and spleens of wild-type and IL-$10^{-/-}$ mice (Fig. 20D); furthermore, as infection progressed, the numbers of M45-specific memory $CD8^+$ T cells remained low in the absence of IL-10 (Fig. 20D). Consistent with previously published data (Munks, Cho et al. 2006), high frequencies of $CD8^+$ T cells specific for M38, m139 and IE3 were observed in wild-type mice at day 90 post-infection; strikingly, however, the corresponding frequencies at the same time-point were even higher in IL-$10^{-/-}$ mice (Fig. 20D). The accumulation of IE3-specific $CD8^+$ T cells was most notable, representing ~15% of all $CD8^+$ T cells in IL-$10^{-/-}$ mice at day 90 post-infection (Fig. 20E) and reaching up to 30% in some individual mice (data not shown).

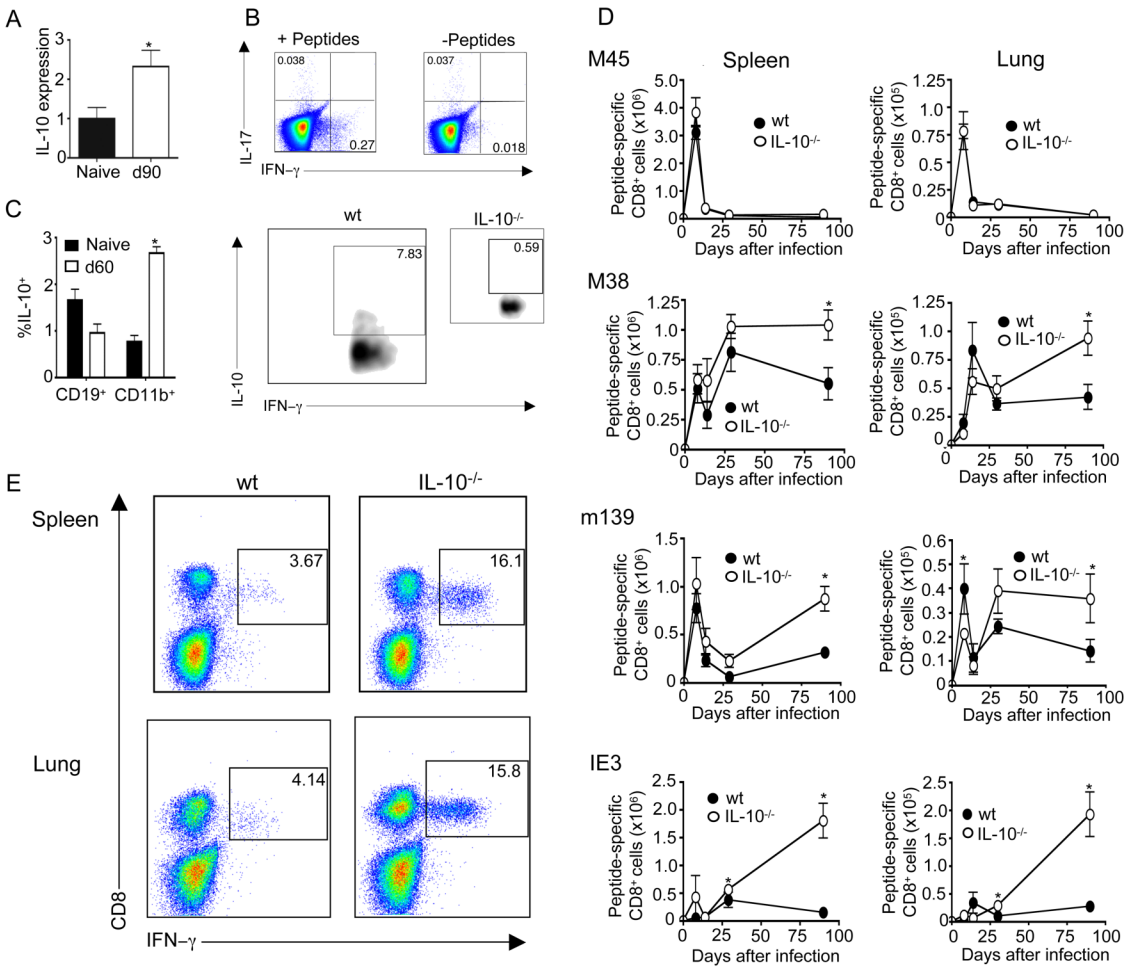

Figure 20. IL-10 limits memory CD8$^+$ T cell inflation during MCMV infection. **(A)** IL-10 expression in spleen extracts from naive C57BL/6 wild-type (wt) mice and wt mice infected for 90 days with MCMV was measured by quantitative RT-PCR and normalized to β-actin. Results represent the mean +/- SEM of four mice from two independent experiments. * p <0.05 with the Mann-Whitney U-test. **(B)** IFN-γ and IL-17 expression by CD4$^+$ T cells derived from spleens of wt mice 90 days post-infection (top panels) following ex vivo stimulation for 16 hours with (top left panel) or without (top right panel) m09, M25, m139 and m142 peptides. Values in quadrants represent percent cytokine$^+$CD4$^+$ cells. Expression of IL-10 by IFN-γ$^+$ peptide-specific CD4$^+$ T cells from wt (bottom left panel) and IL-10$^{-/-}$ (bottom right panel) mice. Quadrants were set using fluorescence minus one controls. Results are representative of two experiments, each comprising four mice per group. **(C)** IL-10 expression by splenic CD19$^+$ and CD11b$^+$ cells derived from naïve (closed bars) and MCMV-infected (day 60 post-infection; open bars) mice following ex vivo stimulation with LPS and PMA/ionomycin (CD19$^+$) or LPS alone (CD11b$^+$). Results are shown as the mean +/- SEM derived from two independent experiments, each comprising four mice per group. *Ex vivo* stimulation of B cells from MCMV-infected mice (day 90 post-infection) did not induce significant apoptosis (6.6 +/- 0.4% AnnV$^+$) as compared with freshly

isolated $CD19^+$ cells (8.2 +/- 2.2% $AnnV^+$). **(D and E)** Wt (closed circles) and IL-$10^{-/-}$ (open circles) mice were infected with MCMV and peptide-specific $CD8^+$ T cells were quantified by intracellular IFN-γ detection. **(D)** Numbers of $CD8^+$ T cells specific for M38, M45, m139 and IE3 on days 0, 7, 14, 30 and 90 post-infection in spleen (left) and lung (right). Results are expressed as mean +/- SEM cells/organ of four to six mice per group, and each time-point represents four to seven experiments. * p <0.05 with Student's t-test. **(E)** Representative bivariate flow cytometry plots showing IFN-γ expression by IE3-reactive $CD8^+$ T cells in the spleens (top panels) and lungs (bottom panels) of wt (left panels) and IL-$10^{-/-}$ (right panels) mice at day 90 post-infection. The percent $CD8^+$ T cells expressing IFN-γ is shown; gates were set using the fluorescence minus one control for FITC. Results are representative of seven experiments, each comprising four to six mice per group. These data were generated in collaboration with Dr. Ian Humphreys and his laboratory.

IL-10 limits the oligoclonal expansion of IE3-specific $CD8^+$ T cells

To investigate further the profound expansion of IE3-specific $CD8^+$ T cells, a comprehensive and unbiased analysis of T cell receptor (TCR) gene usage was undertaken within the cognate populations isolated directly *ex vivo* from both wild-type and IL-$10^{-/-}$ mice (Fig. 21 and, for complete data set, Fig. 22). In both sets of mice at day 90 post-infection, the IE3-specific TCR repertoires were oligoclonal and highly skewed towards the usage of only a few dominant clonotypes; this is consistent with previous studies of HCMV-specific $CD8^+$ T cell populations (Price, Brenchley et al. 2005). Moreover, a diverse array of clonotypic structures was apparent in both wild-type and IL-$10^{-/-}$ mice, although with a strong bias towards TRBV16 usage (Fig. 21 and Fig. 22). Similar patterns were observed as late as day 282 post-infection, at which time IE3-specific $CD8^+$ T cells dominated the response in IL-$10^{-/-}$ mice (Figs. 23, 24 and 25). In addition, a substantial degree of differentially encoded inter-individual TCR sharing was apparent (Figs. 21, 22, 24 and 25); this is consistent with recent studies demonstrating the role of convergent recombination in the generation of "public" clonotypes, which can affect the outcome of infection in certain circumstances (Venturi, Price et al. 2008; Price, Asher et al. 2009). Overall, these data suggest that the enhanced inflation of IE3-specific $CD8^+$ T cells in IL-$10^{-/-}$ mice is due to the expansion of clonotypes selected within the memory pool rather than the recruitment of greater numbers of cognate clonotypes from the naïve pool (Vezys, Masopust et al. 2006).

A

TRBV	CDR3	TRBJ	Freq (%)
16	CASSLGTGDTQY	2-5	64.04
16	CASSLDSGVAEQF	2-1	35.96

TRBV	CDR3	TRBJ	Freq (%)
16	CASSFTGYAEQF	2-1	29.33
16	CASSLDSGNSDYT	1-2	25.33
12-1	CASSPWGVQDTQY	2-5	20.00
12-1	CASSLRDSYTGQLY	2-2	13.33
19	CASSPHRGQEQY	2-7	4.00
16	CASSPGTKNTGQLY	2-2	2.67
12-2	CASSPGLGGYEQY	2-7	2.67
16	CASSFGTGDTQY	2-5	2.67

TRBV	CDR3	TRBJ	Freq (%)
16	CASSLGTGDTQY	2-5	57.14
12-1	CASSLTGGREQY	2-7	22.22
12-1	CASSLRDSYTGQLY	2-2	12.7
16	CASSPRQANTGQLY	2-2	4.76
16	CASSLDGVEQY	2-7	3.17

B

TRBV	CDR3	TRBJ	Freq (%)
16	CASSLDSGVGTQY	2-5	63.29
16	CASSFGTGDTQY	2-5	27.85
29	CASSLRRVYEQY	2-7	2.53
16	CASSLDSGAGTQY	2-5	1.27
16	CASSLDSGLAEQF	2-1	1.27
13-1	CASSDPGLGYEQY	2-7	1.27
16	CASSFGAGDTQY	2-5	1.27
16	CASSFGTGDAQY	2-5	1.27

TRBV	CDR3	TRBJ	Freq (%)
12-2	CASSTDTYQDTQY	2-5	33.33
16	CASSLDSGMTDYT	1-2	28.99
16	CASSLGTGDEQY	2-7	13.04
1	CTCSAEGLGGYEQY	2-7	5.80
26	CASSLDRNTGQLY	2-2	5.80
14	CASSFLGYEQY	2-7	4.35
12-2	CASSPGLGGGEQY	2-7	2.90
16	CASSLDGGGEQY	2-7	2.90
16	CASSLDGQAPL	1-5	2.90

TRBV	CDR3	TRBJ	Freq (%)
16	CASSLDSGNSDYT	1-2	85.00
12-2	CASSSTGPNTGQLY	2-2	10.00
2	CASSQDLGVVNQDTQY	2-5	5.00

Figure 21. Oligoconal expansion of IE-3 specific $CD8^+$ T cells during MCMV infection. TCRB CDR3 amino acid sequences, TCRBV (TCRB variable) and TCRBJ (TCRB joining) usage, and the relative frequencies of individual clonotypes within viable $CD3^+CD8^+$IE3-tetramer$^+$ cell populations isolated by flow cytometric sorting from wt **(A)** and IL-$10^{-/-}$ **(B)** mice at day 90 post-MCMV infection. Three representative mice are shown per group; coloured boxes represent shared clonotypes that were detected in other individual mice. The full data set is shown in Fig. 22; analyses from later time-points are shown in Fig. 24 (day 142 post-infection) and Fig. 25 (day 282 post-infection).

A

TRBV	CDR3	TRBJ	Freq (%)
16	CASSLGTGDTQY	2-5	64.04
16	CASSLDSGVAEQF	2-1	35.96

TRBV	CDR3	TRBJ	Freq (%)
16	CASSFTGYAEQF	2-1	29.33
16	CASSLDSGNSDYT	1-2	25.33
12-1	CASSPWGVQDTQY	2-5	20.00
12-1	CASSLRDSYTGQLY	2-2	13.33
19	CASSPHRGQEQY	2-7	4.00
16	CASSPGTKNTGQLY	2-2	2.67
12-2	CASSPGLGGYEQY	2-7	2.67
16	CASSFGTGDTQY	2-5	2.67

TRBV	CDR3	TRBJ	Freq (%)
16	CASSLGTGDTQY	2-5	57.14
12-1	CASSLTGGREQY	2-7	22.22
12-1	CASSLRDSYTGQLY	2-2	12.7
16	CASSPRQANTGQLY	2-2	4.76
16	CASSLDGVEQY	2-7	3.17

TRBV	CDR3	TRBJ	Freq (%)
16	CASSLDSGNERLF	1-4	28.30
16	CASSLRGADTGQLY	2-2	5.66
16	CASSLDNFAETLY	2-3	3.77
16	CASSLGVGLEEQY	2-7	3.77
13-1	CASRLGVGAETLY	2-3	3.77
1	CTCSADGGEQF	2-1	3.77
1	CTCSADSANSYNSPLY	1-6	1.89
12-2	CAISELGQISNERLF	1-4	1.89
1	CTCSADPGNSGNTLY	1-3	1.89
16	CASSLDSGKRKAYI	1-4	1.89
14	CASSFQTGGYAEQF	2-1	1.89
13-2	CASGDDGGSAETLY	2-3	1.89
12-2	CASSLDGHSSYEQY	2-7	1.89
1	CTCSAGLGGLAEQF	2-1	1.89
31	CAWSQDRGNQAPL	1-5	1.89
15	CASSYWGSSYEQY	2-7	1.89
15	CASSLTGGDAEQF	2-1	1.89
14	CASSFAGDPGQLY	2-2	1.89
13-3	CASRGLGGKNTLY	2-4	1.89
12-2	CASSLSLGADTQY	2-5	1.89
12-2	CASSLGQGGDEQY	2-7	1.89
12-2	CASSRDNANSDYT	1-2	1.89
3	CASSPGTGGDEQY	2-7	1.89
29	CASSGGAGNTLY	1-3	1.89
17	CASSSRAQDTQY	2-5	1.89
13-1	CASSADTNTEVF	1-1	1.89
13-1	CASSDRSQNTLY	2-4	1.89
31	CAGQISNERLF	1-4	1.89
29	CASSFTNSDYT	1-2	1.89
14	CASSHGQYEQY	2-7	1.89
14	CASSLGDAEQF	2-1	1.89
3	CASSLPGEQF	2-1	1.89
13-1	CASRQGEVF	1-1	1.89

B

TRBV	CDR3	TRBJ	Freq (%)
16	CASSLDSGGSGTQY	2-5	77.33
13-1	CASSGTGGAEQF	2-1	14.67
16	CASSLWGGGSAETLY	2-3	6.67
16	CASSLDSGGSGAQY	2-5	1.33

TRBV	CDR3	TRBJ	Freq (%)
16	CASSFNGYAEQF	2-1	81.92
24	CASSLGGLKDTQY	2-5	6.21
29	CASSSGQGYNSPLYFA	1-6	2.82
12-1	CASSPRWGGAETLY	2-3	1.69
12-2	CASSPGLGGYEQY	2-7	1.69
12-2	CASSLGTGGKGNTLY	1-3	1.13
16	CASSLDSGHQAPL	1-5	1.13
26	CASSWTTNSDYT	1-2	1.13
13-1	CASSDGISYNSPLY	1-6	0.56
13-1	CASSDLEANTEVF	1-1	0.56
31	CAWGTGGNTEVF	1-1	0.56
3	CASSLAIGNTLY	1-3	0.56

TRBV	CDR3	TRBJ	Freq (%)
16	CASSLDSGVGTQY	2-5	63.29
16	CASSFGTGDTQY	2-5	27.85
29	CASSLRRVYEQY	2-7	2.53
16	CASSLDSGAGTQY	2-5	1.27
16	CASSLDSGLAEQF	2-1	1.27
13-1	CASSDPGLGYEQY	2-7	1.27
16	CASSFGAGDTQY	2-5	1.27
16	CASSFGTGDAQY	2-5	1.27

TRBV	CDR3	TRBJ	Freq (%)
12-2	CASSTDTYQDTQY	2-5	33.33
16	CASSLDSGMTDYT	1-2	28.99
16	CASSLGTGDEQY	2-7	13.04
1	CTCSAEGLGGYEQY	2-7	5.80
26	CASSLDRNTGQLY	2-2	5.80
14	CASSFLGYEQY	2-7	4.35
12-2	CASSPGLGGGEQY	2-7	2.90
16	CASSLDGGGEQY	2-7	2.90
16	CASSLDGQAPL	1-5	2.90

TRBV	CDR3	TRBJ	Freq (%)
16	CASSLDSGNSDYT	1-2	85.00
12-2	CASSSTGPNTGQLY	2-2	10.00
2	CASSQDLGVVNQDTQY	2-5	5.00

Figure 22. Clonotypic analysis of IE3-specific CD8$^+$ T cell populations at day 90 post-MCMV infection. TCRB CDR3 amino acid sequences, TCRBV and TCRBJ usage, and the relative frequencies of individual clonotypes within viable CD3$^+$CD8$^+$IE3-tetramer$^+$ cell populations isolated by flow cytometric sorting from wt **(A)** and IL-10$^{-/-}$ **(B)** mice at day 90 post-MCMV infection. Coloured boxes depict shared

clonotypes that were detected in other individual mice.

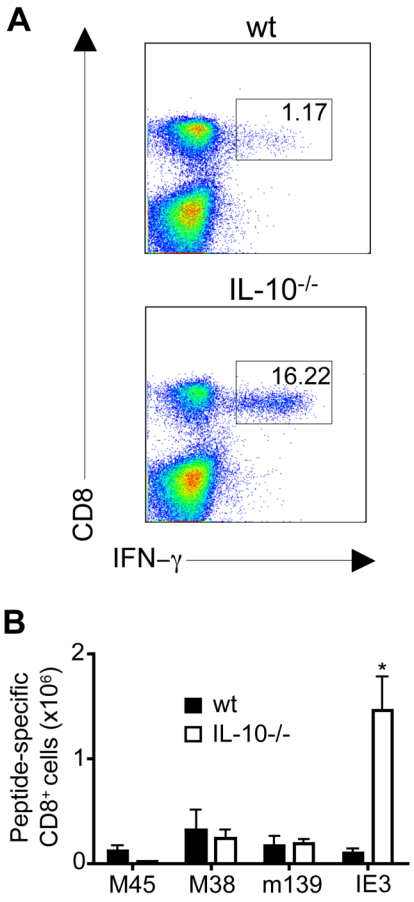

Figure 23. Increased accumulation of IE3-specific $CD8^+$ T cells in IL-$10^{-/-}$ mice 10 months post-infection. Wt (closed bars) and IL-$10^{-/-}$ (open bars) mice were infected with MCMV; peptide-specific $CD8^+$ T cells were detected by IFN-γ expression 282 days later. **(A)** Representative bivariate flow cytometry plots showing IFN-γ expression by IE3-specific $CD8^+$ T cells from spleens of wt (top panel) and IL-$10^{-/-}$ (bottom panel) mice. **(B)** Splenic peptide-specific $CD8^+$ T cells were enumerated. Results are expressed as mean +/- SEM of three to four mice per group and are representative of 2 independent experiments. Significance is indicated by *, which represents p <0.05 with Student's t-test. These data were generated in collaboration with Dr. Ian Humphreys and his laboratory.

A

TRBV	CDR3	TRBJ	Freq (%)
16	CASSLGTGDTQY	2-5	34.88
16	CASSLDSGFAEQF	2-1	16.28
16	CASSSGTGDTQY	2-5	10.47
16	CASSLDSGINTLY	2-4	8.14
13-3	CASSWDRANSDYT	1-2	5.81
14	CASSFLGQYAEQF	2-1	3.49
16	CASSPGTGDTQY	2-5	3.49
12-2	CASSAGWEQY	2-7	3.49
17	CASSSIGTGDAGQF	2-1	2.32
24	CASSLSNSQNTLY	2-4	2.32
5	CASSQETGGVNQDTQY	2-5	1.16
29	CASSPDRVPSGNTLY	1-3	1.16
16	CASSLDSGVAEQF	2-1	1.16
16	CASSLDAGDSDYT	1-2	1.16
13-3	CASSNRGRNSDYT	1-2	1.16
13-2	CASGPGTGGYEQY	2-7	1.16
3	CASSLRDRNSDYT	1-2	1.16
13-3	CASTGGNYAEQF	2-1	1.16

B

TRBV	CDR3	TRBJ	Freq (%)
16	CASSLDAGVGEQY	2-7	91.78
13-3	CASSEDWANYAEQF	2-1	2.74
16	CASSLAAGYAEQF	2-1	1.37
16	CASSFGNYAEQF	2-1	1.37
12-1	CASSLGAGGPQY	2-5	1.37
1	CTCSAGYEQY	2-7	1.37

TRBV	CDR3	TRBJ	Freq (%)
13-1	CASSEQEVF	1-1	30.49
16	CASSLDSGWGTQY	2-5	29.27
12-1	CASSPGHNYAEQF	2-1	14.63
3	CASSLVGTGKDTQY	2-5	12.2
2	CASSQEWGRNSDYT	1-2	10.98
16	CASSLDAGVGEQY	2-7	1.22
13-3	CASSDPGNERLF	1-4	1.22

TRBV	CDR3	TRBJ	Freq (%)
16	CASSLDSGFAEQF	2-1	45.33
13-1	CASSEQEVF	1-1	24.00
1	CTCSPRGRGRAEQF	2-1	4.00
1	CTCSAVANTGQLY	2-2	4.00
3	CASSLAGWGSSQNTLY	2-4	2.67
16	CASSLGTGGAAEQF	2-1	2.67
16	CASSLDAGVGEQY	2-7	2.67
16	CASSLDSGWGTQY	2-5	2.67
16	CASSLASGVAEQF	2-1	2.67
12-1	CASSPGTSYAEQF	2-1	2.67
16	CASSLDSGLAEQF	2-1	1.33
12-1	CASSPGHNYAEQF	2-1	1.33
3	CASSATISNERLF	1-4	1.33
5	CASSPTGNTEVF	1-1	1.33
16	CASSEFYEQY	2-7	1.33

Figure 24. Clonotypic analysis of IE3-specific $CD8^+$ T cell populations at day 142 post-MCMV infection. TCRB CDR3 amino acid sequences, TCRBV and TCRBJ usage, and the relative frequencies of individual clonotypes within viable $CD3^+CD8^+$IE3-tetramer$^+$ cell populations isolated by flow cytometric sorting from wt **(A)** and IL-$10^{-/-}$ **(B)** mice at day 142 post-MCMV infection. Coloured boxes depict shared clonotypes that were detected in other individual mice.

A

TRBV	CDR3	TRBJ	Freq (%)
16	CASSSGTGDTQY	2-5	31.48
16	CASSLDSGWAEQF	2-1	27.78
12-1	CASSPGHNYAEQF	2-1	9.26
13-1	CASRDREDTGQLY	2-2	7.41
16	CASSPTGGNTEVF	1-1	5.56
15	CASSLGWGGYEQY	2-7	3.70
16	CASSLDGQAETLY	2-3	1.85
16	CACSLDSGWAEQF	2-1	1.85
12-1	CASSGLGDFYEQY	2-7	1.85
12-1	CASSPGHDYAEQF	2-1	1.85
17	CASSRGGNYAEQF	2-1	1.85
16	CASSLGTGDTQY	2-5	1.85
20	CGALQGGDTEVF	1-1	1.85
13-3	CASSGVNTEVF	1-1	1.85

TRBV	CDR3	TRBJ	Freq (%)
16	CASSLGTGDTQY	2-5	82.22
4	CASSFWGSQNTLY	2-4	6.67
3	CASSLTGGSYEQY	2-7	4.44
26	CASSLHRGNSDYT	1-2	2.22
15	CASSFGTEGAEQF	2-1	2.22
12-1	CASSLGGANTLY	2-4	2.22

B

TRBV	CDR3	TRBJ	Freq (%)
16	CASSLDAGTAEQF	2-1	86.81
15	CASSLGTANTGQLY	2-2	10.99
16	CASSLGTGDEQY	2-7	2.20

TRBV	CDR3	TRBJ	Freq (%)
16	CASSLDSGISDYT	1-2	73.03
16	CASSLDSGAAEQF	2-1	26.97

Figure 25. Clonotypic analysis of IE3-specific $CD8^+$ T cell populations at day 282 post-MCMV infection. TCRB CDR3 amino acid sequences, TCRBV and TCRBJ usage, and the relative frequencies of individual clonotypes within viable $CD3^+CD8^+$IE3-$tetramer^+$ cell populations isolated by flow cytometric sorting from wt **(A)** and IL-$10^{-/-}$ **(B)** mice at day 282 post-MCMV infection. Coloured boxes depict shared clonotypes that were detected in other individual mice.

Enhanced MCMV-specific $CD4^+$ T cell and professional APC accumulation in IL-$10^{-/-}$ mice during MCMV infection

$CD4^+$ T cells promote MCMV-specific memory $CD8^+$ T cell expansion (Humphreys, Loewendorf et al. 2007; Snyder, Loewendorf et al. 2009). Therefore, the accumulation of virus-specific memory $CD4^+$ T cell populations was measured in wild-type and IL-$10^{-/-}$ mice, investigating previously described distinct $CD4^+$ T cell populations with specificities for four different viral proteins (m09, M25, m139, m142) that are associated with active viral replication (Arens, Wang et al. 2008). Interestingly, it was found that enhanced $CD8^+$ T cell accumulation in IL-$10^{-/-}$ mice at day 90 post-infection was accompanied by a large increase in the number of IFN-γ-expressing $CD4^+$ T cells in the spleen (Fig. 26A and 26B) and lung (Fig. 26C and 26D), detected following *ex vivo* stimulation with MCMV-derived

MHC class II-restricted peptides (Fig. 26A and 26C) or PMA and ionomycin (Fig. 26B and 26D). IL-10 can inhibit $CD4^+$ T cells by suppressing the function of professional APCs (Moore, O'Garra et al. 1993; O'Garra, Barrat et al. 2008) and MCMV-induced IL-10 inhibits MHC class II expression (Redpath, Angulo et al. 1999). In accordance, more splenic DCs (Fig. 26E and 26F), splenic inflammatory monocytes (Fig. 26G), and pulmonary macrophages (Fig. 26H) were observed in IL-$10^{-/-}$ mice compared to wild-type mice. In contrast, B cell accumulation was comparable in spleens and lungs of wild-type and IL-$10^{-/-}$ mice (data not shown).

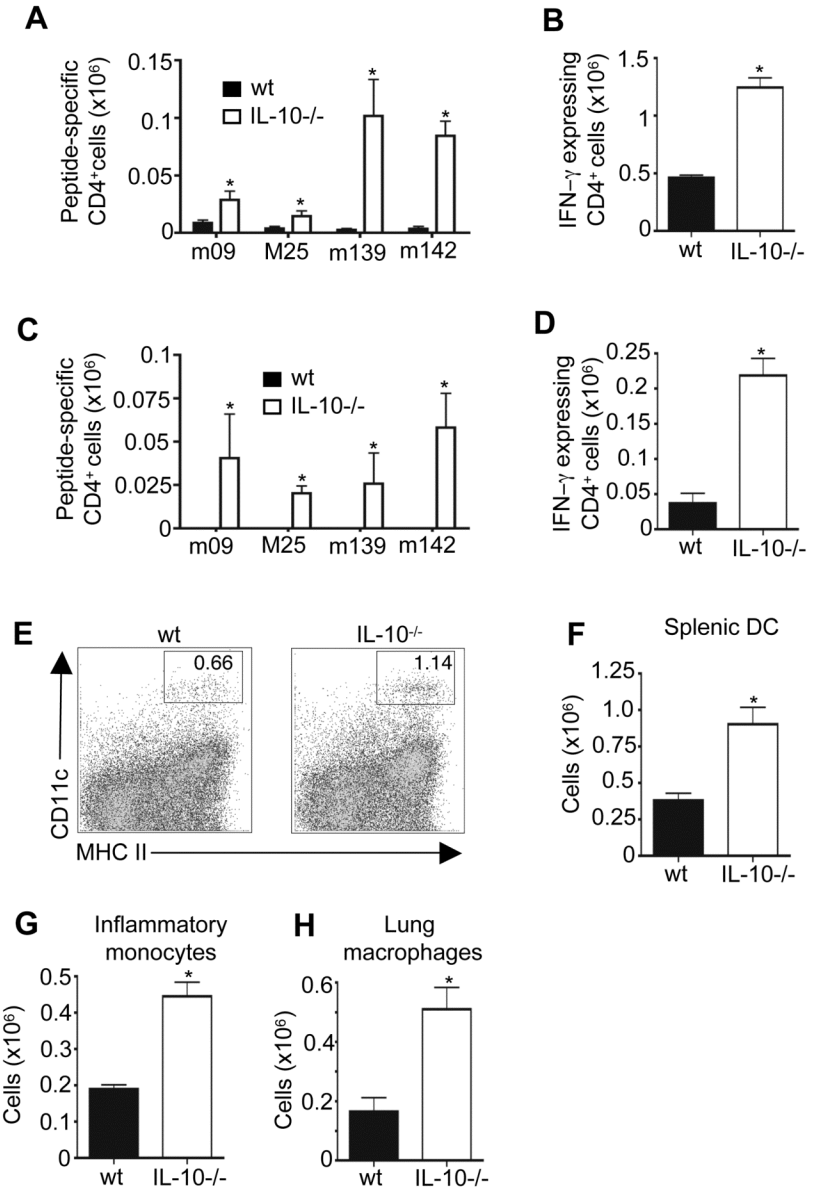

Figure 26. Elevated $CD4^+$ T cell accumulation at day 90 following MCMV infection of IL-$10^{-/-}$ mice.

IFNγ-expressing $CD4^+$ T cells in the spleens **(A, B)** and lungs **(C, D)** of wt (closed bars) and IL-$10^{-/-}$ (open bars) mice at day 90 post-infection following stimulation with peptide **(A, C)** or PMA and ionomycin **(B, D)**. Undetectable virus-specific $CD4^+$ T cells were expressed as an arbitrary value of 1 cell for statistical analyses. **(E)** Representative flow cytometric analyses of splenic $CD11c^{hi}MHCII^+$ dendritic cells from wt (left panel) and IL-$10^{-/-}$ (right panel) mice at day 90 post-infection. Splenic $CD11c^{hi}MHCII^+$ dendritic cells **(F)**, $CD11b^+CD11c^-Gr1^{lo/-}7/4^+$ monocytes **(G)**, and lung $CD11c^{int}CD11b^+Gr1^{lo/-}F4/80^+$ macrophages (**H**) from wt (closed bars) and IL-$10^{-/-}$ (open bars) mice at day 90 post-infection were enumerated. Results represent mean +/- SEM of two to three independent experiments, each comprising four mice per group. * p <0.05 with Student's t-test. These data were generated in collaboration with Dr. Ian Humphreys and his laboratory.

IL-10 inhibition of $CD8^+$ T cell memory occurs during acute and chronic/latent MCMV infection

MCMV-specific memory $CD8^+$ T cell populations are derived both from cells primed during acute infection and from more recent thymic emigrants (Snyder, Cho et al. 2008). Given that IL-10 is expressed during acute MCMV infection (Arens, Wang et al. 2008; Oakley, Garvy et al. 2008; Walton, Wyrsch et al. 2008; Madan, Demircik et al. 2009), and enhances $CD4^+$ (Oakley, Garvy et al. 2008) and, in some models, $CD8^+$ T cell responses (Madan, Demircik et al. 2009), the time point at which IL-10 exerts its inhibitory effect was examined next.

Blockade of IL-10R signalling during initial T cell priming using a monoclonal antibody at the time of infection did not significantly influence $CD8^+$ T cell numbers specific for M38 and m139 at day 96 post-infection (Fig. 27A). However, IE3-specific $CD8^+$ T cells, which are generally undetectable in the first week of infection (Munks, Cho et al. 2006; Snyder, Cho et al. 2008), were enhanced ~2-fold at the day 96 time point (Fig. 27A). This was accompanied by a transient expansion of MCMV-specific $CD4^+$ T cell numbers at day 7 (Fig. 27B) but not day 90 (data not shown) post-infection.

Next, IL-10R signalling was inhibited from day 60 post-infection. Importantly, $CD8^+$ T cell populations specific for M38, m139 and IE3 were all substantially increased (3- to 4-fold) following late IL-10R blockade (Fig. 27C and 27D), as were MCMV-specific $CD4^+$ T cells (Fig. 27E). In the case of IE3-specific $CD8^+$ T cells, this increased accumulation was more dramatic than that observed after early

IL-10R blockade (Fig. 27A). Thus, IL-10 primarily limits memory T cell accumulation during the chronic/latent phase of infection.

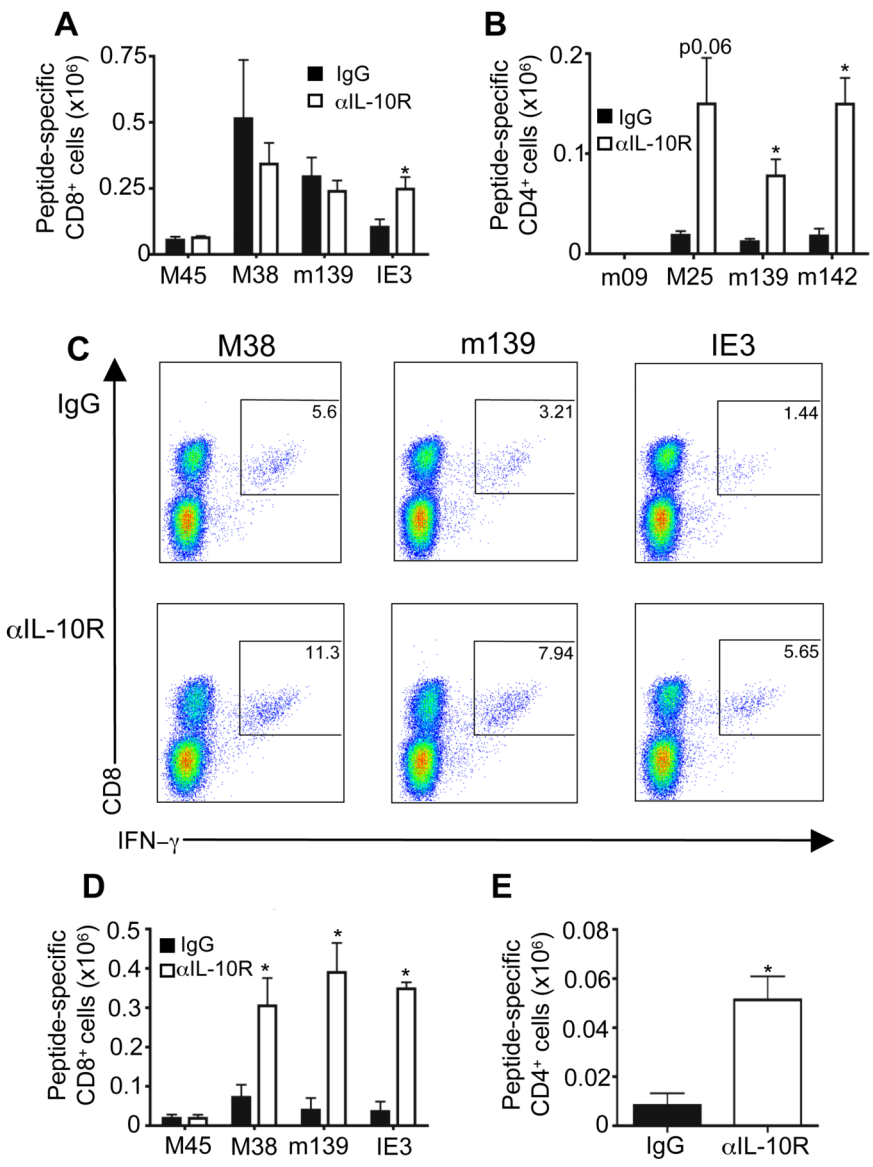

Figure 27. IL-10 inhibits memory $CD8^+$ T cells during acute and chronic/latent MCMV infection. **(A, B)** MCMV-infected wt mice were treated with IgG (closed bars) or αIL-10R (open bars) on day 0, and peptide-specific $CD8^+$ **(A)** and $CD4^+$ **(B)** T cells were enumerated at day 96 **(A)** and day 7 **(B)** post-infection. **(C-E)** Wt mice were treated with IgG or αIL-10R on days 60, 67, 74, and 81 post-infection. **(C)** Representative bivariate flow cytometry plots showing IFN-γ expression by $CD8^+$ T cells specific for M38, m139 and IE3 at day 90 post-infection from mice treated with IgG (top panels) or αIL-10R (bottom panels). Peptide-specific $CD8^+$ **(D)** and $CD4^+$ **(E)** T cells were enumerated at day 90 post-infection. MCMV-specific $CD4^+$ T cells were stimulated with pooled m09, M25, m139 and m142

peptides. Results are expressed as the mean +/- SEM of two independent experiments, each comprising four mice per group. * p <0.05 with Student's t-test. These data were generated in collaboration with Dr. Ian Humphreys and his laboratory.

CD27 expression is down-regulated by MCMV-specific CD8$^+$ T cells from IL-10$^{-/-}$ mice

In contrast to the phenotypic heterogeneity of the total CD8$^+$ T cell population (Fig. 28A), inflationary MCMV-specific memory CD8$^+$ T cells from wild-type mice were CD44^{hi}CD62L^{lo} (Fig. 28A), consistent with an effector memory status. Furthermore, these highly differentiated cells expressed high levels of KLRG-1 and low levels of CD27 (Fig. 28A). Memory CD8$^+$ T cells specific for MCMV from IL-10$^{-/-}$ mice were also CD44^{hi}CD62L^{lo} (Fig. 28A). Notably, however, the frequency of KLRG-1$^+$CD27$^-$ MCMV-specific CD8$^+$ T cells was even higher in IL-10$^{-/-}$ mice (Fig. 28A, 28B) and down-regulation of CD27 was more pronounced (Fig. 28A, 28C). In addition, receptors for the homeostatic cytokines IL-7 and IL-15 were not up-regulated by CD8$^+$ T cells from IL-10$^{-/-}$ mice (data not shown). Collectively, these data suggest that IL-10 does not inhibit memory CD8$^+$ T cells via the regulation of inhibitory or cytokine receptor expression; furthermore, it seems that the enhanced expansion of inflationary MCMV-specific CD8$^+$ T cells in the absence of IL-10 is associated with more advanced differentiation.

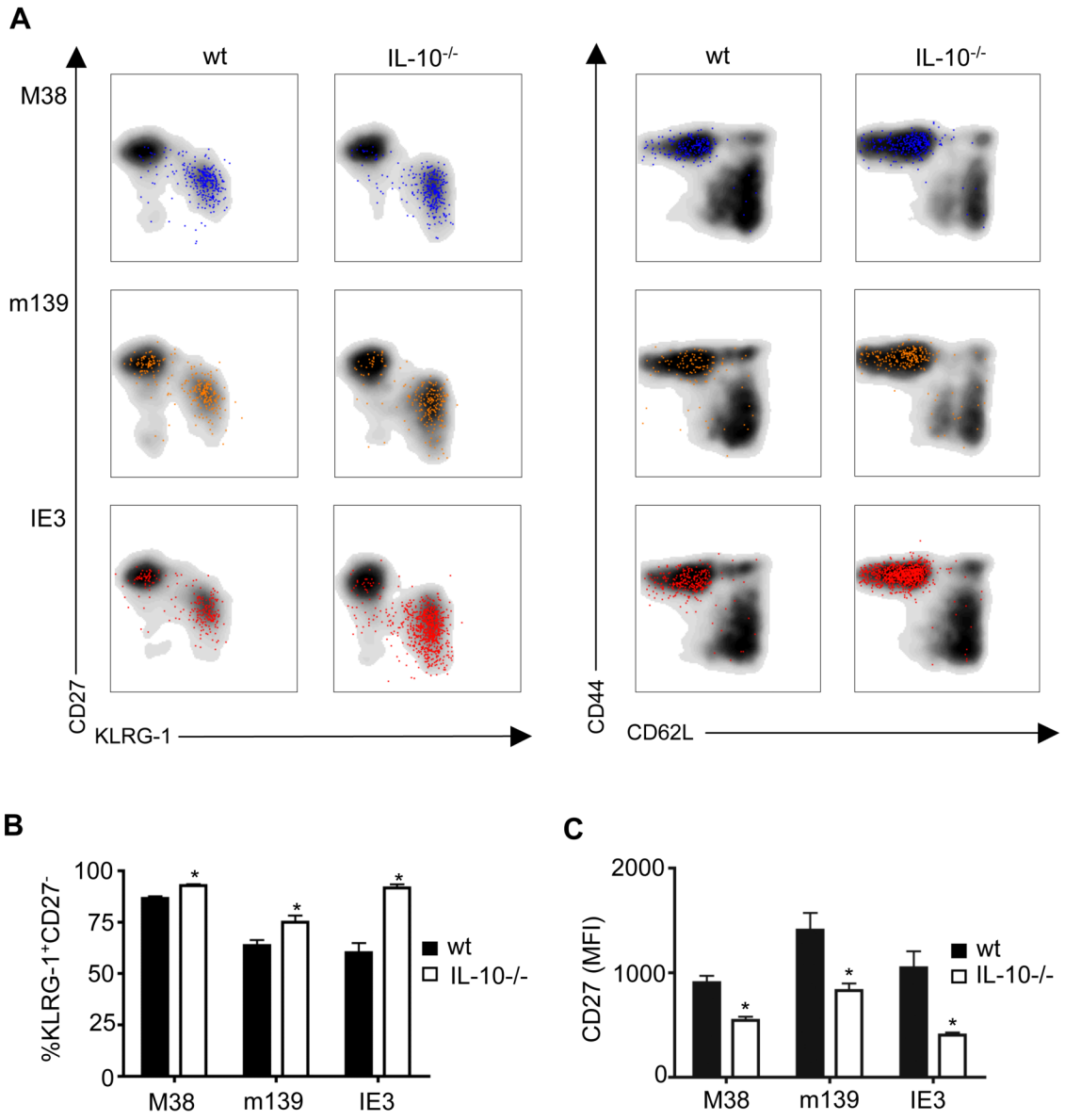

Figure 28. IL-10$^{-/-}$ MCMV-specific CD8^{+} T cells are highly differentiated. MCMV-specific CD8^{+} T cells from spleens of wt and IL-10$^{-/-}$ mice were detected with cognate tetramers and co-expression of CD27, KLRG-1, CD44, and CD62L was examined. **(A)** Co-expression of CD27 and KLRG-1 (left panels), and CD62L and CD44 (right panels), by CD3^{+}CD8^{+}tetramer^{+} cells (coloured dots) and total CD3^{+}CD8^{+} cells (black/grey) from spleens of wt (left panels in each set) and IL-10$^{-/-}$ (right panels in each set) mice. **(B, C)** The frequencies of KLRG-1^{+}CD27^{-} CD3^{+}CD8^{+}tetramer^{+} cells **(B)** and the median fluorescence intensity (MFI) of CD27 expression by CD3^{+}CD8^{+}tetramer^{+} cells **(C)** were assessed. In IL-10$^{-/-}$ mice, the percent KLRG-1^{+}CD27^{-} cells in the total CD3^{+}CD8^{+} population was not significantly decreased (wt = 23.5, IL-10$^{-/-}$ = 24.1; p = 0.91) nor was the CD27 MFI (wt = 2564.75, IL-10$^{-/-}$ = 1979.5; p = 0.22). Results are expressed as the mean +/- SEM of three experiments, each comprising three to four mice per group. * *p* <0.05 with Student's t-test. These data were generated in collaboration with

Dr. Ian Humphreys and his laboratory.

IL-10 restricts the accumulation of functional MCMV-specific CD8$^+$ T cells

Next, it was hypothesized that IL-10 limits the accumulation of functional antiviral memory CD8$^+$ T cells. Hence, cytokine production by MCMV-specific CD8$^+$ T cells was examined. A low proportion (6-10%) of wild-type MCMV-specific IFN-γ^+ CD8$^+$ T cells co-expressed IL-2 following ex vivo peptide stimulation and this was further reduced (2-4%) in IL-10$^{-/-}$ mice (Fig. 29A). In contrast, IL-10 deficiency increased both the proportion (Fig. 29A) and the total number (Fig. 29B) of MCMV-specific IFN-γ^+ CD8$^+$ T cells capable of co-expressing the antiviral cytokine TNF. Recent degranulation based on cell surface CD107a mobilization was also quantified and greater numbers of CD107a$^+$ MCMV-specific CD8$^+$ T cells were observed in the spleens and lungs of IL-10$^{-/-}$ mice compared to wild-type mice after *ex vivo* peptide stimulation (Fig. 29C). Importantly, IL-10R blockade in wild-type mice from day 60 post-infection also led to an increase in the numbers of virus-specific CD8$^+$ T cells that expressed TNF (Fig. 29D) and degranulated (Fig. 29E) in response to peptide stimulation. Collectively, these data suggest that IL-10 restricts the accumulation of functional memory CD8$^+$ T cells.

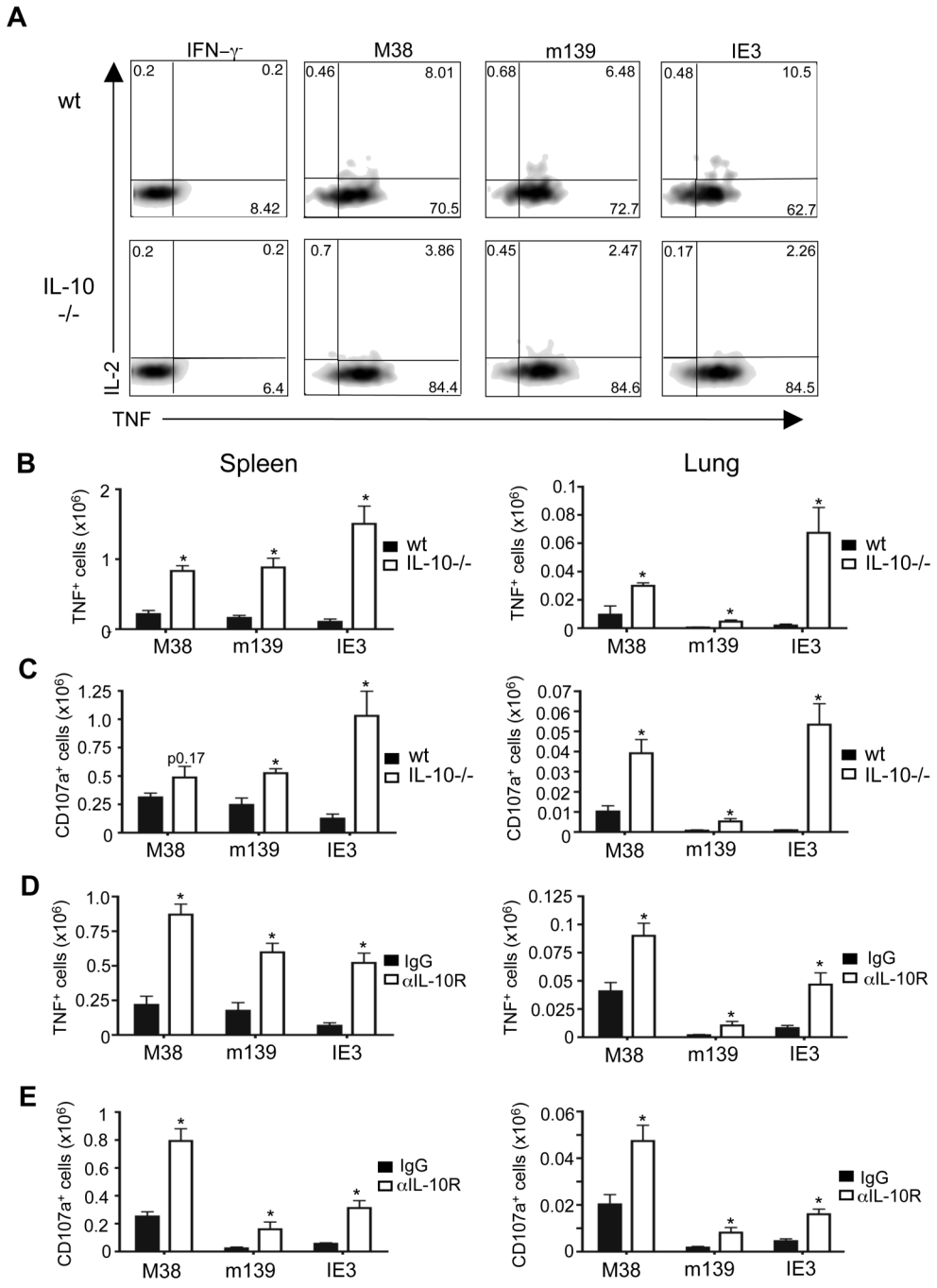

Figure 29. IL-10 limits the accumulation of functional antiviral $CD8^+$ T cells during MCMV infection. TNF, IL-2 and CD107a expression by IFN-γ^+ MCMV peptide-specific $CD8^+$ T cells from wt and IL-$10^{-/-}$ mice **(A-C)** and wt mice treated with IgG or αIL-10R **(D, E)** was assessed at day 90 post-infection. **(A)** Representative bivariate flow cytometry plots showing TNF versus IL2 expression by IFN-γ^- $CD8^+$ T cells (control) and IFN-γ^+ peptide-specific splenic $CD8^+$ T cells from wt (top panels) and IL-$10^{-/-}$ (bottom panels) mice. Results are representative of four experiments, each comprising four to five mice per

group. **(B-E)** Numbers of peptide-specific $CD8^+$ T cells expressing TNF **(B, D)** and surface CD107a **(C, E)** in the spleens (left panels) and lungs (right panels) of wt (closed bars) and IL-$10^{-/-}$ (open bars) mice **(B, C)** and wt mice treated with IgG (closed bars) or αIL-10R (open bars) on days 60, 67, 74 and 81 post-infection **(D, E)**. All results are representative of three experiments and show the mean +/- SEM of evaluations conducted with four to five mice per group. * p <0.05 with Student's t-test. These data were generated in collaboration with Dr. Ian Humphreys and his laboratory.

Latent virus load is reduced in the absence of IL-10R signalling

To determine whether the increased $CD8^+$ T cell responses in IL-$10^{-/-}$ mice reduced latent viral load, MCMV genome content in the lung and spleen was examined. No significant differences were observed at the peak of the primary T cell response (day 7 post-infection, data not shown) or at day 60 post-infection (Fig. 30A). Critically, however, viral DNA load was significantly reduced in both the spleens and lungs of IL-$10^{-/-}$ mice at day 90 post-infection (Fig. 30B). Importantly, late (from day 60 onwards) blockade of IL-10R in wild-type mice also led to a reduction in viral DNA load in spleen and lung at this time (Fig. 30C).

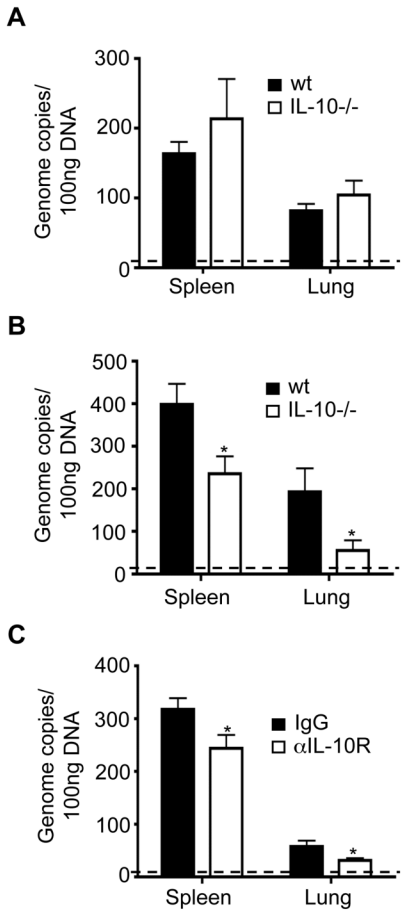

Figure 30. IL-10 increases latent MCMV load during infection. Genomic DNA was isolated from the spleens and lungs of wt (closed bars) and IL-$10^{-/-}$ (open bars) mice at days 60 **(A)** and 90 **(B)** post-infection. **(C)** Infected wt mice were treated on days 60, 67, 74 and 81 with IgG (closed bars) or αIL-10R (open bars) and genomic DNA was isolated from the spleens and lungs at day 90 post-infection. MCMV gB was detected by quantitative PCR and data expressed as genome copy number per 100 ng genomic DNA; horizontal dashed lines depict the lower limit of detection. Results are representative of two independent experiments and show the mean +/- SEM of evaluations conducted with five to fifteen mice per group. * p <0.05 with the Mann-Whitney U-test. These data were generated in collaboration with Dr. Ian Humphreys and his laboratory.

5.5 Discussion

Herein, it is reported that IL-10 suppresses CMV-specific memory T cell inflation. The key findings of this study were that: (i) chronic/latent MCMV infection was associated with IL-10 production by macrophages and virus-specific IFN-γ-expressing $CD4^+$ T cells; (ii) mice deficient in IL-10 exhibited a

profound increase in MCMV-specific $CD8^+$ T cell accumulation and antiviral cytokine production; (iii) IL-10 suppressed the oligoclonal expansion of memory $CD8^+$ T cells; (iv) MCMV viral genome load was reduced in IL-$10^{-/-}$ mice; and, (v) the enhanced memory $CD8^+$ T cell expansion and reduced viral load observed in IL-$10^{-/-}$ mice was recapitulated by delayed IL-10R blockade in wild-type mice. Collectively, these data demonstrate that IL-10 restricts the accumulation of functional MCMV-specific memory T cells during MCMV infection.

In vivo, MCMV infection leads to chronic activation of APCs (Barton, White et al. 2007) and the generation of highly differentiated, activated memory $CD8^+$ T cells (Sierro, Rothkopf et al. 2005; Snyder, Cho et al. 2008); these observations suggest that, after the resolution of acute infection, mice harbour non-replicating, reactivating and, possibly, low levels of chronically replicating CMV that drives the immune activation (Klenerman and Hill 2005; Reddehase, Simon et al. 2008; Virgin, Wherry et al. 2009). In the current study, 3.7%-8.3% of splenic IFN-γ^+ MCMV-specific memory $CD4^+$ T cells from MCMV-infected mice expressed IL-10. The production of IL-10 by Th1-like cells is triggered by chronic stimulation in parasitic infections (Anderson, Oukka et al. 2007; Jankovic, Kullberg et al. 2007), and prolonged stimulation of HCMV-specific $CD4^+$ T cells *in vitro* induces IL-10/IFN-γ co-expression (Haringer, Lozza et al. 2009). Similarly, it was observed that MCMV infection led to an increased frequency of IL-10-expressing $CD11b^+$ cells. Although one cannot exclude the possibility that MCMV may encode a protein(s) that selectively induces IL-10 expression by these cell subsets, the data imply that IL-10 expression by MCMV-specific $CD4^+$ T cells and monocytes/macrophages is a consequence of chronic activation which, in this model, is likely to be provided by persistent viral reactivation from latency and, possibly, undetectable chronic replication.

B cells are a significant source of IL-10 during acute systemic MCMV infection (Madan, Demircik et al. 2009). Although chronic/latent infection did not increase the proportion of IL-10-producing $CD19^+$ cells in the spleen as compared with naïve mice, the possible importance of this cell subset cannot be exlcuded. Intracellular cytokine staining is a relatively insensitive technique and may therefore underestimate the frequency of IL-10-producing $CD19^+$ cells. Furthermore, given that ~50% of

splenocytes were $CD19^+$ at day 90 post-infection (unpublished observation), even the small percentage of $CD19^+$ IL-10 producers suggested by our data could have a significant impact on antiviral immunity.

Interestingly, although IL-10 expression was detected in the lungs of mice at day 90 post-infection, this was not increased compared to naïve controls (data not shown). Whether or not this reflects the small numbers of virus-specific $CD4^+$ T cells in the lungs of chronic/latently infected mice in our model, or the presence of IL-10-producing interstitial macrophages (Bedoret, Wallemacq et al. 2009) in both uninfected and infected mice, is not clear.

The amplification of $CD8^+$ T cell inflation in IL-$10^{-/-}$ mice was striking and maintained 10 months post-infection without causing overt signs of disease (weight loss and cachexia) or pathology (unpublished observation). In some models, IL-10 directly inhibits $CD8^+$ T cells (Taga and Tosato 1992; Rohrer and Coggin 1995), whereas in other situations IL-10 actually promotes primary (Kang and Allen 2005) and memory $CD8^+$ T cell responses (Kang and Allen 2005; Foulds, Rotte et al. 2006). In our system, inflationary $CD8^+$ T cells expressed low levels of IL-10R (data not shown), thereby suggesting that these cells might be refractory to direct IL-10-mediated effects. Interestingly, enhanced $CD8^+$ T cell responses in IL-$10^{-/-}$ mice were accompanied by increased numbers of $CD4^+$ T cells and APCs. Inflationary $CD8^+$ T cell responses are partially dependent upon $CD4^+$ T cells (Humphreys, Loewendorf et al. 2007; Snyder, Loewendorf et al. 2009), thereby implying that elevated $CD4^+$ T cell help in IL-$10^{-/-}$ mice promoted $CD8^+$ T cell expansion. Interestingly, IE3-specific $CD8^+$ T cells, which are more sensitive to $CD4^+$ T cell depletion than other memory $CD8^+$ T cells (Snyder, Loewendorf et al. 2009), were preferentially expanded in IL-$10^{-/-}$ mice. Collectively, these data suggest that IL-10 limits memory $CD8^+$ T cell expansion via the abrogation of effective $CD4^+$ T cell help.

Expansion of $CD8^+$ T cell numbers was not observed 7 days post-infection, as reported previously (Oakley, Garvy et al. 2008). Primary MCMV-specific $CD8^+$ T cell responses occur independently of $CD4^+$ T cell help (Humphreys, Loewendorf et al. 2007; Snyder, Loewendorf et al. 2009), suggesting that IL-10-mediated inhibition of $CD4^+$ T cells only limits memory $CD8^+$ cells. Interestingly, however, B

cell-derived IL-10 inhibits primary $CD8^+$ T cell responses following sub-cutaneous infection (Madan, Demircik et al. 2009). Whether or not these differences reflect the different mouse strains or infection routes used in this study, variation in how peptide-specific $CD8^+$ T cells were enumerated (percentages versus total numbers of splenic $CD8^+$ T cells) or the fact that the IL-$10^{-/-}$ mice were housed in specific pathogen-free conditions (and subsequently no colitis was observed in aged naïve mice or mice infected with MCMV for 14 months; data not shown), is unclear.

The increased expansion of $CD8^+$ T cells in IL-$10^{-/-}$ mice was not due to altered expression of cytokine receptors (CD122, CD127) or the absence of inhibitory molecules (KLRG-1). However, it is known that virus-specific $CD8^+$ T cells down-regulate CD27 during latent MCMV infection (Baars, Sierro et al. 2005; Sierro, Rothkopf et al. 2005), and expression of this surface marker was further reduced in IL-$10^{-/-}$ mice. One possible functional consequence of CD27 down-regulation in this study was reduced IL-2 production in response to Ag stimulation; this is consistent with previous studies linking cellular differentiation to the loss of IL-2 expression (Precopio, Betts et al. 2007; Usharauli and Kamala 2008) and suggests a role for $CD4^+$ T cell help in the maintenance of polyfunctional memory $CD8^+$ T cells (Matter, Claus et al. 2008). Furthermore, highly differentiated $CD8^+$ T cells express high levels of granzyme and perforin (Baars, Sierro et al. 2005; Takata and Takiguchi 2006; Chattopadhyay, Betts et al. 2009), thereby suggesting that these cells are cytotoxic. The increased accumulation in IL-$10^{-/-}$ mice of $CD8^+$ T cells that degranulate more readily on cognate Ag encounter further supports the conclusion that IL-10 restricts MCMV-specific cytotoxic T cell responses.

In chronic lymphocytic choriomeningitis virus infection, dysregulated TNF production by $CD8^+$ T cells is rescued in IL-$10^{-/-}$ mice (Brooks, Trifilo et al. 2006). However, in MCMV infection, virus-specific $CD8^+$ T cells sustain pro-inflammatory cytokine expression during latency (Snyder, Cho et al. 2008). Indeed, 60-70% of virus-specific IFN-γ-producing $CD8^+$ T cells in wild-type mice co-expressed TNF. Therefore, enhanced TNF production by IL-$10^{-/-}$ $CD8^+$ T cells probably reflects increased activation rather than reversal of defective function. Furthermore, $CD8^+$ T cell functionality was not enhanced on a per cell basis following IL-10R blockade in wild-type mice (data not shown), highlighting that the qualitative

restriction of $CD8^+$ T cell function by IL-10 was comparatively small as compared to the large effect on T cell numbers. Collectively, these data suggest that IL-10 predominately regulates inflationary $CD8^+$ T cell responses by inhibiting cellular accumulation at sites of viral infection.

Importantly, MCMV burden was reduced in IL-$10^{-/-}$ mice and wild-type mice treated with an IL-10R blocking antibody. Expanded $CD8^+$ T cells in both situations were reactive to several viral proteins expressed during active replication, thereby implying that these cells do not directly recognize latently infected cells. Of particular interest was the expansion of IE3-specific $CD8^+$ T cells. IE genes are expressed during the early stages of viral replication, and IE3 is a checkpoint gene involved in the maintenance of latency (Kurz and Reddehase 1999). Patrolling IE-specific $CD8^+$ T cells may detect early reactivation events (Simon, Seckert et al. 2006). It is therefore possible that the increased frequency of Ag recognition by IE3-specific cells may contribute to the more dramatic effect of IL-10 on this population. In support of this hypothesis, latent MCMV infection of BALB/c mice induces the inflation of IE1-specific $CD8^+$ T cells (Holtappels, Pahl-Seibert et al. 2000; Karrer, Sierro et al. 2003) that terminate viral reactivation *in vivo* (Simon, Holtappels et al. 2006). Alternatively, however, it is conceivable that enhanced memory T cell responses in the absence of IL-10R signalling may inhibit low levels of undetectable chronic replication which, in turn, restricts the establishment of latent infection in the spleen and lung.

The exact mechanism by which expanded $CD8^+$ T cells reduced viral load following IL-10 gene deletion or IL-10R blockade is also unclear. Both approaches led to enhanced numbers of $CD8^+$ T cells in the spleen and lung that could degranulate efficiently; in conjunction with the reduced levels of CD27 expression, this implies an enhanced capability to kill cells harbouring reactivating and/or replicating virus. Indeed, elevated TNF secretion by $CD8^+$ T cells in the absence of IL-10R signalling may promote splicing of IE3 transcripts and subsequent viral reactivation (Simon, Seckert et al. 2005). In this situation, which could be implied by the preferential expansion of IE3-specific $CD8^+$ T cells in IL-$10^{-/-}$ mice, increased numbers of cytotoxic T cells would detect and kill cells harbouring this reactivating virus. Alternatively, increased accumulation of T cells expressing IFN-γ and TNF might

directly inhibit late gene expression during viral reactivation and/or replication (Gribaudo, Ravaglia et al. 1993; Lucin, Jonjic et al. 1994; Presti, Pollock et al. 1998), and may also activate secondary antiviral mechanisms mediated by other cell types, such as macrophages and NK cells (Weigent, Stanton et al. 1983; Heise and Virgin 1995; Orange and Biron 1996).

The factors that determine whether an MCMV-specific $CD8^+$ T cell population inflates are currently unknown. However, the observation that inflationary but not stable memory $CD8^+$ T cells are enhanced in IL-$10^{-/-}$ mice implies that IL-10 is not a determining factor in this process. Rather, IL-10 appears to limit the expansion of memory $CD8^+$ T cells that are already dividing during chronic/latent infection.

The data presented here provide evidence that, as suggested previously (Jenkins, Garcia et al. 2008; Cheung, Gottlieb et al. 2009), IL-10 orthologs expressed by herpesviruses including HCMV (Kotenko, Saccani et al. 2000) and Epstein-Barr virus (Hsu, de Waal Malefyt et al. 1990) may function to preserve latent viral load within the host. It should be noted, however, that MCMV does not encode an obvious IL-10 ortholog, and the kinetics and locality of expression of host and viral IL-10 proteins may differ *in vivo*. Furthermore, HCMV (Spencer, Cadaoas et al. 2008) and Epstein-Barr virus (Rousset, Garcia et al. 1992) IL-10 orthologs promote B cell growth and differentiation, whereas in this model no effect of murine IL-10 on B cell accumulation was observed. Although it was hypothesized that the increased numbers of $CD4^+$ T cells in IL-$10^{-/-}$ mice may compensate for the absence of direct IL-10R signalling in B cells, the possibility cannot be excluded that mammalian and viral IL-10 proteins could function differently *in vivo*. Irrespective, these data clearly highlight the previously unappreciated role for mammalian IL-10 in the regulation of memory T cell inflation *in vivo* and suggest that this immune regulatory pathway could be manipulated to promote the accumulation of functional antiviral memory T cells.

CHAPTER

6

Expansion of highly differentiated $CD8^+$ T cells or NK cells in patients treated with dasatinib is associated with cytomegalovirus reactivation

6.1 Introduction

Chronic myeloid leukaemia (CML) epitomizes the concept of a haematological malignancy caused by dysregulated signal transduction. More than 90% of all CML patients have the translocation t(9;22), which leads to the formation of a BCR–ABL fusion protein with continuous tyrosine kinase activity that is responsible for the malignant phenotype. Specific tyrosine kinase inhibitor therapy with imatinib (Glivec/Gleevec, Novartis, Basel, Switzerland) is the gold standard for the treatment of CML (Druker, Guilhot et al. 2006). However, as imatinib resistance or intolerance may occur, second-line tyrosine kinase inhibitors have entered the clinic; examples include nilotinib (Tasigna, Novartis) (Kantarjian, Giles et al. 2007), which is highly selective, and dasatinib (Sprycel, Bristol-Myers Squibb, New York, NY, USA) (Hochhaus, Baccarani et al. 2008). In addition to BCR-ABL, dasatinib also targets SRC and TEC kinases that are known to be key players in the regulation of immune responses (Bantscheff, Eberhard et al. 2007; Rix, Hantschel et al. 2007). The broader target profile of dasatinib implies less susceptibility to the development of resistance, but also the potential for more potent modulation of immune cell subsets. Indeed, immunosuppressive effects on T cells and NK cells have been described *in vitro* for dasatinib (Fei, Yu et al. 2008; Schade, Schieven et al. 2008; Weichsel, Dix et al. 2008; Fraser, Blake et al. 2009) and other tyrosine kinase inhibitors (Seggewiss, Lore et al. 2005; Chen, Schmitt et al. 2008; Blake, Lyons et al. 2009). This is in line with observations in single center clinical case series (Sillaber, Herrmann et al. 2009). However, in large phase II/III clinical trials, increased infection rates due to immunosuppression have not been observed (Kantarjian, Shah et al. 2010).

Recently, in a subset of CML or Ph^+ ALL patients receiving dasatinib, the development of a chronic,

oscillating lymphocytosis has been observed *in vivo*. This dasatinib-induced lymphocytosis typically comprises monoclonal or oligoclonal $CD8^+$ T cell or NK cell LGL expansions and is associated with enhanced, long-lasting therapeutic responses in patients with advanced leukaemia (Kim, Kamel-Reid et al. 2009; Mustjoki, Ekblom et al. 2009). The $CD8^+$ T cell or NK cell clones are present during the diagnostic phase of the disease and expand with dasatinib therapy, leading to a numerical and fractional lymphocytosis (Kreutzman, Juvonen et al. 2010). Thus, dasatinib does not induce these clones, but rather appears to promote their preferential expansion.

6.2 Hypotheses

- Lymphocyte populations in dasatinib-associated LGL patients are differentiated effector memory T cells or NK cells.
- LGL patients have elevated cytokine/chemokine levels due to a direct or indirect immunostimulatory effect of dasatinib treatment.
- The LGL expansions that are linked to a favourable outcome during dasatinib therapy are associated with CMV reactivation.

6.3 Specific Aims

- To determine the phenotypic characteristics of T cell subsets and NK cells in patients on continuous dasatinib treatment with and without LGL expansions using polychromatic flow cytometry.
- To elucidate the mechanisms underlying dasatinib-associated LGL expansions in more detail by measuring directly *ex vivo* T cell and NK cell effector functions such as activation, proliferation, degranulation, cytotoxicity and the secretion of soluble factors in PBMC samples treated *in vitro* with clinically relevant doses of 10 and 50nM, thereby mimicking peak and steady state concentrations (Brave, Goodman et al. 2008; Weichsel, Dix et al. 2008).

- To assay plasma samples for soluble immune mediators and CMV load.

6.4 Results

Association of LGL expansions with CMV seropositivity, CMV reactivation and elevated plasma levels of IP-10, IL-6, MIG and IL-2R

15/16 patients in our cohort with LGL expansions were CMV IgG seropositive (IgG serostatus only unknown for patient 9), whereas only 3/9 non-LGL patients were CMV IgG seropositive (Table 3). Most patients with LGL expansions also exhibited high frequencies of CMV-specific $CD8^+$ T cells (range, 0.7-15.6% of the total $CD3^+$ T cell pool) as determined by staining with pHLA-A*0201 tetrameric complexes bearing the immunodominant pp65-derived (residues 495-503) epitope NLVPMVATV (Table 4). Of note, 5/16 LGL patients and 0/9 non-LGL patients experienced symptomatic (persistent low-grade fever) CMV reactivations (Table 3), which were confirmed by PCR. However, it should be noted that CMV load measurements were not performed in asymptomatic patients. There was no evidence for reactivation of other herpes viruses. In addition, significantly elevated levels of IP-10 (CXCL10), IL-6, MIG (CXCL9) and IL-2R were present in the plasma of patients with LGL expansions compared to healthy controls (Fig. 31). Notably, the highest plasma levels of these soluble factors were detected in the patients who experienced symptomatic CMV reactivations during dasatinib therapy (Fig. 31). These data are consistent with previous studies, which have demonstrated increased levels of IFN-γ stimulated gene products, such as IP-10 and MIG, in the plasma of patients with LGL expansions unrelated to dasatinib treatment (Wlodarski, Nearman et al. 2008). There were no significant differences between groups for any of the other 21 soluble factors measured in plasma. Thus, the cytokine perturbations in patients with dasatinib-associated LGL expansions are restricted and may reflect virus-specific responses dominated by IFN-γ rather than general immune activation.

Table 3. Characteristics of study patients with and without LGL expansions during treatment with dasatinib for CML or ALL.

Pt no	Dg	Age* (yrs)	Gender	Therapy response	Duration (months)	LGL lymphocytosis	Clonality status**	CMV serology	CMV reactivation	HLA-A*02
1	ALL t(1;9)	43	Male	CCgR	35[a]	Yes; T cell	TCRγ TCRδ	Pos	Yes, max 700	Pos
2	Ph^+ ALL	48	Male	CMR	5	Yes; T cell	TCRγ	Pos	Yes max 2500	Pos
3	Ph^+ ALL	52	Female	CMR	6	Yes; T cell	ND	Pos	NS	Pos
4	Ph^+ ALL	70	Female	CCgR	23[a]	Yes; T + NK cell	ND	Pos	NS	Neg
5	Ph^+ ALL	76	Female	MMR	4[a]	Yes; T + NK cell	ND	Pos	NS	Neg
6	CML BC	62	Female	CMR	16	Yes; T + NK cell	TCRγ TCRδ	Pos	Yes, max 7500	Pos
7	CML BC	43	Male	CMR	45	Yes; T cell	TCRγ TCRδ	Pos	Yes, max 6200	Pos
8	CML CP	48	Female	MMR	19[a]	Yes; NK cell	ND	Pos	NS	Neg
9	CML CP	52	Female	MMR	6[a]	Yes; T cell	TCRγ	ND	NS	ND
10	CML CP	58	Female	CMR	48	Yes; NK cell	TCRδ	Pos	NS	Pos
11	CML CP	61	Female	MMR	6[a]	Yes; T + NK cell	TCRγ TCRδ	Pos	NS	Pos
12	CML CP	64	Female	CMR	6	Yes; T cell	ND	Pos	Yes, max 15100	Neg
13	CML CP	65	Female	MMR	36[a]	Yes; T + NK cell	TCRγ TCRδ	Pos	NS	Pos
14	CML CP	52	Male	CMR	7	Yes; T cell	TCRγ	Pos	NS	Pos
15	CML CP	60	Male	CMR	39	Yes; T cell	TCRγ TCRδ	Pos	NS	Pos
16	CML CP	76	Male	CMR	59	Yes; NK cell	TCRγ TCRδ	Pos	NS	Pos
17	CML CP	29	Female	CMR	58[a]	No	TCRγ	Pos	NS	Pos
18	CML CP	64	Female	MMR	37[a]	No	TCRγ	Neg	NS	Pos
19	CML CP	71	Female	CMR	6[a]	No	ND	Pos	NS	Pos
20	CML CP	27	Male	MMR	22	No	No	Neg	NS	Pos
21	CML CP	40	Male	MMR	54[a]	No	TCRγ	Neg	NS	Pos
22	CML CP	49	Male	CCgR	57[a]	No	TCRγ	Pos	NS	Neg
23	CML CP	61	Male	CMR	25[a]	No	No	Neg	NS	Neg
24	CML CP	66	Male	MMR	20[a]	No	ND	Neg	NS	Neg
25	CML CP	71	Male	CHR	21[a]	No	ND	Neg	NS	Pos

Abbreviations: Dg, diagnosis; ALL, acute lymphoblastic leukaemia; $Ph^{+,}$ positive Philadelphia chromosome; CML, chronic myeloid leukaemia; CP, chronic phase; BC, blast crisis; CCgR; complete cytogenetic response; CMR, complete molecular response; MMR, major molecular response; CHR, complete haematological response; CMV, cytomegalovirus; copies/mL, genome copies/mL of plasma;

NS, no symptoms, plasma CMV DNA viral load not analyzed; ND, not done. *Age at the time of sampling. [a] Therapy ongoing. ** Clonality of lymphocytes was confirmed by analyzing T cell receptor (TCR) γ- and δ-gene rearrangements by PCR as described earlier (Kreutzman, Juvonen et al. 2010). Of note, clonal TCR rearrangments were found in most LGL and non-LGL CML patients (Kreutzman, Juvonen et al. 2010). Positive products (confirmed by sequencing) are marked in the table.

Table 4. Phenotypic features of $CD8^+$ and $CD4^+$ T cell populations.

Phenotype	T LGL* n=5	NK LGL* n=5	T + NK LGL*[a] n=1	No LGL* n=3
$CD8^+$ (% of $CD3^+$ T cells)	76.0 (31.6-80.3)	36.8 (33.8-42.6)	35.3	30.9 (27.3-48.9)
$CD4^+$ (% of $CD3^+$ T cells)	17.1 (14.0-57.8)	42.2 (29.8-61.1)	37.4	54.2 (35.1-67.7)
$CD57^+$ (% of $CD8^+$ T cells)	78.2 (51.9-83.8)	47.3 (26.5-70.3)	76.1	12.2 (8.0-16.6)
PD-1^+CD57^- (% of $CD8^+$ T cells)	3.4 (0.9-7.6)	9.4 (1.4-15.6)	14.9	18.9 (5.5-22.1)
PD-1^+CD57^+ (% of $CD8^+$ T cells)	5.2 (1.0-19.3)	7.1 (0.5-17.2)	23.9	3.7 (0.7-4.0)
$CD45RO^+CD27^-$ (% of $CD8^+$ T cells)	80.5 (63.8-90.5)	54.8 (27.2-80.6)	90.5	17.6 (15.6-29.0)
$CD57^+$ (% of $CD8^+$ $CD45RO^+CD27^-$)	86.2 (55.2-87.6)	78.9 (73.9-81.2)	79.4	30.0 (20.4-34.2)
$CD57^+$ (% of $CD4^+$ T cells)	39.4 (21.6-80.7)	4.5 (1.3-72.6)	67.6	2.3 (1.0-5.6)
$CD45RO^+CD27^-$ (% of $CD4^+$ T cells)	79.1 (35.1-87.6)	14.6 (4.2-90.8)	90.1	16.5 (5.8-26.7)
$CD57^+$ (% of $CD4^+$ $CD45RO^+CD27^-$)	65.6 (44.9-88.0)	23.5 (6.6-78.8)	73.8	11.1 (3.1-14.2)
$CD8^+NLV^+$ (% of $CD3^+$ T cells)	7.9 (3.7-11.2)[b]	2.6 (0.7-4.2)[c]	15.6	-
$CD45RO^+CD27^-$ (% of NLV^+ T cells)	84.8 (79.4-88.9)	53.3 (39.9-76.2)	93.2	-
$CD57^+$ (% of NLV^+ T cells)	39.8 (26.6-88.1)	29.7 (24.8-46.8)	70.6	-
$CD57^+$ (% of NLV^+ $CD45RO^+CD27^-$)	41.6 (27.7-89.6)	46.3 (30.6-54.2)	72.4	-

[a] Patient 13; longitudinal values for patient 6 are shown in Fig. 36. [b] Patient 12 did not have an NLV-specific $CD8^+$ T cell population due to the absence of HLA-A*02. [c] Patient 8 did not have an NLV-specific $CD8^+$ T cell population due to the absence of HLA-A*02. * Medians with ranges in parenthesis are shown. NLV^+, CMV $pp65_{495-503}$/HLA-A*0201 tetramer-labelled $CD3^+$ T cells.

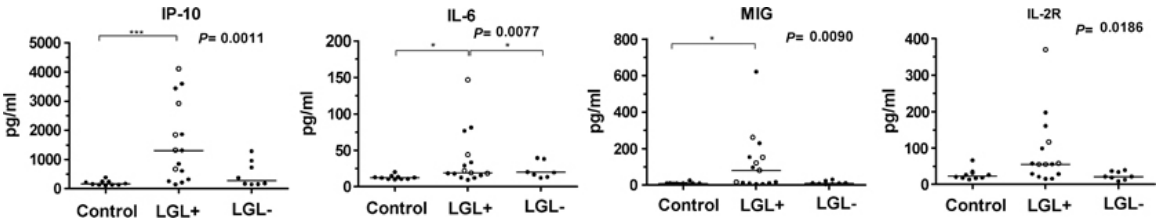

Figure 31. Plasma IP-10, IL-6, MIG and IL-2R levels in CML and Ph^+ ALL patients treated with dasatinib. Plasma levels of 25 cytokines were measured with a multiplex bead-based cytokine assay (Luminex®) in healthy controls (n=10), dasatinib-treated patients with LGL expansions (LGL+, n=15) and patients without LGL expansions during dasatinib therapy (LGL-, n=8). Patients who experienced CMV reactivations during dasatinib therapy (Table 3) are identified with unfilled symbols. Comparisons between groups were performed using the non-parametric Kruskall-Wallis test. Statistically significant differences were observed between healthy controls and LGL patients for IP-10 (p=0.0011), IL-6 (p=0.0077), MIG (p=0.0090) and IL-2R (p=0.0186) levels; these differences held irrespective of the sampling time point (data not shown). In the IL-6 graph, one data point in the LGL- group was out of range (3576.5 pg/ml) and is not shown. The horizontal lines in the graphs denote medians. The data in this figure and this figure were produced by collaborators.

Increased apoptotic susceptibility of T cells from patients with LGL expansions

In vitro, $CD3^+$ T cells from LGL patients (n=8) demonstrated significantly higher rates of apoptosis compared to non-LGL patients (n=6) or healthy controls (n=4) after 4 days without stimulation ($p<0.05$ for both comparisons); no significant differences for NK cells were observed between the 3 groups (data not shown). The $CD3^+$ T cells from LGL patients were also more sensitive to AICD after stimulation with the murine mAb OKT3, which cross-links the CD3 component of the CD3/TCR complex, leading to significantly higher rates of apoptosis compared to healthy controls ($p<0.05$) and a trend towards higher rates of apoptosis compared to non-LGL patients. In contrast, no differences were observed in either untreated or OKT3-stimulated T cells with regard to the fraction of late apoptotic/necrotic cells ($7AAD^+$/annexin V^+; data not shown). Thus, with the caveat that *in vitro* conditions do not necessarily recapitulate the complexity of cellular signalling networks *in vivo*, it appears that enhanced survival does not explain the T cell expansions observed in dasatinib-associated LGL lymphocytosis; instead, these data point towards a proliferative basis for the observed

T cell expansions. Thus, the effects of dasatinib on T cell and NK cell activation, proliferation and function directly *ex vivo* were examined.

Ex vivo modulation of T cell activation, proliferation, degranulation and cytokine production by dasatinib

Initially, the effects of dasatinib on $CD3^+$, $CD4^+$ and $CD8^+$ T cell subsets stimulated non-specifically with OKT3 *ex vivo* were examined. Consistent with previous studies, significant dose-dependent inhibitory effects on T cell activation, proliferation, degranulation and cytokine production were observed in all subsets (Fig. 32). Importantly, no differences in dasatinib sensitivity were observed with respect to any of these effects between LGL patients, non-LGL patients and healthy controls (data not shown). Notably, during these experiments, a dichotomy within the $CD8^+$ T cell compartment of LGL patients was observed. Specifically, two distinct $CD8^+$ T cell subpopulations, $CD8^{high}$ and $CD8^{low}$, could be discerned based on differential CD8 expression levels (Fig. 32C, 32D). The $CD8^{high}$ subset exhibited substantially greater degranulation and cytokine production in response to OKT3 stimulation compared to the $CD8^{low}$ and $CD4^+$ subsets (Fig. 32C-E). Moreover, distinct $CD8^{high}$ and $CD8^{low}$ T cell subsets were not observed in healthy controls or non-LGL patients, with the exception of one non-LGL patient in whom LGL expansions may still develop.

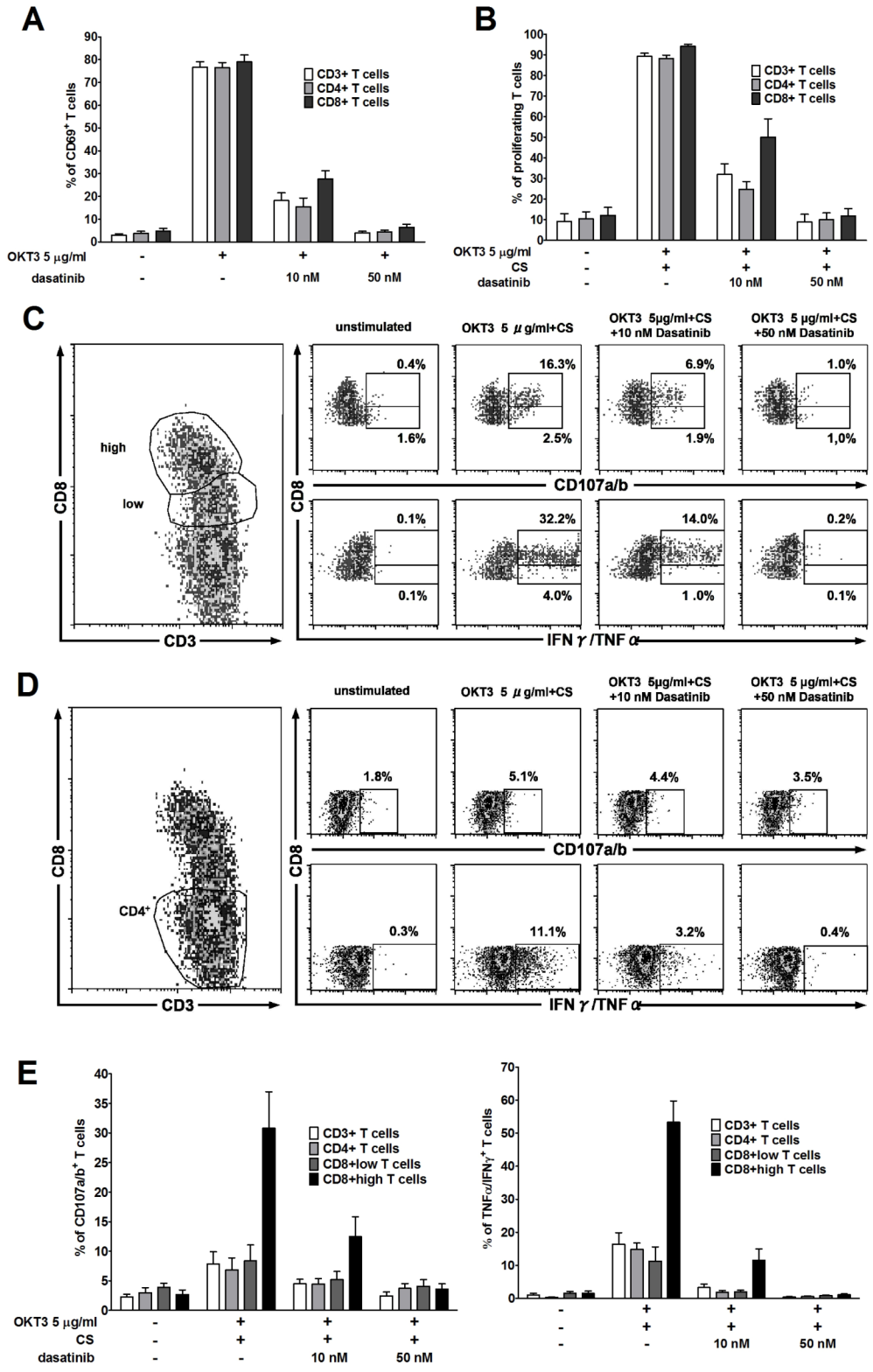

Figure 32. Effects of dasatinib on the activation and proliferation of T cells from LGL patients in response to OKT3 and costimulation. **(A)** T cells from LGL patients were either untreated or pre-

incubated with dasatinib at 10 or 50 nM for 1 hour as indicated, then stimulated for 24 hours with 5 μg/ml OKT3 under the same conditions. CD69 expression in gated live lymphocytes from 9 independent experiments is shown as the mean +/- SEM for $CD3^+$ T cells (white), $CD4^+$ T cells (light grey) and $CD8^+$ T cells (dark grey). Dasatinib led to a significant dose-dependent inhibition of CD69 up-regulation in $CD3^+$, $CD4^+$ and $CD8^+$ T cells ($p<0.001$ for all comparisons of stimulated alone vs. stimulated in the presence of dasatinib at 10 or 50 nM). **(B)** PBMCs from LGL patients were labelled directly *ex vivo* with 0.25 μM CFSE, then either untreated or pre-incubated with 10 or 50 nM dasatinib for 1 hour prior to stimulation with 5 μg/ml OKT3 in the presence of αCD28/αCD49d at 1 μg/ml each (CS: costimulation) for 4 days under the same conditions. The % proliferating T cells in gated live lymphocytes from 8 independent experiments is shown as the mean +/- SEM for $CD3^+$ T cells (white), $CD4^+$ T cells (light grey) and $CD8^+$ T cells (dark grey). A significant dose-dependent inhibition of OKT3-induced T cell proliferation in $CD3^+$, $CD4^+$ and $CD8^+$ T cells was observed ($p<0.0001$ for all comparisons of stimulated alone vs. stimulated in the presence of dasatinib at 10 or 50 nM). **(C-E)** Frequencies of $CD8^{high}$, $CD8^{low}$ and $CD8^-$ T cells from LGL patients that expressed CD107a/b and produced IFN-γ/TNF-α in response to stimulation with 5 μg/ml OKT3 and αCD28/αCD49d at 1 μg/ml each (CS: costimulation) in 5 hour assays directly *ex vivo*. **(C & D)** Representative plots are shown from patient 14. Gates were set on live lymphocytes, then $CD3^+CD8^+$ **(C)** or $CD3^+CD8^-$ **(D)** cells. **(E)** CD107a/b expression (left graph) and IFN-γ/TNF-α production (right graph) in gated live lymphocytes from 8 independent experiments are shown as mean values +/- SEMs for $CD3^+$ T cells (white), $CD4^+$ T cells (light grey; gated as $CD8^-$), $CD8^{low}$ T cells (dark grey) and $CD8^{high}$ T cells (black). The $CD8^{high}$ subset appeared to be marginally more resistant to dasatinib inhibition compared to the $CD8^{low}$ T cell subset, as cytokine production was not completely suppressed at 10 nM dasatinib; however, the fractional decrease in cytokine functionality induced by dasatinib was similar compared to the $CD8^{low}$ and $CD4^+$ subsets, and was significant ($p<0.0001$ for all comparisons) in all cases. Dasatinib led to a significant reduction of CD107a/b expression only in the $CD8^{high}$ subset ($p<0.0001$); there was minimal CD107a/b mobilization in the $CD8^{low}$ and $CD4^+$ subsets, even in the absence of dasatinib. The data in this figure and this figure were produced by co-investigators.

As $CD8^+$ T cell-mediated immunity is essential for the long-term control of persistent DNA viruses, and 5/16 LGL patients experienced symptomatic CMV reactivation (Table 3), $CD8^+$ T cell proliferation was evaluated in response to the CMV $pp65_{495-503}$ peptide Ag (NLVPMVATV) over a period of 6 days. CMV-specific $CD8^+$ T cell proliferation was suppressed *in vitro* in the presence of 50 nM dasatinib ($p<0.001$); however, in contrast to bulk $CD8^+$ T cell populations (Fig. 32B), no inhibition was observed

with 10 nM dasatinib (Fig. 33A). No differences were observed when LGL patients (n=4) were compared with either healthy controls (n=2) or a non-LGL patient (patient 19, Table 3). Of note, the majority of non-LGL patients in our cohort were either HLA-A*02$^-$ or CMV IgG seronegative; thus, only extremely limited CMV-specific functional studies were possible in this group (Fig. 33A, 33D).

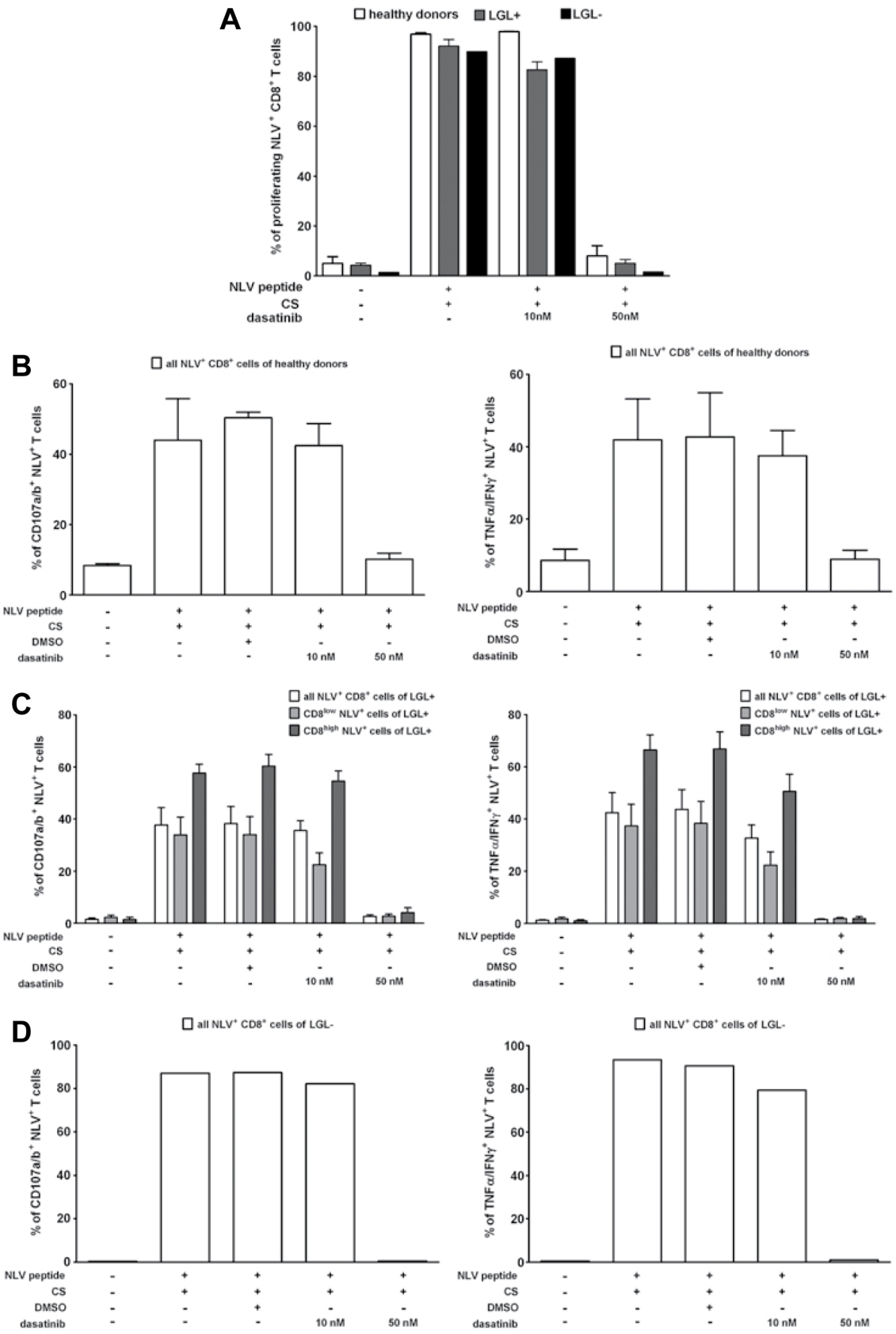

Figure 33. Effects of dasatinib on activation and proliferation of CMV-specific $CD8^+$ T cells from LGL patients and healthy controls in response to cognate viral Ag directly *ex vivo*. **(A)** PBMCs were

labelled with CFSE, then stimulated with the CMV $pp65_{495-503}$ peptide NLVPMVATV (NLV) at a concentration of 2 μM for 6 days in the presence of αCD28/αCD49d at 1 μg/ml each (CS: costimulation). Ag-specific proliferation in the absence and presence of dasatinib at 10 or 50 nM was evaluated for $CD8^+$ T cells that stained with the CMV $pp65_{495-503}$/HLA-A*0201 tetramer. Data are shown as the mean +/- SEM for LGL patients (n=4, grey), healthy controls (n=2, white) and a non-LGL patient (n=1, black). **(B)** Direct *ex vivo* functional analysis of CMV-specific $CD8^+$ T cell populations from healthy controls. CD107a/b expression (left panel) and IFN-γ/TNF-α production (right panel) in gated live lymphocytes from 3 independent experiments are shown as mean values +/- SEMs for $CD3^+CD8^+$ T cells specific for the NLVPMVATV (NLV) peptide (white). **(C)** Direct *ex vivo* functional analysis of CMV-specific $CD8^+$ T cell populations from LGL patients. CD107a/b expression (left panel) and IFN-γ/TNF-α production (right panel) in gated live lymphocytes from 8 independent experiments are shown as mean values +/- SEMs for NLVPMVATV-specific (NLV^+) $CD3^+CD8^+$ T cells (white), NLVPMVATV-specific (NLV^+) $CD3^+CD8^{low}$ T cells (light grey) and NLVPMVATV-specific (NLV^+) $CD3^+CD8^{high}$ T cells (dark grey). **(D)** Direct *ex vivo* functional analysis of CMV specific $CD8^+$ T cell populations from a non-LGL patient (patient 19, Table 3). CD107a/b expression (left panel) and IFN-γ/TNF-α production (right panel) in gated live lymphocytes from a single experiment are shown for $CD3^+CD8^+$ T cells specific for the NLVPMVATV (NLV) peptide (white). The data in this figure and this figure were produced by co-investiagtors.

Strikingly, distinct $CD8^{high}$ and $CD8^{low}$ subsets were observed within the NLVPMVATV-specific $CD8^+$ T cell populations in patients with LGL expansions (n=8). In healthy controls (n=3) and one non-LGL patient (patient 19, Table 3), only NLVPMVATV-specific $CD8^{high}$ subpopulations were detected; the distinct $CD8^{low}$ subpopulation was confined to LGL patients (Fig. 34A, 34B). When NLVPMVATV-specific $CD8^+$ T cells were stimulated with cognate peptide, both the $CD8^{high}$ and $CD8^{low}$ subsets exhibited degranulation and cytokine production; these functions were inhibited by dasatinib in a dose-dependent fashion, with minimal and almost complete suppression at concentrations of 10 and 50 nM, respectively (Fig. 33B-D). Of note, in LGL patients, both degranulation and cytokine production were significantly more pronounced in the $CD8^{high}$ subset (n=8; Fig. 33C). Furthermore, dasatinib effectively abrogated downregulation of both TCR and CD8 in the $CD8^{high}$ subpopulation *in vitro*, which could be a contributing factor in the generation and maintenance of persistent LGL expansions (data not shown) (Lissina, Ladell et al. 2009). Importantly, the dominant TCR clonotypes and phenotypic

features of the CD8^{high} and CD8^{low} NLVPMVATV-specific subsets were similar (Fig. 34), thereby indicating that these cells were derived from the same precursors and that the observed CD8 downregulation likely reflected a state of recent activation. One minor deviation from this general observation occurred in patient 13, in whom the NLVPMVATV-specific CD8^{low} population appeared more differentiated (CD45RO^{dim}CD57^{+}) and expressed greater levels of programmed death-1 (PD-1); this is consistent with Ag-driven effects in the context of combined T cell and NK cell LGL expansions.

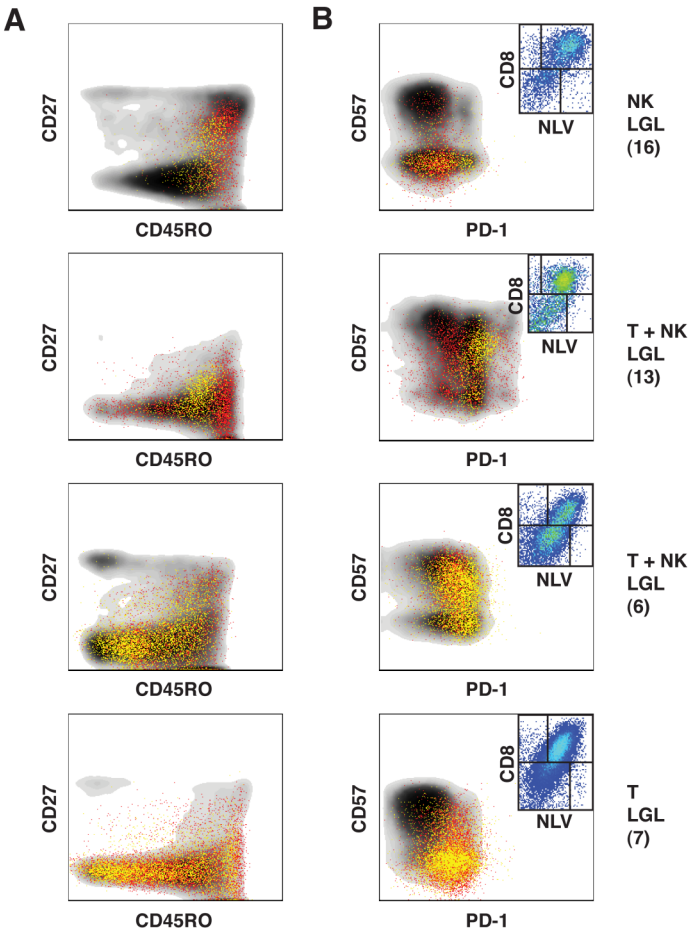

C

TRBV	CDR3	TRBJ	Freq (%)
12-3*/12-4*	CASSSANYGYT	1-2	45.2
6-5	CASTLGTGGRELF	2-2	28.8
11-1	CASSFWDRASGANVLT	2-6	23.3
11-1	CASSSWDRASGANVLT	2-6	1.4
11-1	CASSFWDGASGANVLT	2-6	1.4

D

TRBV	CDR3	TRBJ	Freq (%)
12-3*/12-4*	CASSSANYGYT	1-2	63.2
6-5	CASTLGTGGRELF	2-2	32.9
11-1	CASSFWDRASGANVLT	2-6	2.6
13	CASSRQGGYYGYT	1-2	1.3

Figure 34. Phenotypes and clonotypes of CMV-specific CD8^{high} and CD8^{low} T cell subsets in LGL

patients. **(A & B)** Phenotypic profiles of NLVPMVATV-specific $CD8^{high}$ and $CD8^{low}$ T cell populations from four representative LGL patients (1 x NK LGL, 2 x T + NK LGL, 1 x T LGL). Coloured dots depict individual NLVPMVATV-specific $CD8^{high}$ (red) and $CD8^{low}$ (yellow) T cells super-imposed on density plots showing the phenotypic profile of the overall $CD8^+$ T cell population. **(A)** CD27 vs. CD45RO; **(B)** CD57 vs. PD-1. Inset plots in **(B)** display the CMV $pp65_{495-503}$/HLA-A*0201 tetramer-labelled $CD3^+$ T cell populations in each case. The magnitudes (% values with respect to the total $CD3^+$ T cell population) of the tetramer-labelled (NLV) $CD8^{high}$ and $CD8^{low}$ subpopulations, respectively, were: 2.28% and 1.12% for patient 16, 10.1% and 4.6% for patient 13, 2.04% and 3.06% for patient 6, and 2.67% and 0.85% for patient 7. **(C)** Clonotypic composition of NLVPMVATV-specific $CD8^{high}$ T cells from patient 6. **(D)** Clonotypic composition of NLVPMVATV-specific $CD8^{low}$ T cells from patient 6. The clonotype sequence data shown are derived from 2385 and 4055 sorted cells, respectively. TRBV and TRBJ usage, CDR3 amino acid sequence and percent frequency are shown for each distinct clonotype. *TRBV12-3 and TRBV12-4 could not be distinguished.

Ex vivo modulation of expanded NK cell cytotoxic activity, degranulation and cytokine production by dasatinib

A modified biophotonic luciferase assay was used to measure NK cell cytotoxic activity against transiently transfected K562 cells. Expanded NK cells from LGL patients showed significantly impaired cytotoxic activity against K562 cells compared to NK cells from non-LGL patients or healthy controls ($p<0.05$ for both comparisons, Fig. 35A). Of note, insufficient numbers of NK cells were available from LGL patients with $CD8^+$ T cell expansions to conduct this assay. The impaired *in vitro* cytotoxic activity of NK cells from LGL patients may be due to exhaustion based on excessive *in vivo* proliferation or a state of reversible anergy. In line with this hypothesis, NK cell cytotoxic activity was restored to a substantial extent after pre-treatment with IL-2 for 18 hours (Fig. 35B). The cytotoxic activity of NK cells, either with or without IL-2 pre-treatment, was inhibited by dasatinib in all three groups irrespective of differences in activity (Fig. 35C, 35D). In contrast, when PBMCs were stimulated with untransfected K562 cells without IL-2 pre-treatment, no differences in NK cell degranulation and cytokine production were observed for NK LGL patients (n=5; Fig. 35E, 35F) compared to non-LGL patients (n=3) or healthy controls (n=3). Dasatinib led to a significant reduction in CD107a/b

expression and cytokine production in NK LGL patients and healthy controls at a concentration of 10 nM ($p<0.01$ for all comparisons); however, significant inhibition was not achieved at this concentration in non-LGL patients, which may reflect the small sample size (n=3). Degranulation and cytokine production were completely inhibited by dasatinib at a concentration of 50 nM in all three groups. The contrasting cytotoxicity and degranulation data could reflect differential assay conditions or differences in the cytotoxic arsenal available for deployment.

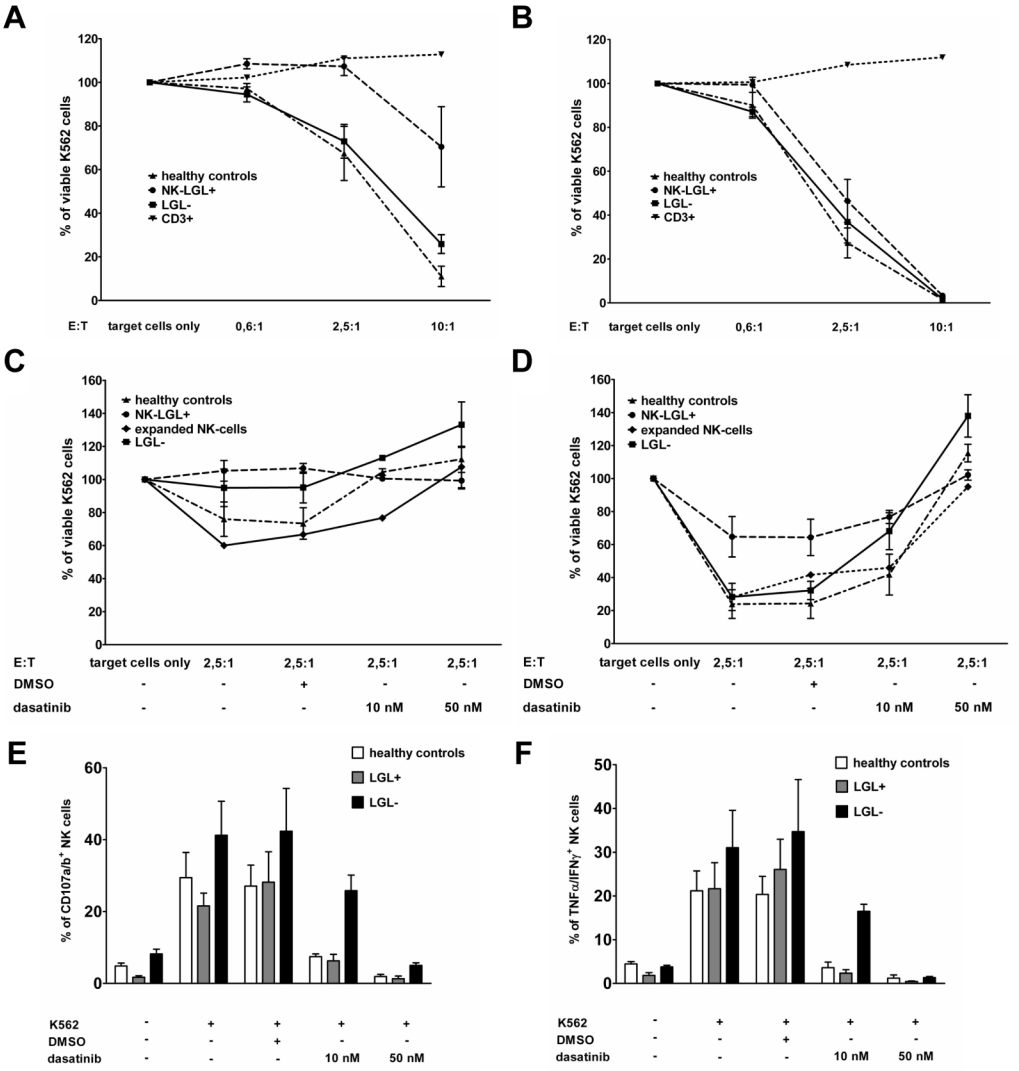

Figure 35. Effects of dasatinib on the functionality of NK cells from LGL patients, non-LGL patients and healthy controls. **(A-D)** Target cell lysis mediated by NK cells was monitored by a decrease in detected luminescence flux (RLU) in a biophotonic luciferase assay. RLU in the condition without

effector cells was set as 100% to establish relative values for other evaluations. **(A)** The cytotoxic activity of NK cells from healthy controls (n=4), non-LGL patients (n=3) and NK LGL patients (n=5) was measured at the indicated effector:target (E:T) ratios. Sorted $CD3^+$ T cells from a healthy control were included as a negative control. **(B)** NK cells were pre-treated with 2000 IU/ml IL-2 for 18 h. The cytotoxic activity of NK cells from healthy controls (n=4), non-LGL patients (n=3) and NK LGL patients (n=5) was then measured at the indicated E:T ratios. Sorted $CD3^+$ T cells from a healthy control were included as a negative control. **(C)** NK cell cytotoxic activity at the indicated E:T ratios in the presence of dasatinib at the indicated doses is shown for NK LGL patients (n=3) and non-LGL patients (n=2), and compared to expanded NK cells (n=2) or untreated NK cells from healthy controls (n=3). **(D)** NK cells were pre-treated with 2000 IU/ml IL-2 for 18 h. The cytotoxic activity of NK cells at the indicated E:T ratios was then measured in the presence of dasatinib at the indicated doses for NK LGL patients (n=3), non-LGL patients (n=2), healthy controls (n=5) and expanded polyclonal NK cells (n=1) as a positive control. **(E & F)** PBMCs ($1.5x10^5$ $CD16^+/CD56^+$ NK-cells) from NK LGL patients (n=5), non-LGL patients (n=3) and healthy controls (n=3) were stimulated with K562 cells ($2x10^4$) at an E:T ratio of 7.5:1. CD107a/b expression **(E)** and IFN-α/TNF-α production **(F)** were measured in the absence or presence of dasatinib at the indicated concentrations after 5 h. Mean values +/- SEMs are shown. The data in this figure and this figure were produced by co-investigators.

Detailed phenotypic characterization of T cells and NK cells in subjects with or without LGL expansions

Analyzed directly *ex vivo*, patients with dasatinib-associated T LGL expansions had higher frequencies of $CD8^+$ T cells and lower frequencies of $CD4^+$ T cells compared to non-LGL patients or patients with NK LGL or T + NK LGL expansions (Table 4). Although the frequencies of PD-1^+CD57^- cells in the $CD8^+$ T cell compartment were highest in non-LGL patients, subjects with LGL tended to have higher frequencies of PD-1^+ cells that also expressed CD57. Annexin V was only expressed by very few cells in patients with or without LGL expansions, and there were no differences between groups (data not shown). The majority of $CD8^+$ and $CD4^+$ T cells from patients with T or T + NK LGL expansions were $CD45RO^+CD27^-$ and many of these cells, especially in the $CD8^+$ T cell compartment, co-expressed CD57 (with lower percentages in $CD4^+$ T cells; Table 4). As described above, high frequencies of CMV-specific $CD8^+$ T cells were observed in patients with LGL expansions; these cells also exhibited

a predominant $CD45RO^{+}CD27^{-}$ phenotype and many co-expressed CD57 (Table 4). The latter could not be assessed in non-LGL patients, as they were mostly either HLA-A*02^{-} or CMV IgG seronegative. Collectively, these phenotypic features indicate that these cells are primed, late differentiated effector memory T cells (Appay, van Lier et al. 2008). The majority of NK-cells exhibited a $CD45RO^{-}CD27^{-}$ $CD57^{+}$ phenotype, especially in patients with NK or T + NK LGL expansions (Table 5). This phenotype is typical for terminally differentiated effector memory cells that are characterized by replicative senescence and are found at higher frequencies in chronic viral infections (Cooper, Elliott et al. 2009; Sun, Beilke et al. 2009). Of note, 3 LGL patients (patients 1, 3 and 7; Table 3) had $CD8^{+}$ T cell populations specific for the PR1 leukaemia-associated peptide derived from proteinase 3 (1.1%, 0.6% and 0.05% of the total $CD8^{+}$ T cell population, respectively); of these, >90% were $CD45RO^{+}CD27^{-}$ and the majority (71-100%) were also $CD57^{+}$. All of these patients had advanced disease (ALL and CML in blast crisis) that had relapsed after allogeneic BM transplantation and, in 2 patients (patients 1 and 7; Table 3) the disease had subsequently quiesced into prolonged remission (>2 years) with dasatinib monotherapy, suggesting an unexpectedly good response to treatment. In other patients studied, no PR1-specific $CD8^{+}$ T cells were observed. Overall, these analyses demonstrate that T cells and NK cells in dasatinib-associated T, NK and T + NK LGL expansions characteristically display a late or terminally differentiated phenotype ($CD45RO^{+/-}CD27^{-}CD57^{+}$).

Table 5. Phenotypic features of NK cells (either gated on $CD16^+$ or $CD56^+$ first) in patients with T, NK or T + NK LGL expansion.

Phenotype	T LGL* n=4	NK LGL* N=3	T + NK LGL* n=4	No LGL* n=2
$CD16^+$ (% of live $CD14^-$ $CD3^-$ cells)	27.7 (3.5-84.2)	91.8 (64.3-97)	63.4 (49.4-72.7)	9.6 (7.0-12.2)
$CD57^+$ (% of $CD16^+$ NK cells)	53.1 (15.3-90.0)	83.3 (76.3-88.2)	76.9 (30.4-85.9)	73.5 (65.9-81.0)
$CD45RO^+CD27^-$ (% of $CD16^+$)	21.4 (17.4-36.8)	22.0 (15.8-33.5)	10.9 (7.6-20.3)	26.6 (21.7-31.5)
$CD45RO^-CD27^-$ (% of $CD16^+$)	77.1 (58.7-80.6)	78.0 (66.3-84.2)	88.6 (78.8-90.7)	71.8 (67.5-76.1)
$CD57^+$ (% of $CD16^+CD45RO^-CD27^-$)	54.8 (47.6-92.2)	85.1 (82.8-89.2)	79.4 (31.4-88.4)	80.6 (69.9-91.3)
$CD56^+$ (% of $CD16^+$ NK cells)	68.9 (25.8-75.5)	30.3 (19.5-77.8)	42.9 (29.0-70.7)	55.9 (32.9-78.8)
$CD57^+$ (% of $CD16^+CD56^+$ NK cells)	55.5 (25.8-91.8)	81.9 (77.8-89.7)	77.3 (29.0-85.9)	86.6 (83.0-90.1)
$CD45RO^+CD27^-$ (% of $CD16^+CD56^+$)	17.5 (13.4-23.6)	28.5 (23.5-33.5)	10.5 (7.5-20.8)	9.9 (6.1-13.7)
$CD45RO^-CD27^-$ (% of $CD16^+CD56^+$)	77.6 (75.1-83.4)	71.4 (66.3-76.5)	88.5 (77.6-90.5)	88.4 (83.7-93.0)
$CD56^+$ (% of live $CD14^-$ $CD3^-$ cells)	28.7 (6.2-65.0)	28.5 (19.8-93.7)	37.1 (29.7-59.6)	12.5 (8.3-16.7)
$CD57^+$ (% of $CD56^+$ NK cells)	31.6 (24.6-90.1)	78.4 (78.3-88.4)	67.6 (27.7-75.1)	61.4 (53.4-69.4)
$CD45RO^+CD27^-$ (% of $CD56^+$)	20.7 (12.0-31.9)	38.0 (27.0-40.0)	14.1 (11.1-22.4)	12.0 (11.1-12.9)
$CD45RO^-CD27^-$ (% of $CD56^+$)	72.2 (67.5-76.7)	61.8 (59.7-72.8)	83.5 (73.8-86.1)	83.4 (81.2-85.6)
$CD57^+$ (% of $CD56^+CD45RO^-CD27^-$)	40.6 (26.2-90.9)	81.6 (79.4-88.8)	73.0 (26.1-81.3)	75.9 (70.1-81.6)
$CD16^+$ (% of $CD56^+$ NK cells)	59.7 (36.2-95.1)	96.7 (77.1-98.2)	73.8 (65.5-88.0)	43.9 (27.9-59.8)
$CD57^+$ (% of $CD56^+CD16^+$ NK cells)	55.2 (31.4-91.8)	81.9 (77.2-89.7)	77.2 (30.9-85.2)	86.4 (83.0-89.7)
$CD45RO^+CD27^-$ (% of $CD56^+CD16^+$)	30.7 (11.0-40.6)	45.6 (35.6-46.5)	19.6 (17.1-33.9)	18.2 (13.1-23.2)
$CD45RO^-CD27^-$ (% of $CD56^+CD16^+$)	66.2 (59.3-80.9)	54.2 (53.4-64.3)	79.5 (64.6-81.5)	80.6 (74.6-86.5)

* Medians with ranges in parenthesis are shown.

Longitudinal phenotypic characterization of T cell subsets in a patient with combined T and NK LGL expansion

To increase our understanding of the LGL phenomenon, a longitudinal examination of T cell subsets was conducted in one patient (patient 6, CML in blast crisis; Table 3) with T + NK LGL expansion (TCRδ rearrangement in NK-cells and TCRγ rearrangement in $CD8^+$ T cells) (Kreutzman, Juvonen et al. 2010). Dramatic expansions of both total and NLVPMVATV-specific $CD8^+$ T cells were observed; the latter comprised up to 14.2% of the total $CD3^+$ T cell population in PBMCs and up to 15.1% in BMMCs (Fig. 36A). The clonal T + NK LGL expansions emerged 12 weeks after dasatinib was first administered (time point 2; Fig. 36). This paralleled the expansion of NLVPMVATV-specific $CD8^+$ T cells. A high fraction of $CD8^+$ T cells expressed CD45RO, but not CD27 (Fig. 36B); furthermore, a very high fraction of $CD8^+$ T cells expressed CD57, but relatively few expressed or co-expressed PD-1 (Fig. 36C). The latter was also true for $CD4^+$ T cells (Fig. 36H). Only a minority of total $CD8^+$ T cells and NLVPMVATV-specific $CD8^+$ T cells exhibited an activated phenotype ($CD69^+$), but more activated cells were present at the first time point (Fig. 36D, 36G). Similarly, the majority of total $CD8^+$ T cells and NLVPMVATV-specific $CD8^+$ T cells were $CD127^-$ during the period of study, although higher expression of this homeostatic memory marker was apparent at the first time point (Fig. 36D, 36G). Most NLVPMVATV-specific $CD8^+$ T cells (both $CD8^{high}$ and $CD8^{low}$) expressed CD45RO, but not CD27 (Fig. 36E); a high fraction also expressed CD57 (Fig. 36F). However, in contrast to the total $CD8^+$ T cell population, a high fraction of NLVPMVATV-specific $CD8^+$ T cells expressed both PD-1 and CD57; this PD-1^+CD57^+ fraction was less prominent at time points characterized by higher CMV loads, whereas the PD-1^+CD57^- fraction displayed the opposite pattern (Fig. 36F). Overall, these data are consistent with the contrasting effects of an Ag-driven activation and differentiation process attenuated by the inhibitory effects of dasatinib.

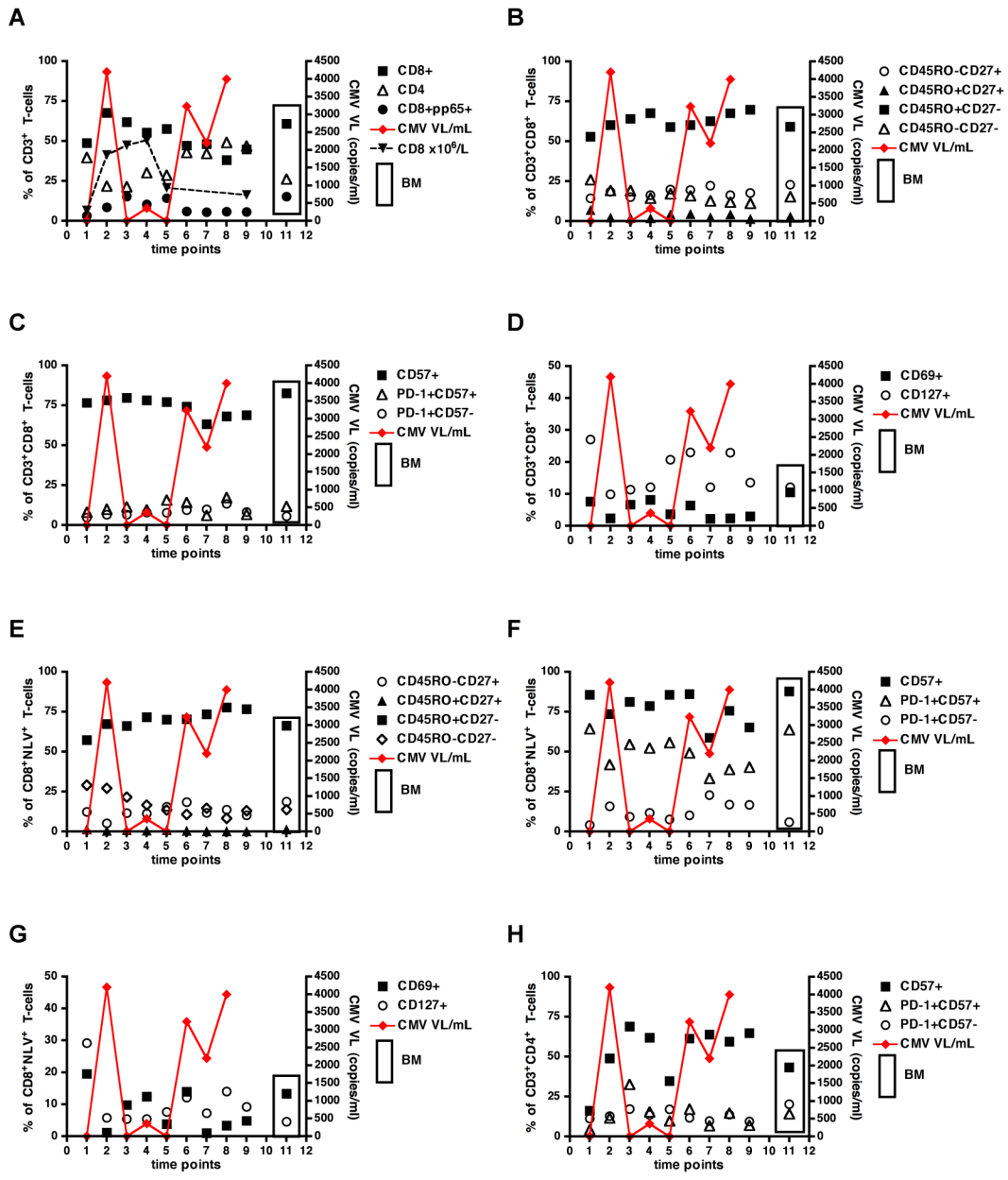

Figure 36. Longitudinal phenotypic characterization of T cell subsets in a patient with combined T and NK LGL expansion. **(A)** Frequencies of $CD8^+$, $CD4^+$ and NLVPMVATV-specific ($pp65^+$) $CD8^+$ T cells longitudinally in PBMCs and in bone marrow (BM). The $CD8^+$ T cell counts (x 10^6/L) were calculated using the absolute lymphocyte count and the percentage of $CD8^+$ T cells in PBMCs as determined by flow cytometry. **(B)** CD45RO and CD27 expression profiles of $CD3^+CD8^+$ T cells. **(C)** Fraction of $CD3^+CD8^+$ T cells that expressed CD57, PD-1 and CD57, or PD-1 without CD57. **(D)** CD69 and CD127 expression profiles of $CD3^+CD8^+$ T cells. **(E)** CD45RO and CD27 expression profiles of NLVPMVATV-specific (NLV^+) $CD3^+CD8^+$ T cells. **(F)** Fraction of NLVPMVATV-specific (NLV^+)

$CD3^+CD8^+$ T cells that expressed CD57, PD-1 and CD57, or PD-1 without CD57. **(G)** CD69 and CD127 expression profiles of NLVPMVATV-specific (NLV^+) $CD3^+CD8^+$ T cells. **(H)** Fraction of $CD3^+CD4^+$ T cells that expressed CD57, PD-1 and CD57, or PD-1 without CD57. PBMCs or BMMCs were stained sequentially with a live/dead fixable dye, CMV $pp65_{495-503}$/HLA-A*0201-allophycocyanin tetramer, and one of two different polychromatic surface marker-specific mAb panels; for one of the surface marker-specific mAb panels, cells were then also stained with streptavidin-Pacific Blue. Data were acquired on a 20-parameter FACSAria II flow cytometer and analyzed with FlowJo software. The time points were: 1 = 46 days, 2 = 107 days, 3 = 117 days, 4 = 138 days, 5 = 358 days, 6 = 446 days, 7 = 463 days, 8 = 488 days, 9 = 491 days; 11 = BM sample from 358 days after the start of dasatinib therapy. The CMV load (copies/ml) is shown in all panels. All analyses were conducted with cryopreserved samples from patient 6 (Table 3).

6.5 Discussion

The dose-dependent immunosuppressive effects of dasatinib observed *in vitro* are at odds with apparent immunostimulatory effects observed *in vivo*. These differences may be explained, at least in part, by the short half-life of dasatinib *in vivo*, which leads to intermittent kinase-mediated target inhibition (Shah, Kantarjian et al. 2008). Previously, it was shown that $CD4^+$ regulatory T_{REG} cell numbers were significantly lower in CML patients compared to healthy controls; this distinction was especially marked in LGL patients, who exhibited substantially lower T_{REG} cell numbers compared to non-LGL patients (data not shown) (Mustjoki, Ekblom et al. 2009; Rohon, Porkka et al. 2010). However, the observation herein that LGL expansions in dasatinib-treated patients are associated with CMV reactivation provides additional insight into these seemingly contradictory observations.

In this study, high frequencies of $CD8^+$ T cells specific for the CMV $pp65_{495-503}$ peptide Ag (NLVPMVATV) were observed in LGL patients; furthermore, a high proportion of LGL patients (31%) experienced symptomatic CMV reactivation during dasatinib therapy, while there was no evidence for reactivation of other herpes viruses. It is feasible that CMV reactivation was triggered in these patients by the immunosuppressive effects of dasatinib, subsequently leading to the preferential expansion of individual $CD8^+$ T cell or NK cell clones with properties that rendered them more resistant to dasatinib-mediated inhibition in the context of enhanced viral antigenic load. Our dasatinib sensitivity studies

support this hypothesis (Figs. 32 and 33). Furthermore, monoclonal or oligoclonal LGL expansions have been described in states of reduced immunity, for example after allogeneic stem cell transplantation (Mohty, Faucher et al. 2002), and during chronic viral infections (Strickler, Movahed et al. 1990; Rossi, Franceschetti et al. 2007). After allogeneic stem cell transplantation, LGL expansions typically occur within 3-15 months and are primarily observed in the context of chronic viral infections. This indicates that chronic Ag-driven T cell stimulation may contribute to, or even cause, LGL expansions. Of note, LGL expansions have been associated with long-term remission in leukaemic states (Mohty, Faucher et al. 2002). Indeed, this favourable outcome also applies to dasatinib-treated patients with monoclonal or oligoclonal LGL expansions (Table 3) (Kim, Kamel-Reid et al. 2009; Mustjoki, Ekblom et al. 2009; Kreutzman, Juvonen et al. 2010). It is tempting to speculate that cross-reactive $CD8^+$ T cells (Nahill and Welsh 1993; Burrows, Khanna et al. 1994), driven by viral recrudescence and fortuitously targeting leukaemia-associated Ags, might mediate these beneficial effects. In this light, it is notable that the majority of LGL patients (11/16) in this study were HLA-A*02^+, which might restrict both virus-specific and leukaemia-associated Ag-specific epitopes in this setting. Previous descriptions of improved survival associated with HLA-A*02^+ and CMV IgG seropositivity in the allogeneic transplantation setting are consistent with this notion (Nachbaur, Bonatti et al. 2001).

All LGL patients exhibited distinct $CD8^+$ T cell populations comprising both $CD8^{high}$ and $CD8^{low}$ T cells. This was true for both the total and NLVPMVATV-specific $CD8^+$ T cell populations. The $CD8^{high}$ T cell subset was uniformly the most functionally responsive on restimulation. A similar phenotypic dichotomy ($CD8^{high}$ vs $CD8^{low}$) has been described previously for HIV-specific $CD8^+$ T cells, both during the initiation and discontinuation of antiretroviral therapy (Oxenius, Gunthard et al. 2001). Thus, dynamic perturbations of viral load can elicit such phenotypic patterns within the cognate $CD8^+$ T cell population. Consistent with this explanation, both the $CD8^{high}$ and $CD8^{low}$ NLVPMVATV-specific $CD8^+$ T cell populations were phenotypically and clonotypically similar within individuals, thereby indicating that the same Ag-specific clonotypes can exist in different states of activation during dasatinib-associated LGL expansion. Of further note in this regard, it has been shown previously that CMV-specific $CD8^+$ T cells can dominate the memory pool in IgG seropositive individuals (Sylwester,

Mitchell et al. 2005; Scheinberg, Melenhorst et al. 2009); thus, CMV reactivation could potentially explain the dichotomous pattern of CD8 expression within the total $CD8^+$ T cell population, as the NLVPMVATV-specific response likely only measures a small fraction of the overall $CD8^+$ T cell response to CMV. In addition, high CD8 expression may reflect the inhibition of co-receptor downregulation by dasatinib (Weichsel, Dix et al. 2008; Lissina, Ladell et al. 2009). $CD8^{low}$ T cells have been observed primarily in chronic infections with persistent antigenic stimulation, such as HIV infection (Schmitz, Forman et al. 1998; Keir, Rosenberg et al. 2002), and may represent long-lived anergic cells in some cases (Blish, Dillon et al. 1999).

In LGL patients, an increased frequency of apoptotic T cells was found compared to non-LGL patients and healthy controls. This finding may reflect strong *in vivo* proliferation of the LGL cells, potentially driven by viral Ags, leading to exhaustion and increased susceptibility to apoptosis. The observed relative impairment of NK cell cytotoxic activity against K562 cells in NK LGL patients could be due to a similar process. In line with these findings, both $CD8^+$ T cells and NK cells expressed high levels of CD57 in patients with LGL expansions of the corresponding cell subsets. CD57 expression is a marker of replicative senescence and indicative of altered functional capacities (Brenchley, Karandikar et al. 2003). However, this reduced cytotoxic activity was restorable after pre-treatment of NK cells with IL-2, which argues for a transient effect with sustained functionality as typifies recently primed or anergic cells.

The increased IP-10, IL-6, MIG and IL-2R levels observed in LGL patients could conceivably contribute to improved therapeutic responses because these cytokines/chemokines direct the chemotaxis of monocytes, T cells, NK cells and dendritic cells. Such chemotactic effects have been shown to be relevant for leukaemia control (Sun, Finger et al. 2005; Choi, Hildebrandt et al. 2007). Of note, some of these soluble factors are typically produced by Ag-specific $CD8^+$ T cells during viral infections and are associated with anti-viral processes. Indeed, a causative role for infections with herpes viruses has already been postulated in the pathogenesis of LGL expansions (Swa, Wright et al. 2001). The elevated cytokine/chemokine levels in LGL patients could therefore indicate a higher

degree of viral Ag-driven cellular immune activation enhanced by an intrinsic dysregulation of homeostasis. Consistent with these ideas, the highest levels of IP-10, IL-6, MIG and IL-2R were observed in the plasma of LGL patients with symptomatic CMV reactivation. Notably, $CD8^+$ T cells specific for the leukaemia-associated Ag PR1 were detected in 3 LGL patients with complete remission status despite initially poor prognoses. Such $CD8^+$ T cell populations are difficult to detect in peripheral blood (Melenhorst, Scheinberg et al. 2009); it is therefore possible that larger numbers of these cells might reside in the bone marrow of patients with dasatinib-associated LGL, contributing to the link between elevated levels of cytokines/chemokines and favourable outcome.

In summary, the expanded lymphocyte populations in dasatinib-associated LGL patients are primarily $CD27^-$ and $CD57^+$, a phenotype associated with late differentiated effector memory cells. This finding is in general agreement with previous descriptions of anergic clonal T cell expansions in other malignant diseases such as multiple myeloma (Sze, Giesajtis et al. 2001), myelodysplastic syndrome (Epling-Burnette, Painter et al. 2007) and Waldenstrom's macroglobulinaemia (Li, Sze et al. 2010). In addition, strong evidence is provided that the LGL expansions, which are linked to a favourable outcome during dasatinib therapy, are associated with CMV reactivation. A causative role for CMV in this process has yet to be proven, but the possibility that a recrudescent virus can elicit cellular immune responses capable of controlling leukaemia is worthy of further study.

CHAPTER

7

Discussion

7.1 Discussion

In this thesis, T cell responses to chronic antigenic stimulation were investigated in a variety of settings to generate insights into the processes that regulate T cell memory. The *in vivo* turnover (rates of proliferation and cell death) of antigen-specific and phenotypically defined T cell populations was studied in transgenic mice and HIV-1-infected humans, respectively. In addition, memory $CD8^+$ T cell expansions were examined in MCMV-infected mice and patients with dasatinib-induced LGL.

Other investigators have published discrepant results on the issue of whether continuous s.c. administration of peptide without adjuvant leads to T cell tolerance or immunity / inflammation. In **chapter 3** of this thesis, experiments were performed using intact TCR tg mice to resolve these discrepancies in an appropriately controlled setting. Use of a murine model was necessary to study the cellular composition of the thymus and sort sufficient numbers of Ag-specific T_M and T_N cells to assess label enrichment after *in vivo* labelling. The main objectives were to study the *in vivo* proliferation rates of naïve and effector memory Ag-specific T cells, and to study the expansion of these cells, as well $CD4^+CD25highFoxP3^+$ T_{REG} cells, in terms of complete organ counts. *In vitro*, the number of T cell divisions has been used as an argument for or against tolerance. Specifically, tolerized T cells are thought to undergo fewer divisions than non-tolerized T cells. The data presented here show that immunological tolerance is established through “aborted” immune activation in DO11.10 $CD4^+$ TCR tg mice during and after s.c. administration of peptide without adjuvant. Significantly, the *in vivo* T cell labelling data indicate that Ag-specific $CD4^+$ T cells divide initially even when Ag is given without adjuvant, which suggests the occurrence of active priming. However, the efficacy of priming and peripheral expansion was limited and confined to the peripheral LNs. This finding is in line with recent data showing that the induction of $CD4^+$ T cell tolerance versus priming *in*

vivo is independent of the rate and number of cell divisions (Adler, Huang et al. 2000). It is also consistent with the possibility that tolerized T cells are impaired with respect to T cell trafficking (Marelli-Berg, Okkenhaug et al. 2007). In this context, it is feasible that Ag given without adjuvant failed to upregulate and subsequently downregulate the expression of activation markers, such as CD69, a process that is thought to be necessary for the initiation of T cell trafficking (Shiow, Rosen et al. 2006). Unfortunately, however, CD69 cell surface expression was not assessed in the presented study. Conversion of T_N to memory/effector phenotype T cell subsets was also limited and not sustained in the absence of adjuvant. Furthermore, T_{REG} cells were induced and increased both numerically and relatively in peripheral LNs, and relatively in PBMCs and the spleen. In addition, a significant transient depletion of $CD4^+$ T cells was observed under these conditions, which might have contributed to immunological tolerance. The data described here also show that cognate Ag given with adjuvant leads to the systemic induction and expansion of all memory/effector phenotype T cell subsets studied (at the expense of naïve T cells) in $CD4^+$ TCR tg mice and that this immunological response is accompanied by typical symptoms, such as scruffy fur and weight loss, suggestive of a state of heightened immune activation. The latter finding is unexpected had one believed the assumptions of Kearney *et al.* (Kearney, Pape et al. 1994). Indeed, the data presented in this thesis likely represent the first demonstration that immune responses can be generated in TCR tg mice with considerable similarities to those observed in wild-type mice.

CD57 expression has been associated with $CD8^+$ T cell senescence (Brenchley, Karandikar et al. 2003), one feature of which is the inability of cells to further divide. *Ex vivo*, $CD57^+$ memory $CD8^+$ T cells appeared to proliferate much less than other memory T cell subsets in response to non-specific stimuli (Brenchley, Karandikar et al. 2003). Memory $CD8^+$ $CD57^+$ T cells would therefore be expected to proliferate less *in vivo* than their $CD57^-$ counterparts. The preliminary *in vivo* labelling data shown in **chapter 4** suggest that long-term ^2H_2O labelling needs to be carried out to resolve this issue definitively. Short-term labelling gave less consistent results. One relevant consideration here is the

fact that memory $CD57^+$ and $CD57^-$ $CD8^+$ T cells are more heterogeneous than the two other populations studied, namely $CD3^+CD8^+CD45RA^-CCR7^-CD57^+$ T cells and $CD3^+CD8^+CD45RA^-CCR7^-CD57^-$ T cells. The labelling curves for the latter two populations suggest that $CD3^+CD8^+CD45RA^-CCR7^-CD57^+$ T cells indeed proliferate less than $CD3^+CD8^+CD45RA^-CCR7^-CD57^-$ T cells, but further experiments are needed to consolidate these findings.

CMV expresses a viral homologue of the anti-inflammatory cytokine IL-10. However, little is known regarding the role of IL-10 in the regulation of CMV-specific memory $CD8^+$ T cell responses, including the phenomenon of inflation, a characteristic of CMV infection in both humans and mice whereby antigen-specific T cells progressively accumulate over time (Gillespie, Wills et al. 2000; Sylwester, Mitchell et al. 2005). In **chapter 5**, the effect of IL-10 on memory $CD8^+$ T cells, including Ag-specific $CD8^+$ T cells, was studied. The data clearly show that IL-10 suppresses CMV-specific memory T cell inflation. Chronic/latent MCMV infection was associated with IL-10 production by macrophages and virus-specific IFN-γ-expressing $CD4^+$ T cells. The induction of Th1-like cells that express IL-10 is likely due to chronic antigenic stimulation, as shown for parasitic infections (Anderson, Oukka et al. 2007; Jankovic, Kullberg et al. 2007). In addition, prolonged stimulation of HCMV-specific $CD4^+$ T cells *in vitro* induces IL-10/IFN-γ co-expression (Haringer, Lozza et al. 2009). Another finding was that mice deficient in IL-10 exhibited a profound increase in MCMV-specific $CD8^+$ T cell accumulation and antiviral cytokine production, even though inflationary $CD8^+$ T cells expressed low levels of IL-10R and may, therefore, have been refractory to direct IL-10-mediated effects. However, as inflationary T cell responses are partially dependent upon $CD4^+$ T cells (Humphreys, Loewendorf et al. 2007; Snyder, Loewendorf et al. 2009), elevated $CD4^+$ T cell help in $IL\text{-}10^{-/-}$ mice probably promotes $CD8^+$ T cell expansion as well as increased cytokine production. Furthermore, IL-10 deficiency was associated with IE3-specific $CD8^+$ T cell expansion, which suggests that IL-10 preferentially promotes inflation of defined specificities. MCMV viral genome load was reduced in $IL\text{-}10^{-/-}$ mice, most likely due to enhanced memory $CD8^+$ T cell expansion as well as more potent effector outputs (for example greater

cytokine production). The latter was recapitulated by delayed IL-10R blockade in wild-type mice. Collectively, these data demonstrate that IL-10 restricts the accumulation of functional MCMV-specific memory T cells during MCMV infection. These findings may also have direct therapeutic implications.

The cancer drug dasatinib is an oral BCR/ABL and Src family tyrosine kinase inhibitor approved for use in patients with CML after imatinib (a specific BCR/ABL tyrosine kinase inhibitor) treatment and in patients with Ph^+ ALL. Dasatinib treatment of patients with CML is associated with the occurrence of LGL expansions. Antigenic stimulation from latent pathogens such as CMV may drive these LGL expansions in some cases, and this could be related to the published dose-dependent immunosuppressive effects of dasatinib that have been observed *in vitro*. Indeed, one could envisage a scenario in which latent virus reactivation occurs due to dasatinib-mediated immunosuppression, consequently leading, to Ag-driven immune activation and the expansion of granular $CD8^+$ T cells and NK cells. The data presented in **chapter 6** suggest that this scenario is likely to happen *in vivo*, as high frequencies of $CD8^+$ T cells specific for CMV $pp65_{495\text{-}503}$ (NLVPMVATV) were observed in LGL patients. Furthermore, symptomatic CMV reactivation was observed during dasatinib therapy in 31% of LGL patients. Monoclonal or oligoclonal LGL expansions have been observed in states of reduced immunity, for example after stem cell transplantation (Mohty, Faucher et al. 2002), and during chronic viral infections (Strickler, Movahed et al. 1990; Rossi, Franceschetti et al. 2007). Of note, LGL expansions have also been associated with long-term remission in leukaemic states (Mohty, Faucher et al. 2002), and a favourable outcome also applies to dasatinib-treated patients as shown both in this thesis and in previous reports (Kim, Kamel-Reid et al. 2009; Mustjoki, Ekblom et al. 2009; Kreutzman, Juvonen et al. 2010). It is also notable that the majority of patients studied in **chapter 6** were HLA-$A*02^+$. In the setting of allogeneic transplantation, CMV-seropositive HLA-$A*02^+$ patients show improved survival rates (Nachbaur, Bonatti et al. 2001). The reason for this favourable response is currently under investigation. Potential contributory factors include cross-reactivity of expanded T cell clones that respond to viral Ags and heightened immune activation due to viral reactivation.

In summary, this thesis examined: (i) the impact of continuous antigenic stimulation on Ag-specific naïve and memory $CD4^+$ T cell turnover; (ii) a subset of $CD8^+$ T cells that are assumed to be senescent T cells and that accumulate in humans harbouring chronic viruses, such as CMV and HIV; (iii) the impact of the immunosuppressive cytokine IL-10 on the inflation of CMV-specific $CD8^+$ T cell populations; and, (iv) the detailed phenotypic and functional characteristics of T and NK cells in leukaemic patients with LGL expansions during dasatinib treatment. First, it was found that continuous antigenic stimulation without adjuvant leads to increased *in vivo* turnover of Ag-specific $CD4^+$ T cells in TCR tg mice, but that adjuvant is needed for expansion of all memory/effector $CD4^+$ T cell subsets in this setting. Only in the presence of adjuvant did the mice exhibit any symptoms that would suggest immune activation, such as weight loss and inflammation at the site of continuous Ag administration. In other words, continuous antigenic stimulation lead to aborted immune activation. Second, it does indeed appear as if $CD57^+$ T cells turnover less *in vivo* than their $CD57^-$ counterparts, at least in the $CD8^+$ T cell compartment. However, more data are needed to confirm this finding and work is ongoing in this respect. Third, chronic/latent MCMV infection was found to be associated with the production of IL-10 by macrophages and virus-specific Th1-like cells, and that IL-10 suppresses memory T cell inflation. Conversely, mice deficient in IL-10 exhibited a profound increase in MCMV-specific $CD8^+$ T cell accumulation and antiviral cytokine production, even though inflationary $CD8^+$ T cells expressed low levels of IL-10R and may therefore have been refractory to direct IL-10-mediated effects. Defined T cell specificities were inflated in mice with IL-10 deficiency, and MCMV viral genome load was reduced in $IL\text{-}10^{-/-}$ mice, most likely due to enhanced memory $CD8^+$ T cell expansions with more potent antiviral weaponry. Lastly, evidence is presented that dasatinib-associated LGL expansion is linked to CMV reactivation, at least in the cohort of patients studied here, which could represent a potential mechanism for this phenomenon. The expanded cells, which were either of T cell or NK cell origin, exhibited a late differentiated ($CD27^-CD57^+$) phenotype, which suggests that these cells were expanded due to antigenic stimulation. In addition $CD8^{high}$ and $CD8^{low}$ T cells were observed in the whole CD8 compartment as well as in the CMV-specific $CD8^+$ T cell populations of LGL patients, and plasma levels of pro-inflammatory cytokines were significantly increased, all of which are consistent

with Ag-driven activation.

7.2 Future work

Future work has already begun and is focussed on understanding memory T cell differentiation and senescence in more detail. In particular, long-term isotope labelling studies combined with accurate measurements of telomere length and telomerase activity within T cell subsets defined in high resolution multi-parametric space using advanced polychromatic flow cytometry are underway and should enable accurate determination of lineage relationships within the memory T cell pool. Experiments are also ongoing to identify the precise viral antigens that trigger LGL expansions and determine whether the expanded $CD8^+$ T cells cross-recognize leukaemia-associated antigens.

7.3 Concluding remarks

The aim of this thesis has been to study Ag-specific T cell turnover (proliferation and death rates) and expansion *in vivo* under conditions of chronic antigenic stimulation. New insights have been gained into Ag-specific naïve and memory $CD4^+$ T cell turnover in mice during chronic immune stimulation with cognate peptide in the presence and absence of adjuvant. In addition, the turnover of memory $CD57^+CD8^+$ T cells in humans was examined, although these data should be considered preliminary. Chronic antigenic stimulation in the presence of adjuvant, which is naturally present in persistent viral infection due to pathogen-expressed motifs that activate immune pathways, not only leads to increased T cell turnover, but also to T cell expansion. Further insights have been provided into how IL-10 influences T cell expansion and inflation during MCMV infection, with possible implications for immunotherapeutic interventions. Finally, this work has provided evidence that LGL expansions in leukaemia patients treated with dasatinib are associated with CMV reactivation and chronic stimulation with viral antigen.

Bibliography

Addo, M. M., R. Draenert, et al. (2007). "Fully differentiated HIV-1 specific CD8+ T effector cells are more frequently detectable in controlled than in progressive HIV-1 infection." PLoS One **2**(3): e321.

Adler, A. J., C. T. Huang, et al. (2000). "In vivo CD4+ T cell tolerance induction versus priming is independent of the rate and number of cell divisions." J Immunol **164**(2): 649-55.

Almeida, A. R., N. Legrand, et al. (2002). "Homeostasis of peripheral CD4+ T cells: IL-2R alpha and IL-2 shape a population of regulatory cells that controls CD4+ T cell numbers." J Immunol **169**(9): 4850-60.

Almeida, J. R., D. A. Price, et al. (2007). "Superior control of HIV-1 replication by CD8+ T cells is reflected by their avidity, polyfunctionality, and clonal turnover." J Exp Med **204**(10): 2473-85.

Altman, J. D., P. A. Moss, et al. (1996). "Phenotypic analysis of antigen-specific T lymphocytes." Science **274**(5284): 94-6.

Anderson, C. F., M. Oukka, et al. (2007). "CD4(+)CD25(-)Foxp3(-) Th1 cells are the source of IL-10-mediated immune suppression in chronic cutaneous leishmaniasis." J Exp Med **204**(2): 285-97.

Andersson, J., D. Q. Tran, et al. (2008). "CD4+ FoxP3+ regulatory T cells confer infectious tolerance in a TGF-beta-dependent manner." J Exp Med **205**(9): 1975-81.

Annacker, O., O. Burlen-Defranoux, et al. (2000). "Regulatory CD4 T cells control the size of the peripheral activated/memory CD4 T cell compartment." J Immunol **164**(7): 3573-80.

Annacker, O., R. Pimenta-Araujo, et al. (2001). "CD25+ CD4+ T cells regulate the expansion of peripheral CD4 T cells through the production of IL-10." J Immunol **166**(5): 3008-18.

Apostolou, I. and H. von Boehmer (2004). "In vivo instruction of suppressor commitment in naive T cells." J Exp Med **199**(10): 1401-8.

Appay, V., P. R. Dunbar, et al. (2002). "Memory CD8+ T cells vary in differentiation phenotype in different persistent virus infections." Nat Med **8**(4): 379-85.

Appay, V., R. A. van Lier, et al. (2008). "Phenotype and function of human T lymphocyte subsets: consensus and issues." Cytometry A **73**(11): 975-83.

Arens, R., P. Wang, et al. (2008). "Cutting edge: murine cytomegalovirus induces a polyfunctional CD4 T cell response." J Immunol **180**(10): 6472-6.

Asquith, B., C. Debacq, et al. (2002). "Lymphocyte kinetics: the interpretation of labelling data." Trends Immunol **23**(12): 596-601.

Asseman, C., S. Mauze, et al. (1999). "An essential role for interleukin 10 in the function of regulatory

T cells that inhibit intestinal inflammation." J Exp Med **190**(7): 995-1004.

Asseman, C. and F. Powrie (1998). "Interleukin 10 is a growth factor for a population of regulatory T cells." Gut **42**(2): 157-8.

Baars, P. A., S. Sierro, et al. (2005). "Properties of murine (CD8+)CD27- T cells." Eur J Immunol **35**(11): 3131-41.

Baldwin, T. A., M. M. Sandau, et al. (2005). "The timing of TCR alpha expression critically influences T cell development and selection." J Exp Med **202**(1): 111-21.

Banks, T. A., S. Rickert, et al. (2005). "A lymphotoxin-IFN-beta axis essential for lymphocyte survival revealed during cytomegalovirus infection." J Immunol **174**(11): 7217-25.

Bantscheff, M., D. Eberhard, et al. (2007). "Quantitative chemical proteomics reveals mechanisms of action of clinical ABL kinase inhibitors." Nat Biotechnol **25**(9): 1035-44.

Barton, E. S., D. W. White, et al. (2007). "Herpesvirus latency confers symbiotic protection from bacterial infection." Nature **447**(7142): 326-9.

Bedoret, D., H. Wallemacq, et al. (2009). "Lung interstitial macrophages alter dendritic cell functions to prevent airway allergy in mice." J Clin Invest **119**(12): 3723-38.

Ben-Sasson, S. Z., J. Hu-Li, et al. (2009). "IL-1 acts directly on CD4 T cells to enhance their antigen-driven expansion and differentiation." Proc Natl Acad Sci U S A **106**(17): 7119-24.

Betts, M. R., M. C. Nason, et al. (2006). "HIV nonprogressors preferentially maintain highly functional HIV-specific CD8+ T cells." Blood **107**(12): 4781-9.

Blake, S. J., A. B. Lyons, et al. (2009). "Nilotinib inhibits the Src-family kinase LCK and T-cell function in vitro." J Cell Mol Med **13**(3): 599-601.

Blish, C. A., S. R. Dillon, et al. (1999). "Anergic CD8+ T cells can persist and function in vivo." J Immunol **163**(1): 155-64.

Bonasio, R., M. L. Scimone, et al. (2006). "Clonal deletion of thymocytes by circulating dendritic cells homing to the thymus." Nat Immunol **7**(10): 1092-100.

Bopp, T., C. Becker, et al. (2007). "Cyclic adenosine monophosphate is a key component of regulatory T cell-mediated suppression." J Exp Med **204**(6): 1303-10.

Borghans, J. A. and R. J. de Boer (2007). "Quantification of T-cell dynamics: from telomeres to DNA labeling." Immunol Rev **216**: 35-47.

Brave, M., V. Goodman, et al. (2008). "Sprycel for chronic myeloid leukemia and Philadelphia chromosome-positive acute lymphoblastic leukemia resistant to or intolerant of imatinib mesylate." Clin Cancer Res **14**(2): 352-9.

Brenchley, J. M., N. J. Karandikar, et al. (2003). "Expression of CD57 defines replicative senescence

and antigen-induced apoptotic death of CD8+ T cells." Blood **101**(7): 2711-20.

Bridgeman, J. S., A. K. Sewell, et al. (2012). "Structural and biophysical determinants of alphabeta T-cell antigen recognition." Immunology **135**(1): 9-18.

Brooks, D. G., M. J. Trifilo, et al. (2006). "Interleukin-10 determines viral clearance or persistence in vivo." Nat Med **12**(11): 1301-9.

Brown, C. E., C. L. Wright, et al. (2005). "Biophotonic cytotoxicity assay for high-throughput screening of cytolytic killing." J Immunol Methods **297**(1-2): 39-52.

Burrows, S. R., R. Khanna, et al. (1994). "An alloresponse in humans is dominated by cytotoxic T lymphocytes (CTL) cross-reactive with a single Epstein-Barr virus CTL epitope: implications for graft-versus-host disease." J Exp Med **179**(4): 1155-61.

Busch, R., D. Cesar, et al. (2004). "Isolation of peripheral blood CD4(+) T cells using RosetteSep and MACS for studies of DNA turnover by deuterium labeling." J Immunol Methods **286**(1-2): 97-109.

Busch, R., R. A. Neese, et al. (2007). "Measurement of cell proliferation by heavy water labeling." Nat Protoc **2**(12): 3045-57.

Campisi, J. (1996). "Replicative senescence: an old lives' tale?" Cell **84**(4): 497-500.

Cantor, H., J. Hugenberger, et al. (1978). "Immunoregulatory circuits among T-cell sets. Identification of a subpopulation of T-helper cells that induces feedback inhibition." J Exp Med **148**(4): 871-7.

Cao, X., S. F. Cai, et al. (2007). "Granzyme B and perforin are important for regulatory T cell-mediated suppression of tumor clearance." Immunity **27**(4): 635-46.

Casalegno-Garduno, R., A. Schmitt, et al. (2010). "Multimer technologies for detection and adoptive transfer of antigen-specific T cells." Cancer Immunol Immunother **59**(2): 195-202.

Chambers, C. A., M. F. Krummel, et al. (1996). "The role of CTLA-4 in the regulation and initiation of T-cell responses." Immunol Rev **153**: 27-46.

Chappert, P., M. Leboeuf, et al. (2008). "Antigen-driven interactions with dendritic cells and expansion of Foxp3+ regulatory T cells occur in the absence of inflammatory signals." J Immunol **180**(1): 327-34.

Chattopadhyay, P. K., M. R. Betts, et al. (2009). "The cytolytic enzymes granyzme A, granzyme B, and perforin: expression patterns, cell distribution, and their relationship to cell maturity and bright CD57 expression." J Leukoc Biol **85**(1): 88-97.

Chaube, S. and M. L. Murphy (1995). "The Teratogenic Effects of Recent Drugs Active in Cancer Chemotherapy." Advanced Teratology **3**: 181-237.

Chen, J., A. Schmitt, et al. (2008). "Nilotinib hampers the proliferation and function of CD8+ T

lymphocytes through inhibition of T cell receptor signalling." J Cell Mol Med **12**(5B): 2107-18.

Chen, L. (2004). "Co-inhibitory molecules of the B7-CD28 family in the control of T-cell immunity." Nat Rev Immunol **4**(5): 336-47.

Chen, W., W. Jin, et al. (2003). "Conversion of peripheral CD4+CD25- naive T cells to CD4+CD25+ regulatory T cells by TGF-beta induction of transcription factor Foxp3." J Exp Med **198**(12): 1875-86.

Chess, L. and H. Jiang (2004). "Resurrecting CD8+ suppressor T cells." Nat Immunol **5**(5): 469-71.

Cheung, A. K., D. J. Gottlieb, et al. (2009). "The role of the human cytomegalovirus UL111A gene in down-regulating CD4+ T-cell recognition of latently infected cells: implications for virus elimination during latency." Blood **114**(19): 4128-37.

Cho, H. J., S. G. Edmondson, et al. (2003). "Cutting edge: identification of the targets of clonal deletion in an unmanipulated thymus." J Immunol **170**(1): 10-3.

Choi, S. W., G. C. Hildebrandt, et al. (2007). "CCR1/CCL5 (RANTES) receptor-ligand interactions modulate allogeneic T-cell responses and graft-versus-host disease following stem-cell transplantation." Blood **110**(9): 3447-55.

Chong, L. K., R. J. Aicheler, et al. (2008). "Proliferation and interleukin 5 production by CD8hi CD57+ T cells." Eur J Immunol **38**(4): 995-1000.

Chtanova, T., S. G. Tangye, et al. (2004). "T follicular helper cells express a distinctive transcriptional profile, reflecting their role as non-Th1/Th2 effector cells that provide help for B cells." J Immunol **173**(1): 68-78.

Cobbold, M., N. Khan, et al. (2005). "Adoptive transfer of cytomegalovirus-specific CTL to stem cell transplant patients after selection by HLA-peptide tetramers." J Exp Med **202**(3): 379-86.

Cohen, A., J. Barankiewicz, et al. (1983). "Purine and pyrimidine metabolism in human T lymphocytes. Regulation of deoxyribonucleotide metabolism." J Biol Chem **258**(20): 12334-40.

Collison, L. W., C. J. Workman, et al. (2007). "The inhibitory cytokine IL-35 contributes to regulatory T-cell function." Nature **450**(7169): 566-9.

Connor, L. M., M. C. Harvie, et al. (2010). "A key role for lung-resident memory lymphocytes in protective immune responses after BCG vaccination." Eur J Immunol **40**(9): 2482-92.

Cooper, M. A., J. M. Elliott, et al. (2009). "Cytokine-induced memory-like natural killer cells." Proc Natl Acad Sci U S A **106**(6): 1915-9.

Curotto de Lafaille, M. A. and J. J. Lafaille (2009). "Natural and adaptive foxp3+ regulatory T cells: more of the same or a division of labor?" Immunity **30**(5): 626-35.

Dahlberg, P. E., J. M. Schartner, et al. (2007). "Daily subcutaneous injections of peptide induce CD4+

CD25+ T regulatory cells." Clin Exp Immunol **149**(2): 226-34.

Daniel, C., B. Weigmann, et al. (2011). "Prevention of type 1 diabetes in mice by tolerogenic vaccination with a strong agonist insulin mimetope." J Exp Med **208**(7): 1501-10.

Davenport, M. P., C. Fazou, et al. (2002). "Clonal selection, clonal senescence, and clonal succession: the evolution of the T cell response to infection with a persistent virus." J Immunol **168**(7): 3309-17.

Davis, M. M., J. J. Boniface, et al. (1998). "Ligand recognition by alpha beta T cell receptors." Annu Rev Immunol **16**: 523-44.

Day, C. L., D. E. Kaufmann, et al. (2006). "PD-1 expression on HIV-specific T cells is associated with T-cell exhaustion and disease progression." Nature **443**(7109): 350-4.

Deaglio, S., K. M. Dwyer, et al. (2007). "Adenosine generation catalyzed by CD39 and CD73 expressed on regulatory T cells mediates immune suppression." J Exp Med **204**(6): 1257-65.

Douek, D. C., M. R. Betts, et al. (2002). "A novel approach to the analysis of specificity, clonality, and frequency of HIV-specific T cell responses reveals a potential mechanism for control of viral escape." J Immunol **168**(6): 3099-104.

Druker, B. J., F. Guilhot, et al. (2006). "Five-year follow-up of patients receiving imatinib for chronic myeloid leukemia." N Engl J Med **355**(23): 2408-17.

Einsele, H., E. Roosnek, et al. (2002). "Infusion of cytomegalovirus (CMV)-specific T cells for the treatment of CMV infection not responding to antiviral chemotherapy." Blood **99**(11): 3916-22.

Ejrnaes, M., C. M. Filippi, et al. (2006). "Resolution of a chronic viral infection after interleukin-10 receptor blockade." J Exp Med **203**(11): 2461-72.

Epling-Burnette, P. K., J. S. Painter, et al. (2007). "Prevalence and clinical association of clonal T-cell expansions in Myelodysplastic Syndrome." Leukemia **21**(4): 659-67.

Eyerich, S., K. Eyerich, et al. (2009). "Th22 cells represent a distinct human T cell subset involved in epidermal immunity and remodeling." J Clin Invest **119**(12): 3573-85.

Fahlen, L., S. Read, et al. (2005). "T cells that cannot respond to TGF-beta escape control by CD4(+)CD25(+) regulatory T cells." J Exp Med **201**(5): 737-46.

Fei, F., Y. Yu, et al. (2008). "Dasatinib exerts an immunosuppressive effect on CD8+ T cells specific for viral and leukemia antigens." Exp Hematol **36**(10): 1297-308.

Fishman, J. A., V. Emery, et al. (2007). "Cytomegalovirus in transplantation - challenging the status quo." Clin Transplant **21**(2): 149-58.

Foulds, K. E., M. J. Rotte, et al. (2006). "IL-10 is required for optimal CD8 T cell memory following Listeria monocytogenes infection." J Immunol **177**(4): 2565-74.

Fraser, C. K., S. J. Blake, et al. (2009). "Dasatinib inhibits recombinant viral antigen-specific murine CD4+ and CD8+ T-cell responses and NK-cell cytolytic activity in vitro and in vivo." Exp Hematol **37**(2): 256-65.

Freeman, G. J., E. J. Wherry, et al. (2006). "Reinvigorating exhausted HIV-specific T cells via PD-1-PD-1 ligand blockade." J Exp Med **203**(10): 2223-7.

Fukaura, H., S. C. Kent, et al. (1996). "Induction of circulating myelin basic protein and proteolipid protein-specific transforming growth factor-beta1-secreting Th3 T cells by oral administration of myelin in multiple sclerosis patients." J Clin Invest **98**(1): 70-7.

Gao, G. F., Z. Rao, et al. (2002). "Molecular coordination of alphabeta T-cell receptors and coreceptors CD8 and CD4 in their recognition of peptide-MHC ligands." Trends Immunol **23**(8): 408-13.

Garboczi, D. N., D. T. Hung, et al. (1992). "HLA-A2-peptide complexes: refolding and crystallization of molecules expressed in Escherichia coli and complexed with single antigenic peptides." Proc Natl Acad Sci U S A **89**(8): 3429-33.

Garin, M. I., C. C. Chu, et al. (2007). "Galectin-1: a key effector of regulation mediated by CD4+CD25+ T cells." Blood **109**(5): 2058-65.

Gea-Banacloche, J. C., S. A. Migueles, et al. (2000). "Maintenance of large numbers of virus-specific CD8+ T cells in HIV-infected progressors and long-term nonprogressors." J Immunol **165**(2): 1082-92.

Gillespie, G. M., M. R. Wills, et al. (2000). "Functional heterogeneity and high frequencies of cytomegalovirus-specific CD8(+) T lymphocytes in healthy seropositive donors." J Virol **74**(17): 8140-50.

Gondek, D. C., L. F. Lu, et al. (2005). "Cutting edge: contact-mediated suppression by CD4+CD25+ regulatory cells involves a granzyme B-dependent, perforin-independent mechanism." J Immunol **174**(4): 1783-6.

Green, D. R., N. Droin, et al. (2003). "Activation-induced cell death in T cells." Immunol Rev **193**: 70-81.

Gribaudo, G., S. Ravaglia, et al. (1993). "Interferons inhibit onset of murine cytomegalovirus immediate-early gene transcription." Virology **197**(1): 303-11.

Grohmann, U., C. Orabona, et al. (2002). "CTLA-4-Ig regulates tryptophan catabolism in vivo." Nat Immunol **3**(11): 1097-101.

Hand, T. and Y. Belkaid (2010). "Microbial control of regulatory and effector T cell responses in the gut." Curr Opin Immunol **22**(1): 63-72.

Haringer, B., L. Lozza, et al. (2009). "Identification and characterization of IL-10/IFN-gamma-producing

effector-like T cells with regulatory function in human blood." J Exp Med **206**(5): 1009-17.

Harrington, L. E., P. R. Mangan, et al. (2006). "Expanding the effector CD4 T-cell repertoire: the Th17 lineage." Curr Opin Immunol **18**(3): 349-56.

Heise, M. T. and H. W. t. Virgin (1995). "The T-cell-independent role of gamma interferon and tumor necrosis factor alpha in macrophage activation during murine cytomegalovirus and herpes simplex virus infections." J Virol **69**(2): 904-9.

Hellerstein, M. K. (1999). "Measurement of T-cell kinetics: recent methodologic advances." Immunol Today **20**(10): 438-41.

Hellerstein, M. K., R. A. Hoh, et al. (2003). "Subpopulations of long-lived and short-lived T cells in advanced HIV-1 infection." J Clin Invest **112**(6): 956-66.

Hellerstein, M. K. and R. A. Neese (1992). "Mass isotopomer distribution analysis: a technique for measuring biosynthesis and turnover of polymers." Am J Physiol **263**(5 Pt 1): E988-1001.

Hellerstein, M. K. and R. A. Neese (1999). "Mass isotopomer distribution analysis at eight years: theoretical, analytic, and experimental considerations." Am J Physiol **276**(6 Pt 1): E1146-70.

Hindley, J. P., C. Ferreira, et al. "Analysis of the T-cell receptor repertoires of tumor-infiltrating conventional and regulatory T cells reveals no evidence for conversion in carcinogen-induced tumors." Cancer Res **71**(3): 736-46.

Hochhaus, A., M. Baccarani, et al. (2008). "Dasatinib induces durable cytogenetic responses in patients with chronic myelogenous leukemia in chronic phase with resistance or intolerance to imatinib." Leukemia **22**(6): 1200-6.

Hogquist, K. A., T. A. Baldwin, et al. (2005). "Central tolerance: learning self-control in the thymus." Nat Rev Immunol **5**(10): 772-82.

Holtappels, R., M. F. Pahl-Seibert, et al. (2000). "Enrichment of immediate-early 1 (m123/pp89) peptide-specific CD8 T cells in a pulmonary CD62L(lo) memory-effector cell pool during latent murine cytomegalovirus infection of the lungs." J Virol **74**(24): 11495-503.

Hsu, D. H., R. de Waal Malefyt, et al. (1990). "Expression of interleukin-10 activity by Epstein-Barr virus protein BCRF1." Science **250**(4982): 830-2.

Hu, D., K. Ikizawa, et al. (2004). "Analysis of regulatory CD8 T cells in Qa-1-deficient mice." Nat Immunol **5**(5): 516-23.

Huang, C. T., C. J. Workman, et al. (2004). "Role of LAG-3 in regulatory T cells." Immunity **21**(4): 503-13.

Humphreys, I. R., C. de Trez, et al. (2007). "Cytomegalovirus exploits IL-10-mediated immune regulation in the salivary glands." J Exp Med **204**(5): 1217-25.

Humphreys, I. R., A. Loewendorf, et al. (2007). "OX40 costimulation promotes persistence of cytomegalovirus-specific CD8 T Cells: A CD4-dependent mechanism." J Immunol **179**(4): 2195-202.

Itoh, M., T. Takahashi, et al. (1999). "Thymus and autoimmunity: production of CD25+CD4+ naturally anergic and suppressive T cells as a key function of the thymus in maintaining immunologic self-tolerance." J Immunol **162**(9): 5317-26.

Janeway, C. A., Jr. (1988). "Do suppressor T cells exist? A reply." Scand J Immunol **27**(6): 621-3.

Janeway, C. A., Jr. (1992). "The T cell receptor as a multicomponent signalling machine: CD4/CD8 coreceptors and CD45 in T cell activation." Annu Rev Immunol **10**: 645-74.

Janeway, C. A. J., P. Travers, et al. (2005). Immunobiology: The Immune System in Health and Disease. New York and London, Graland Science Publishing.

Jankovic, D., M. C. Kullberg, et al. (2007). "Conventional T-bet(+)Foxp3(-) Th1 cells are the major source of host-protective regulatory IL-10 during intracellular protozoan infection." J Exp Med **204**(2): 273-83.

Jenkins, C., A. Abendroth, et al. (2004). "A novel viral transcript with homology to human interleukin-10 is expressed during latent human cytomegalovirus infection." J Virol **78**(3): 1440-7.

Jenkins, C., W. Garcia, et al. (2008). "Immunomodulatory properties of a viral homolog of human interleukin-10 expressed by human cytomegalovirus during the latent phase of infection." J Virol **82**(7): 3736-50.

Jonuleit, H., E. Schmitt, et al. (2002). "Infectious tolerance: human CD25(+) regulatory T cells convey suppressor activity to conventional CD4(+) T helper cells." J Exp Med **196**(2): 255-60.

Jordan, M. S., A. Boesteanu, et al. (2001). "Thymic selection of CD4+CD25+ regulatory T cells induced by an agonist self-peptide." Nat Immunol **2**(4): 301-6.

Kabelitz, D. and O. Janssen (1997). "Antigen-induced death of T-lymphocytes." Front Biosci **2**: d61-77.

Kang, S. S. and P. M. Allen (2005). "Priming in the presence of IL-10 results in direct enhancement of CD8+ T cell primary responses and inhibition of secondary responses." J Immunol **174**(9): 5382-9.

Kantarjian, H., N. P. Shah, et al. (2010). "Dasatinib versus imatinib in newly diagnosed chronic-phase chronic myeloid leukemia." N Engl J Med **362**(24): 2260-70.

Kantarjian, H. M., F. Giles, et al. (2007). "Nilotinib (formerly AMN107), a highly selective BCR-ABL tyrosine kinase inhibitor, is effective in patients with Philadelphia chromosome-positive chronic myelogenous leukemia in chronic phase following imatinib resistance and intolerance." Blood **110**(10): 3540-6.

Kappler, J. W., N. Roehm, et al. (1987). "T cell tolerance by clonal elimination in the thymus." Cell **49**(2): 273-80.

Karrer, U., S. Sierro, et al. (2003). "Memory inflation: continuous accumulation of antiviral CD8+ T cells over time." J Immunol **170**(4): 2022-9.

Kearney, E. R., K. A. Pape, et al. (1994). "Visualization of peptide-specific T cell immunity and peripheral tolerance induction in vivo." Immunity **1**(4): 327-39.

Keir, M. E., M. G. Rosenberg, et al. (2002). "Generation of CD3+CD8low thymocytes in the HIV type 1-infected thymus." J Immunol **169**(5): 2788-96.

Kern, F., E. Khatamzas, et al. (1999). "Distribution of human CMV-specific memory T cells among the CD8pos. subsets defined by CD57, CD27, and CD45 isoforms." Eur J Immunol **29**(9): 2908-15.

Killebrew, J. R., N. Perdue, et al. (2011). "A Self-Reactive TCR Drives the Development of Foxp3+ Regulatory T Cells That Prevent Autoimmune Disease." J Immunol **187**(2): 861-9.

Kim, D. H., S. Kamel-Reid, et al. (2009). "Natural killer or natural killer/T cell lineage large granular lymphocytosis associated with dasatinib therapy for Philadelphia chromosome positive leukemia." Haematologica **94**(1): 135-9.

Kisielow, P., H. Bluthmann, et al. (1988). "Tolerance in T-cell-receptor transgenic mice involves deletion of nonmature CD4+8+ thymocytes." Nature **333**(6175): 742-6.

Klenerman, P., V. Cerundolo, et al. (2002). "Tracking T cells with tetramers: new tales from new tools." Nat Rev Immunol **2**(4): 263-72.

Klenerman, P. and A. Hill (2005). "T cells and viral persistence: lessons from diverse infections." Nat Immunol **6**(9): 873-9.

Knoechel, B., J. Lohr, et al. (2006). "Functional and molecular comparison of anergic and regulatory T lymphocytes." J Immunol **176**(11): 6473-83.

Kotenko, S. V., S. Saccani, et al. (2000). "Human cytomegalovirus harbors its own unique IL-10 homolog (cmvIL-10)." Proc Natl Acad Sci U S A **97**(4): 1695-700.

Kretschmer, K., I. Apostolou, et al. (2005). "Inducing and expanding regulatory T cell populations by foreign antigen." Nat Immunol **6**(12): 1219-27.

Kreutzman, A., V. Juvonen, et al. (2010). "Mono/oligoclonal T and NK cells are common in chronic myeloid leukemia patients at diagnosis and expand during dasatinib therapy." Blood **116**(5): 772-82.

Kurz, S. K. and M. J. Reddehase (1999). "Patchwork pattern of transcriptional reactivation in the lungs indicates sequential checkpoints in the transition from murine cytomegalovirus latency to recurrence." J Virol **73**(10): 8612-22.

Lachman, L. B., S. O. Page, et al. (1980). "Purification of human interleukin 1." J Supramol Struct **13**(4): 457-66.

Ladell, K., M. K. Hellerstein, et al. (2008). "Central memory CD8+ T cells appear to have a shorter lifespan and reduced abundance as a function of HIV disease progression." J Immunol **180**(12): 7907-18.

Lan, R. Y., I. R. Mackay, et al. (2007). "Regulatory T cells in the prevention of mucosal inflammatory diseases: patrolling the border." J Autoimmun **29**(4): 272-80.

Le Priol, Y., D. Puthier, et al. (2006). "High cytotoxic and specific migratory potencies of senescent CD8+ CD57+ cells in HIV-infected and uninfected individuals." J Immunol **177**(8): 5145-54.

Lee, S. S., W. Gao, et al. (2007). "Heme oxygenase-1, carbon monoxide, and bilirubin induce tolerance in recipients toward islet allografts by modulating T regulatory cells." Faseb J **21**(13): 3450-7.

Lefranc, M. P., C. Pommie, et al. (2003). "IMGT unique numbering for immunoglobulin and T cell receptor variable domains and Ig superfamily V-like domains." Dev Comp Immunol **27**(1): 55-77.

Li, J., D. M. Sze, et al. (2010). "Clonal expansions of cytotoxic T cells exist in the blood of patients with Waldenstrom macroglobulinemia but exhibit anergic properties and are eliminated by nucleoside analogue therapy." Blood **115**(17): 3580-8.

Liblau, R. S., R. Tisch, et al. (1996). "Intravenous injection of soluble antigen induces thymic and peripheral T-cells apoptosis." Proc Natl Acad Sci U S A **93**(7): 3031-6.

Lissina, A., K. Ladell, et al. (2009). "Protein kinase inhibitors substantially improve the physical detection of T-cells with peptide-MHC tetramers." J Immunol Methods **340**(1): 11-24.

Lombardo, L. J., F. Y. Lee, et al. (2004). "Discovery of N-(2-chloro-6-methyl- phenyl)-2-(6-(4-(2-hydroxyethyl)- piperazin-1-yl)-2-methylpyrimidin-4- ylamino)thiazole-5-carboxamide (BMS-354825), a dual Src/Abl kinase inhibitor with potent antitumor activity in preclinical assays." J Med Chem **47**(27): 6658-61.

Lucin, P., S. Jonjic, et al. (1994). "Late phase inhibition of murine cytomegalovirus replication by synergistic action of interferon-gamma and tumour necrosis factor." J Gen Virol **75 (Pt 1)**: 101-10.

Macallan, D. C., B. Asquith, et al. (2009). "Measurement of proliferation and disappearance of rapid turnover cell populations in human studies using deuterium-labeled glucose." Nat Protoc **4**(9): 1313-27.

Macallan, D. C., C. A. Fullerton, et al. (1998). "Measurement of cell proliferation by labeling of DNA with stable isotope-labeled glucose: studies in vitro, in animals, and in humans." Proc Natl

Acad Sci U S A **95**(2): 708-13.

Madan, R., F. Demircik, et al. (2009). "Nonredundant roles for B cell-derived IL-10 in immune counter-regulation." J Immunol **183**(4): 2312-20.

Marelli-Berg, F. M., K. Okkenhaug, et al. (2007). "A two-signal model for T cell trafficking." Trends Immunol **28**(6): 267-73.

Marie, J. C., J. J. Letterio, et al. (2005). "TGF-beta1 maintains suppressor function and Foxp3 expression in CD4+CD25+ regulatory T cells." J Exp Med **201**(7): 1061-7.

Martin, B., C. Bourgeois, et al. (2003). "On the role of MHC class II molecules in the survival and lymphopenia-induced proliferation of peripheral CD4+ T cells." Proc Natl Acad Sci U S A **100**(10): 6021-6.

Martin, S. and M. J. Bevan (1997). "Antigen-specific and nonspecific deletion of immature cortical thymocytes caused by antigen injection." Eur J Immunol **27**(10): 2726-36.

Matsuoka, K., K. Nomura, et al. (1990). "Mutagenic Effects of Brief Exposure to Broodeoxyuridine on Mouse FM3A Cells." Cell Tissue Kinetics **5**: 495-503.

Matter, M. S., C. Claus, et al. (2008). "CD4+ T cell help improves CD8+ T cell memory by retained CD27 expression." Eur J Immunol **38**(7): 1847-56.

Mayer, G. and J. Nyland. (2006, July 12, 2010). "Cells involved in immune responses and antigen recognition." Microbiology and Immunology On-line Retrieved July 24, 2011, 2011.

McCune, J. M., M. B. Hanley, et al. (2000). "Factors influencing T-cell turnover in HIV-1-seropositive patients." J Clin Invest **105**(5): R1-8.

McKinstry, K. K., T. M. Strutt, et al. (2009). "IL-10 deficiency unleashes an influenza-specific Th17 response and enhances survival against high-dose challenge." J Immunol **182**(12): 7353-63.

Medzhitov, R. and C. Janeway, Jr. (2000). "Innate immunity." N Engl J Med **343**(5): 338-44.

Melenhorst, J. J., P. Scheinberg, et al. (2009). "High avidity myeloid leukemia-associated antigen-specific CD8+ T cells preferentially reside in the bone marrow." Blood **113**(10): 2238-44.

Melenhorst, J. J., P. Scheinberg, et al. (2008). "Regulatory T-cell depletion does not prevent emergence of new CD25+ FOXP3+ lymphocytes after antigen stimulation in culture." Cytotherapy **10**(2): 152-64.

Miller, J. F. (1992). "Post-thymic tolerance to self antigens." J Autoimmun **5 Suppl A**: 27-35.

Mohri, H., A. S. Perelson, et al. (2001). "Increased turnover of T lymphocytes in HIV-1 infection and its reduction by antiretroviral therapy." J Exp Med **194**(9): 1277-87.

Mohty, M., C. Faucher, et al. (2002). "Features of large granular lymphocytes (LGL) expansion following allogeneic stem cell transplantation: a long-term analysis." Leukemia **16**(10): 2129-

33.

Mollet, L., B. Sadat-Sowti, et al. (1998). "CD8hi+CD57+ T lymphocytes are enriched in antigen-specific T cells capable of down-modulating cytotoxic activity." Int Immunol **10**(3): 311-23.

Moore, K. W., A. O'Garra, et al. (1993). "Interleukin-10." Annu Rev Immunol **11**: 165-90.

Morrissey, P. J., K. Charrier, et al. (1988). "In vivo administration of IL-1 induces thymic hypoplasia and increased levels of serum corticosterone." J Immunol **141**(5): 1456-63.

Munks, M. W., K. S. Cho, et al. (2006). "Four distinct patterns of memory CD8 T cell responses to chronic murine cytomegalovirus infection." J Immunol **177**(1): 450-8.

Munks, M. W., M. C. Gold, et al. (2006). "Genome-wide analysis reveals a highly diverse CD8 T cell response to murine cytomegalovirus." J Immunol **176**(6): 3760-6.

Murphy, K. M., A. B. Heimberger, et al. (1990). "Induction by antigen of intrathymic apoptosis of CD4+CD8+TCRlo thymocytes in vivo." Science **250**(4988): 1720-3.

Mustjoki, S., M. Ekblom, et al. (2009). "Clonal expansion of T/NK-cells during tyrosine kinase inhibitor dasatinib therapy." Leukemia **23**(8): 1398-405.

Nachbaur, D., H. Bonatti, et al. (2001). "Survival after bone marrow transplantation from cytomegalovirus seropositive sibling donors." Lancet **358**(9288): 1157-9.

Nahill, S. R. and R. M. Welsh (1993). "High frequency of cross-reactive cytotoxic T lymphocytes elicited during the virus-induced polyclonal cytotoxic T lymphocyte response." J Exp Med **177**(2): 317-27.

Nakaguchi, T., T. Usui, et al. (1971). "Acute, Subacute and Chronic Toxicities of 5-Bromo-2'-Deoxyuridine in Mice and Rats." Chemical Abstract **76**: 108022s.

Nakamura, K., A. Kitani, et al. (2001). "Cell contact-dependent immunosuppression by CD4(+)CD25(+) regulatory T cells is mediated by cell surface-bound transforming growth factor beta." J Exp Med **194**(5): 629-44.

Naramura, M., I. K. Jang, et al. (2002). "c-Cbl and Cbl-b regulate T cell responsiveness by promoting ligand-induced TCR down-modulation." Nat Immunol **3**(12): 1192-9.

Neese, R. A., L. M. Misell, et al. (2002). "Measurement in vivo of proliferation rates of slow turnover cells by 2H2O labeling of the deoxyribose moiety of DNA." Proc Natl Acad Sci U S A **99**(24): 15345-50.

Neese, R. A., S. Q. Siler, et al. (2001). "Advances in the stable isotope-mass spectrometric measurement of DNA synthesis and cell proliferation." Anal Biochem **298**(2): 189-95.

Neujahr, D. C., C. Chen, et al. (2006). "Accelerated memory cell homeostasis during T cell depletion and approaches to overcome it." J Immunol **176**(8): 4632-9.

Nociari, M. M., W. Telford, et al. (1999). "Postthymic development of CD28-CD8+ T cell subset: age-associated expansion and shift from memory to naive phenotype." J Immunol **162**(6): 3327-35.

Northfield, J. W., C. P. Loo, et al. (2007). "Human immunodeficiency virus type 1 (HIV-1)-specific CD8+ T(EMRA) cells in early infection are linked to control of HIV-1 viremia and predict the subsequent viral load set point." J Virol **81**(11): 5759-65.

O'Garra, A., F. J. Barrat, et al. (2008). "Strategies for use of IL-10 or its antagonists in human disease." Immunol Rev **223**: 114-31.

Oakley, O. R., B. A. Garvy, et al. (2008). "Increased weight loss with reduced viral replication in interleukin-10 knock-out mice infected with murine cytomegalovirus." Clin Exp Immunol **151**(1): 155-64.

Oderup, C., L. Cederbom, et al. (2006). "Cytotoxic T lymphocyte antigen-4-dependent down-modulation of costimulatory molecules on dendritic cells in CD4+ CD25+ regulatory T-cell-mediated suppression." Immunology **118**(2): 240-9.

Orange, J. S. and C. A. Biron (1996). "Characterization of early IL-12, IFN-alphabeta, and TNF effects on antiviral state and NK cell responses during murine cytomegalovirus infection." J Immunol **156**(12): 4746-56.

Oxenius, A., H. F. Gunthard, et al. (2001). "Direct ex vivo analysis reveals distinct phenotypic patterns of HIV-specific CD8(+) T lymphocyte activation in response to therapeutic manipulation of virus load." Eur J Immunol **31**(4): 1115-21.

Pandiyan, P., L. Zheng, et al. (2007). "CD4+CD25+Foxp3+ regulatory T cells induce cytokine deprivation-mediated apoptosis of effector CD4+ T cells." Nat Immunol **8**(12): 1353-62.

Pape, K. A., A. Khoruts, et al. (1997). "Inflammatory cytokines enhance the in vivo clonal expansion and differentiation of antigen-activated CD4+ T cells." J Immunol **159**(2): 591-8.

Paust, S., L. Lu, et al. (2004). "Engagement of B7 on effector T cells by regulatory T cells prevents autoimmune disease." Proc Natl Acad Sci U S A **101**(28): 10398-403.

Petrovas, C., J. P. Casazza, et al. (2006). "PD-1 is a regulator of virus-specific CD8+ T cell survival in HIV infection." J Exp Med **203**(10): 2281-92.

Petrovas, C., B. Chaon, et al. (2009). "Differential association of programmed death-1 and CD57 with ex vivo survival of CD8+ T cells in HIV infection." J Immunol **183**(2): 1120-32.

Podlech, J., R. Holtappels, et al. (1998). "Reconstitution of CD8 T cells is essential for the prevention of multiple-organ cytomegalovirus histopathology after bone marrow transplantation." J Gen Virol **79 (Pt 9)**: 2099-104.

Polansky, J. K., K. Kretschmer, et al. (2008). "DNA methylation controls Foxp3 gene expression." Eur J Immunol **38**(6): 1654-63.

Polic, B., H. Hengel, et al. (1998). "Hierarchical and redundant lymphocyte subset control precludes cytomegalovirus replication during latent infection." J Exp Med **188**(6): 1047-54.

Precopio, M. L., M. R. Betts, et al. (2007). "Immunization with vaccinia virus induces polyfunctional and phenotypically distinctive CD8(+) T cell responses." J Exp Med **204**(6): 1405-16.

Presti, R. M., J. L. Pollock, et al. (1998). "Interferon gamma regulates acute and latent murine cytomegalovirus infection and chronic disease of the great vessels." J Exp Med **188**(3): 577-88.

Price, D. A., T. E. Asher, et al. (2009). "Public clonotype usage identifies protective Gag-specific CD8+ T cell responses in SIV infection." J Exp Med **206**(4): 923-36.

Price, D. A., J. M. Brenchley, et al. (2005). "Avidity for antigen shapes clonal dominance in CD8+ T cell populations specific for persistent DNA viruses." J Exp Med **202**(10): 1349-61.

Price, D. A., S. M. West, et al. (2004). "T cell receptor recognition motifs govern immune escape patterns in acute SIV infection." Immunity **21**(6): 793-803.

Quinnan, G. V., Jr., N. Kirmani, et al. (1982). "Cytotoxic t cells in cytomegalovirus infection: HLA-restricted T-lymphocyte and non-T-lymphocyte cytotoxic responses correlate with recovery from cytomegalovirus infection in bone-marrow-transplant recipients." N Engl J Med **307**(1): 7-13.

Rallon, N. I., M. Lopez, et al. (2009). "Level, phenotype and activation status of CD4+FoxP3+ regulatory T cells in patients chronically infected with human immunodeficiency virus and/or hepatitis C virus." Clin Exp Immunol **155**(1): 35-43.

Read, S., V. Malmstrom, et al. (2000). "Cytotoxic T lymphocyte-associated antigen 4 plays an essential role in the function of CD25(+)CD4(+) regulatory cells that control intestinal inflammation." J Exp Med **192**(2): 295-302.

Read, S., S. Mauze, et al. (1998). "CD38+ CD45RB(low) CD4+ T cells: a population of T cells with immune regulatory activities in vitro." Eur J Immunol **28**(11): 3435-47.

Reddehase, M. J., S. Jonjic, et al. (1988). "Adoptive immunotherapy of murine cytomegalovirus adrenalitis in the immunocompromised host: CD4-helper-independent antiviral function of CD8-positive memory T lymphocytes derived from latently infected donors." J Virol **62**(3): 1061-5.

Reddehase, M. J., W. Mutter, et al. (1987). "CD8-positive T lymphocytes specific for murine cytomegalovirus immediate-early antigens mediate protective immunity." J Virol **61**(10): 3102-8.

Reddehase, M. J., C. O. Simon, et al. (2008). "Murine model of cytomegalovirus latency and reactivation." Curr Top Microbiol Immunol **325**: 315-31.

Reddehase, M. J., F. Weiland, et al. (1985). "Interstitial murine cytomegalovirus pneumonia after

irradiation: characterization of cells that limit viral replication during established infection of the lungs." J Virol **55**(2): 264-73.

Redpath, S., A. Angulo, et al. (1999). "Murine cytomegalovirus infection down-regulates MHC class II expression on macrophages by induction of IL-10." J Immunol **162**(11): 6701-7.

Reichard, P. (1988). "Interactions between deoxyribonucleotide and DNA synthesis." Annu Rev Biochem **57**: 349-74.

Reinhardt, R. L., A. Khoruts, et al. (2001). "Visualizing the generation of memory CD4 T cells in the whole body." Nature **410**(6824): 101-5.

Reusser, P., S. R. Riddell, et al. (1991). "Cytotoxic T-lymphocyte response to cytomegalovirus after human allogeneic bone marrow transplantation: pattern of recovery and correlation with cytomegalovirus infection and disease." Blood **78**(5): 1373-80.

Riddell, S. R. (1995). "Pathogenesis of cytomegalovirus pneumonia in immunocompromised hosts." Semin Respir Infect **10**(4): 199-208.

Riddell, S. R., K. S. Watanabe, et al. (1992). "Restoration of viral immunity in immunodeficient humans by the adoptive transfer of T cell clones." Science **257**(5067): 238-41.

Rix, U., O. Hantschel, et al. (2007). "Chemical proteomic profiles of the BCR-ABL inhibitors imatinib, nilotinib, and dasatinib reveal novel kinase and nonkinase targets." Blood **110**(12): 4055-63.

Robey, E. A., B. J. Fowlkes, et al. (1991). "Thymic selection in CD8 transgenic mice supports an instructive model for commitment to a CD4 or CD8 lineage." Cell **64**(1): 99-107.

Rohon, P., K. Porkka, et al. (2010). "Immunoprofiling of patients with chronic myeloid leukemia at diagnosis and during tyrosine kinase inhibitor therapy." Eur J Haematol **85**(5): 387-98.

Rohrer, J. W. and J. H. Coggin, Jr. (1995). "CD8 T cell clones inhibit antitumor T cell function by secreting IL-10." J Immunol **155**(12): 5719-27.

Rossi, D., S. Franceschetti, et al. (2007). "Transient monoclonal expansion of CD8+/CD57+ T-cell large granular lymphocytes after primary cytomegalovirus infection." Am J Hematol **82**(12): 1103-5.

Rousset, F., E. Garcia, et al. (1992). "Interleukin 10 is a potent growth and differentiation factor for activated human B lymphocytes." Proc Natl Acad Sci U S A **89**(5): 1890-3.

Rus, H., C. Cudrici, et al. (2005). "The role of the complement system in innate immunity." Immunol Res **33**(2): 103-12.

Sakaguchi, S. (2004). "Naturally arising CD4+ regulatory t cells for immunologic self-tolerance and negative control of immune responses." Annu Rev Immunol **22**: 531-62.

Sakaguchi, S., N. Sakaguchi, et al. (1995). "Immunologic self-tolerance maintained by activated T

cells expressing IL-2 receptor alpha-chains (CD25). Breakdown of a single mechanism of self-tolerance causes various autoimmune diseases." J Immunol **155**(3): 1151-64.

Sakaguchi, S., K. Wing, et al. (2009). "Regulatory T cells: how do they suppress immune responses?" Int Immunol **21**(10): 1105-11.

Sant'Angelo, D. B. and C. A. Janeway, Jr. (2002). "Negative selection of thymocytes expressing the D10 TCR." Proc Natl Acad Sci U S A **99**(10): 6931-6.

Sarangi, P. P., S. Sehrawat, et al. (2008). "IL-10 and natural regulatory T cells: two independent anti-inflammatory mechanisms in herpes simplex virus-induced ocular immunopathology." J Immunol **180**(9): 6297-306.

Schade, A. E., G. L. Schieven, et al. (2008). "Dasatinib, a small-molecule protein tyrosine kinase inhibitor, inhibits T-cell activation and proliferation." Blood **111**(3): 1366-77.

Scheinberg, P., J. J. Melenhorst, et al. (2009). "The transfer of adaptive immunity to CMV during hematopoietic stem cell transplantation is dependent on the specificity and phenotype of CMV-specific T cells in the donor." Blood **114**(24): 5071-80.

Schmitz, J. E., M. A. Forman, et al. (1998). "Expression of the CD8alpha beta-heterodimer on CD8(+) T lymphocytes in peripheral blood lymphocytes of human immunodeficiency virus- and human immunodeficiency virus+ individuals." Blood **92**(1): 198-206.

Scholzen, T. and J. Gerdes (2000). "The Ki-67 protein: from the known and the unknown." J Cell Physiol **182**(3): 311-22.

Scott, B., H. Bluthmann, et al. (1989). "The generation of mature T cells requires interaction of the alpha beta T-cell receptor with major histocompatibility antigens." Nature **338**(6216): 591-3.

Seggewiss, R., K. Lore, et al. (2005). "Imatinib inhibits T-cell receptor-mediated T-cell proliferation and activation in a dose-dependent manner." Blood **105**(6): 2473-9.

Seggewiss, R., D. A. Price, et al. (2008). "Immunomodulatory effects of imatinib and second-generation tyrosine kinase inhibitors on T cells and dendritic cells: an update." Cytotherapy **10**(6): 633-41.

Shah, N. P., H. M. Kantarjian, et al. (2008). "Intermittent target inhibition with dasatinib 100 mg once daily preserves efficacy and improves tolerability in imatinib-resistant and -intolerant chronic-phase chronic myeloid leukemia." J Clin Oncol **26**(19): 3204-12.

Shen, S., Y. Ding, et al. (2005). "Control of homeostatic proliferation by regulatory T cells." J Clin Invest **115**(12): 3517-26.

Shiow, L. R., D. B. Rosen, et al. (2006). "CD69 acts downstream of interferon-alpha/beta to inhibit S1P1 and lymphocyte egress from lymphoid organs." Nature **440**(7083): 540-4.

Sierro, S., R. Rothkopf, et al. (2005). "Evolution of diverse antiviral CD8+ T cell populations after murine cytomegalovirus infection." Eur J Immunol **35**(4): 1113-23.

Sillaber, C., H. Herrmann, et al. (2009). "Immunosuppression and atypical infections in CML patients treated with dasatinib at 140 mg daily." Eur J Clin Invest **39**(12): 1098-109.

Simon, C. O., R. Holtappels, et al. (2006). "CD8 T cells control cytomegalovirus latency by epitope-specific sensing of transcriptional reactivation." J Virol **80**(21): 10436-56.

Simon, C. O., C. K. Seckert, et al. (2005). "Role for tumor necrosis factor alpha in murine cytomegalovirus transcriptional reactivation in latently infected lungs." J Virol **79**(1): 326-40.

Simon, C. O., C. K. Seckert, et al. (2006). Murine model of cytomegalovirus latency and reactivation: the silencing/desilencing and immune sensing hypothesis. Cytomegaloviruses: Molecular Biology and Immunology. M. J. Reddehase, ed. Wymondham, Norfolk, U.K., Caister Academic Press**:** p. 483-500.

Slobedman, B., P. A. Barry, et al. (2009). "Virus-encoded homologs of cellular interleukin-10 and their control of host immune function." J Virol **83**(19): 9618-29.

Smith-Garvin, J. E., G. A. Koretzky, et al. (2009). "T cell activation." Annu Rev Immunol **27**: 591-619.

Snyder, C. M., K. S. Cho, et al. (2008). "Memory inflation during chronic viral infection is maintained by continuous production of short-lived, functional T cells." Immunity **29**(4): 650-9.

Snyder, C. M., A. Loewendorf, et al. (2009). "CD4+ T cell help has an epitope-dependent impact on CD8+ T cell memory inflation during murine cytomegalovirus infection." J Immunol **183**(6): 3932-41.

Spencer, J. V., J. Cadaoas, et al. (2008). "Stimulation of B lymphocytes by cmvIL-10 but not LAcmvIL-10." Virology **374**(1): 164-9.

Stefanova, I., B. Hemmer, et al. (2003). "TCR ligand discrimination is enforced by competing ERK positive and SHP-1 negative feedback pathways." Nat Immunol **4**(3): 248-54.

Strickler, J. G., L. A. Movahed, et al. (1990). "Oligoclonal T cell receptor gene rearrangements in blood lymphocytes of patients with acute Epstein-Barr virus-induced infectious mononucleosis." J Clin Invest **86**(4): 1358-63.

Sun, J. C., J. N. Beilke, et al. (2009). "Adaptive immune features of natural killer cells." Nature **457**(7229): 557-61.

Sun, Y., C. Finger, et al. (2005). "Chronic gene delivery of interferon-inducible protein 10 through replication-competent retrovirus vectors suppresses tumor growth." Cancer Gene Ther **12**(11): 900-12.

Surh, C. D. and J. Sprent (1994). "T-cell apoptosis detected in situ during positive and negative

selection in the thymus." Nature **372**(6501): 100-3.

Suri-Payer, E. and H. Cantor (2001). "Differential cytokine requirements for regulation of autoimmune gastritis and colitis by CD4(+)CD25(+) T cells." J Autoimmun **16**(2): 115-23.

Swa, S., H. Wright, et al. (2001). "Constitutive activation of Lck and Fyn tyrosine kinases in large granular lymphocytes infected with the gamma-herpesvirus agents of malignant catarrhal fever." Immunology **102**(1): 44-52.

Sweet, C. (1999). "The pathogenicity of cytomegalovirus." FEMS Microbiol Rev **23**: 457-482.

Switzer, S. K., B. P. Wallner, et al. (1998). "Bolus injection of aqueous antigen leads to a high density of T-cell-receptor ligand in the spleen, transient T-cell activation and anergy induction." Immunology **94**(4): 513-22.

Sylwester, A. W., B. L. Mitchell, et al. (2005). "Broadly targeted human cytomegalovirus-specific CD4+ and CD8+ T cells dominate the memory compartments of exposed subjects." J Exp Med **202**(5): 673-85.

Sze, D. M., G. Giesajtis, et al. (2001). "Clonal cytotoxic T cells are expanded in myeloma and reside in the CD8(+)CD57(+)CD28(-) compartment." Blood **98**(9): 2817-27.

Tada, T., T. Takemori, et al. (1978). "Two distinct types of helper T cells involved in the secondary antibody response: independent and synergistic effects of Ia- and Ia+ helper T cells." J Exp Med **147**(2): 446-58.

Taga, K. and G. Tosato (1992). "IL-10 inhibits human T cell proliferation and IL-2 production." J Immunol **148**(4): 1143-8.

Takahashi, T., Y. Kuniyasu, et al. (1998). "Immunologic self-tolerance maintained by CD25+CD4+ naturally anergic and suppressive T cells: induction of autoimmune disease by breaking their anergic/suppressive state." Int Immunol **10**(12): 1969-80.

Takata, H. and M. Takiguchi (2006). "Three memory subsets of human CD8+ T cells differently expressing three cytolytic effector molecules." J Immunol **177**(7): 4330-40.

Teh, H. S., A. M. Garvin, et al. (1991). "Participation of CD4 coreceptor molecules in T-cell repertoire selection." Nature **349**(6306): 241-3.

Thomas, P. G., S. A. Brown, et al. (2010). "Physiological numbers of CD4+ T cells generate weak recall responses following influenza virus challenge." J Immunol **184**(4): 1721-7.

Thornton, A. M. and E. M. Shevach (1998). "CD4+CD25+ immunoregulatory T cells suppress polyclonal T cell activation in vitro by inhibiting interleukin 2 production." J Exp Med **188**(2): 287-96.

Tough, D. F. and J. Sprent (1994). "Turnover of naive- and memory-phenotype T cells." J Exp Med

179(4): 1127-35.

Trautmann, L., L. Janbazian, et al. (2006). "Upregulation of PD-1 expression on HIV-specific CD8+ T cells leads to reversible immune dysfunction." Nat Med **12**(10): 1198-202.

Turner, S. M. (2006). "Stable isotopes, mass spectrometry, and molecular fluxes: applications to toxicology." J Pharmacol Toxicol Methods **53**(1): 75-85.

Usharauli, D. and T. Kamala (2008). "Brief antigenic stimulation generates effector CD8 T cells with low cytotoxic activity and high IL-2 production." J Immunol **180**(7): 4507-13.

Valiante, N. M., M. Rengaraju, et al. (1992). "Role of the production of natural killer cell stimulatory factor (NKSF/IL-12) in the ability of B cell lines to stimulate T and NK cell proliferation." Cell Immunol **145**(1): 187-98.

van Leeuwen, E. M., L. E. Gamadia, et al. (2002). "Proliferation requirements of cytomegalovirus-specific, effector-type human CD8+ T cells." J Immunol **169**(10): 5838-43.

Veldhoen, M., C. Uyttenhove, et al. (2008). "Transforming growth factor-beta 'reprograms' the differentiation of T helper 2 cells and promotes an interleukin 9-producing subset." Nat Immunol **9**(12): 1341-6.

Venturi, V., D. A. Price, et al. (2008). "The molecular basis for public T-cell responses?" Nat Rev Immunol **8**(3): 231-8.

Vezys, V., D. Masopust, et al. (2006). "Continuous recruitment of naive T cells contributes to heterogeneity of antiviral CD8 T cells during persistent infection." J Exp Med **203**(10): 2263-9.

Virgin, H. W., E. J. Wherry, et al. (2009). "Redefining chronic viral infection." Cell **138**(1): 30-50.

Voehringer, D., H. E. Liang, et al. (2008). "Homeostasis and effector function of lymphopenia-induced "memory-like" T cells in constitutively T cell-depleted mice." J Immunol **180**(7): 4742-53.

von Boehmer, H. and P. Kisielow (1990). "Self-nonself discrimination by T cells." Science **248**(4961): 1369-73.

von Boehmer, H., H. S. Teh, et al. (1989). "The thymus selects the useful, neglects the useless and destroys the harmful." Immunol Today **10**(2): 57-61.

Vukmanovic-Stejic, M., Y. Zhang, et al. (2006). "Human CD4+ CD25hi Foxp3+ regulatory T cells are derived by rapid turnover of memory populations in vivo." J Clin Invest **116**(9): 2423-33.

Walter, E. A., P. D. Greenberg, et al. (1995). "Reconstitution of cellular immunity against cytomegalovirus in recipients of allogeneic bone marrow by transfer of T-cell clones from the donor." N Engl J Med **333**(16): 1038-44.

Walton, S. M., P. Wyrsch, et al. (2008). "The dynamics of mouse cytomegalovirus-specific CD4 T cell responses during acute and latent infection." J Immunol **181**(2): 1128-34.

Weichsel, R., C. Dix, et al. (2008). "Profound inhibition of antigen-specific T-cell effector functions by dasatinib." Clin Cancer Res **14**(8): 2484-91.

Weigent, D. A., G. J. Stanton, et al. (1983). "Interleukin 2 enhances natural killer cell activity through induction of gamma interferon." Infect Immun **41**(3): 992-7.

Wells, F. B., S. J. Gahm, et al. (1991). "Requirement for positive selection of gamma delta receptor-bearing T cells." Science **253**(5022): 903-5.

Wherry, E. J. (2011). "T cell exhaustion." Nat Immunol **12**(6): 492-9.

Wlodarski, M. W., Z. Nearman, et al. (2008). "Phenotypic differences between healthy effector CTL and leukemic LGL cells support the notion of antigen-triggered clonal transformation in T-LGL leukemia." J Leukoc Biol **83**(3): 589-601.

Wooldridge, L., A. Lissina, et al. (2009). "Tricks with tetramers: how to get the most from multimeric peptide-MHC." Immunology **126**(2): 147-64.

Yamagiwa, S., J. D. Gray, et al. (2001). "A role for TGF-beta in the generation and expansion of CD4+CD25+ regulatory T cells from human peripheral blood." J Immunol **166**(12): 7282-9.

Zhan, Y., J. F. Purton, et al. (2003). "Without peripheral interference, thymic deletion is mediated in a cohort of double-positive cells without classical activation." Proc Natl Acad Sci U S A **100**(3): 1197-202.

Zhao, D. M., A. M. Thornton, et al. (2006). "Activated CD4+CD25+ T cells selectively kill B lymphocytes." Blood **107**(10): 3925-32.